Zürcher Hochschule
für Angewandte Wissenschaften

zh
aw

Life Sciences und
Facility Management

IUNR Institut für Umwelt und
Natürliche Ressourcen

UNIVERSITY
OF WARSAW

SAPERE AUDE!
1917
KHERSON STATE UNIVERSITY

Report from the

7th Master Summer School
"Biodiversity Monitoring",
Preda, Switzerland, 18–29 August 2025

Edited by Jürgen Dengler

Coordinators

Jürgen Dengler, ZHAW, Switzerland, Iwona Dembicz, University of Warsaw, Poland & Iwan Moysienko, Kherson State University, Ukraine

Teachers

Regula Billeter, Olha Chusova, Jürgen Dengler, Roland Graf, Marcin T. Mazurkiewicz, Ludmiła Szewczak, Stefan Widmer

Participants

Sophie Bürgi, Dylan Derradj, Janick Ehrsam, Katharina Genucchi, Binod Kafle, Nadiia Kapets, Dunin Karwicki, Felix Krogh Vissing, Svitlana Kyiak, Bartosz Norek, Anders Raagaard Larsen, Iryna Rabyk, Fabian Rätz, Lukas Andre Rieben, Joëlle Truniger, Oksana Tyshchenko, Jonas Uhland, Patryk Werner, Anna Wiewiorowska

Recommended citation

Dengler, J. (ed.) 2026. *Report from the 7th Master Summer School "Biodiversity Monitoring", Preda, Switzerland, 18–29 August 2025*. Institute of Natural Resource Sciences (IUNR), Zurich University of Applied Sciences (ZHAW), Wädenswil, CH.

Cover photos

Field work during the summer school (Photos: Jürgen Dengler, Oksana Tyshchenko and Anders Raagaard Larsen).

Disclaimer

The given authors are responsible for the content of the individual chapters.

Table of contents

Preface

Jürgen Dengler

The Master Summer School "Biodiversity Monitoring" started in 2019 as a joint initiative between the Institute of Natural Resource Sciences (IUNR) of the Zurich University of Applied Sciences (ZHAW) Wädenswil in Switzerland and the Faculty of Biology of the University of Warsaw in Poland (Dengler 2020a, 2020b), while Kherson State University, Ukraine, later joined as a third partner. The Summer School is currently conducted alternatingly in Białowieża, Poland (even years; e.g. Dembicz & Dengler 2025) and Preda, Switzerland (uneven years; e.g. Dengler 2024).

For the seventh conductance in August 2025, we returned to Park Ela, Grisons, where we stayed as usual at the group house "Sonnenhof", perfectly located in the very diverse subalpine Albula flood plain, with two beautiful remote alpine valleys on both sides: the acidic Val Mulix to the South and the base-rich Val Zavretta to the North. Under the guidance of seven teachers, 19 participants learned for 11 days how to sample biodiversity in different taxonomic groups (vascular plants, orthopterans and small mammals), how to set up monitoring schemes and how to analyse these data with modern statistical methods in R. Both teachers and students were from all three countries, Switzerland, Poland and Ukraine. Additionally, we had Danish master students (who were on exchange in Warsaw) and a Nepalese PhD student (working in Finland). Thus, it was the most international Summer School so far.

While the Summer School primarily is an is focussed on skill development of the participants, the high-quality sampling from time to time also facilitates international publications. The records of our permanent elevational transect in Preda from 2019 form part of the global DarkDivNet network (as part of site D095; https://macroecology.ut.ee/en/darkdivnet/), which yielded a high-impact publication on the impact of human footprint of different aspects of plant diversity (Pärtel et al. 2025). A student project from the Summer School in Preda 2023 yielded a methodological paper on the use of mean ecological indicator values for the prediction of site conditions (Ostrowski et al. 2025). And from the Summer School 2025 in Preda even two papers are in preparation, one on the scale- and taxon-dependence of bioindication with ecological indicator values, one on the scale-dependence of a wide set of biodiversity metrics. The first of these could already be presented by one of the students on an international conference (Mazurkiewicz et al. 2026), while the second has been invited for submission in a Special Feature of an international journal (Wiewiorowska et al. in prep.).

References

Dembicz, I. & Dengler, J. (eds.) 2025. *Report from the 6th Master Summer School "Biodiversity Monitoring",* Białowieża*, Poland, 16–27 August 2024.* University of Warsaw, Warsaw, PL: 94 pp.

Dengler, J. (ed.) 2020a. *Report from the International Master Summer School "Biodiversity Monitoring", Preda, Parc Ela, Switzerland, 14–25 August 2019*. Institute of Natural Resource Sciences (IUNR). Zurich University of Applied Sciences, Wädenswil, CH.

Dengler, J. 2020b. Internationale Summer School "Biodiversity Monitoring": Lernen, wie man Biodiversität erfasst und ihre Veränderungen analysiert. *IUNR Magazin* 2020(1): 6–7.

Dengler, J. (ed.) 2024. *Report from the 5th Master Summer School "Biodiversity Monitoring", Preda, Switzerland, 14–25 August 2023*. Institute of Natural Resource Sciences (IUNR), Zurich University of Applied Sciences (ZHAW), Wädenswil, CH: 108 pp.

Mazurkiewicz, M.T., Wiewiorowska, A., Kapets, N., Karwicki, D., Norek, B., Rabyk, I., Tyshchenko, O., Chusova, O., Gillet, F., Widmer, S. & Dengler, J. 2026. Scale- and taxon-dependence of mean ecological indicator values. Poster that the 68th IAVS Annual Symposium - Gijón, Spain, 22–26 June 2026.

Ostrowski, G., Aicher, S., Mankiewicz, A., Chusova, O., Dembicz, I., Widmer, S. & Dengler, J. (2025) Mean ecological indicator values: use EIVE but no cover-weighting. *Vegetation Classification and Survey* 6: 57–67. https://doi.org/10.3897/VCS.134800

Pärtel, M., Tamme, R., Carmona, C.P., Riibak, K., Moora, M., Bennett, J.A., Chiarucci, A., Chytrý, M., de Bello, F., (…), Dembicz, I., Dengler, J., (…) & Zobel, M. (2025) Global-scale impoverishment of natural vegetation revealed by dark diversity. *Nature* 641: 917–922. https://doi.org/10.1038/s41586-025-08814-5

Reports from the student projects

The participants of the Summer School have carried out three research projects in small teams of three to five students from mostly at least two countries. These reports were prepared in the style of scientific papers. Please note that the projects are published as submitted by the students, except minor adjustments in the layout. The responsibility for the content solely rests with the authors.

Vegetation changes along an elevational gradient in the subalpine Mulix Valley, Switzerland (2019-2025)

Sophie Bürgi, Binod Kafle, Lukas Rieben

Abstract

Species-related values and mean indicator values are key indicators in biodiversity monitoring, while ecological parameters such as air temperature, light, and soil moisture are known to influence biodiversity patterns. However, the fine-scale interplay between vegetation dynamics and local microclimatic variation remains poorly understood. We aimed to quantify temporal changes in vascular plant species richness, mean ecological indicator values, and species composition across multiple vegetation types, and to assess the influence of local microclimatic variation. We assessed these patterns over a six-year period (2019–2025) across five vegetation types situated between 1706 and 2595 m a.s.l. in the subalpine Mulix Valley near Preda in the Swiss Alps. Thirteen plots were examined, with two subplots of 10 m² recorded per location, resulting in a total of 26 subplots. Across the study period and across all vegetation types, mean species richness ranged from 15 to 49 species per subplot, while mean species turnover varied between 0.3 and 0.6. Species richness reached its lowest value in 2025, indicating greater species loss and correspondingly higher turnover compared to previous years. We detected significant differences among vegetation types ($p < 0.05$) for species richness, Shannon diversity index, competitiveness, stress tolerance, mean air temperature, and mean light availability. We observed a significant correlation between air and soil temperatures based on logger data collected in 2020 and 2025. The findings suggest that, within Mulix Valley, biodiversity dynamics are primarily structured by vegetation type and intrinsic community properties rather than short-term variation in local temperature. In summary, the findings provide a robust baseline for long-term monitoring and emphasize the need for continued resampling to detect directional vegetation changes and inform conservation strategies for alpine ecosystems under climate and land use change.

Keywords

Alpine vegetation, ecological indicator values, elevation gradient, microclimate, species-related values, species richness, subalpine vegetation, time series, vascular plants, vegetation types.

Introduction

The elevation gradients and complex topography of mountain regions create substantial environmental variation, giving rise to a diverse range of ecosystems. These mountain ecosystems support a significant share of global biodiversity and provide vital ecosystem services, such as water regulation, carbon sequestration and grazing resources that sustain local communities as well as downstream populations beyond mountain boundaries (Ioan et al., 2025; Körner, 2004). However, they are among the ecosystems most vulnerable to climate change, with temperatures in the European Alps rising at nearly twice the global average (Begert & Frei, 2018; Kotlarski et al., 2023). Accelerated warming affects alpine biodiversity by causing habitat contraction, shifts in species distributions, declining snowpacks, and retreating glaciers, with cascading consequences for ecological functioning and ecosystem services (Pepin et al., 2022). These

climatic changes interact with local environmental gradients and land-use history, shaping alpine vegetation patterns. While the elevational zonation of plant communities is primarily determined by abiotic conditions, human activity has substantially modified these natural distributions. Historical forest clearing for pastures created species-rich semi-natural grasslands in the Alps, which remain among the most diverse habitats in the region, particularly for vascular plant species (Dengler et al., 2014). More recently, land-use intensification (increased fertilization, mowing frequency, and animal stocking density) as well as large-scale abandonment have emerged as major drivers of biodiversity loss and compositional change in mountain grasslands (Elliott et al., 2023; Spörri et al., 2023; Weber et al., 2024). Together, these climatic and land-use shifts have already altered alpine vegetation composition and productivity, with consequences for ecological functioning as well as for the cultural and economic services that mountain landscapes provide. Understanding how biodiversity and vegetation structure respond along elevational gradients is therefore crucial for ecologists, conservation practitioners, and land managers seeking to anticipate and mitigate the impacts of environmental change.

Elevational gradients provide natural laboratories for studying biodiversity patterns and species distributions, as they encompass pronounced climatic variation and associated changes in productivity over relatively short spatial distances (Körner, 2007; Vetaas, 2021). In the context of ongoing climate change, alpine ecosystems are of particular interest because their vegetation is expected to respond sensitively to shifts in temperature, snow cover, and microclimatic heterogeneity (IPBES, 2019; Theurillat & Guisan, 2001). Recent research highlights that microclimatic variability, such as fine-scale differences in soil and air temperature, can substantially influence vegetation dynamics and species interactions in mountain landscapes (Dolezal et al., 2016; Zellweger et al., 2024).

Long-term monitoring along alpine gradients, such as the GLORIA project across Europe, has documented consistent increases in species richness on mountain summits, driven by upward migration of thermophilous species in response to warming (Pauli et al., 2012; Steinbauer et al., 2018). However, these short-term increases in diversity may mask impending declines in cold-adapted specialists, suggesting a transient phase of community reorganization (Gottfried et al., 2012). Furthermore, while macroscale trends are well documented, less is known about the fine-scale interplay between vegetation dynamics and microclimatic heterogeneity within valleys and across habitat types. Such knowledge gaps highlight the need for repeated local monitoring along elevational transects that integrate vegetation resampling with microclimatic data (Häberlin & Dengler, 2025; Zellweger et al., 2024).

Building on national and international monitoring efforts, we contribute to understanding fine-scale vegetation dynamics and the role of microclimate by resampling a permanent elevational transect in the subalpine Mulix Valley near Preda (Canton of Grisons, Switzerland). Established in 2019, the transect consists of 13 permanent plots distributed across five major vegetation types — floodplain, subalpine forest, subalpine heathland, subalpine grassland, and alpine grassland — spanning approximately 1700–2600 m a.s.l. Each plot is equipped with soil and air temperature loggers, allowing for continuous monitoring of microclimatic conditions. Building on the previous surveys conducted within the framework of the Biodiversity Monitoring Summer School (Dengler, 2024), we aim to address the following research questions in this study:

1. How do the species-related values[1] and mean indicator values[2] change across different vegetation types during the period 2019 – 2025?

[1] Biodiversity indices, specifically species richness, species turnover, Shannon index, Shannon evenness and Simpson index; see Büchler et al. (2020).
[2] Air temperature, light, soil moisture and CSR strategies; see Büchler et al. (2020).

2. Do vegetation types significantly differ in their species-related values and mean indicator values?
3. To what extent do soil temperature and air temperature influence species richness and species turnover?

Methods

Study site

The research area is located in the acidic Mulix Valley in the Swiss Alps near Preda, Canton of Grisons. Along an elevational transect from approximately 1700 to 2600 m a.s.l., we worked with 13 permanent plots of 100 m², each containing two 10 m² subplots, only these were relevant to us (Figure 1). The permanent plots were established in 2019. All plots were georeferenced using GPS and marked at two corners with wooden stakes, with additional buried magnets at the remaining corners to ensure accurate relocation in subsequent years. Each plot was equipped with a TMS-4 datalogger with three sensors for record air temperature, one positioned underground, one at surface level and the other above ground (Wild et al., 2019). Of the 13 loggers that were placed and controlled in 2023 there were just 6 still there or collecting data when we were doing the resampling in August 2025.

Resampling was done before this year's Summer School in 2020, 2021, 2023. In 2025 we resampled the plots between 20th and 25th of August. The plots are located in different vegetation types and are distributed more or less evenly over the whole elevational transect. The vegetation types are: floodplain (C10 and C11), subalpine forest (C01–C03, N1C), subalpine heathland (C04–C05), subalpine grassland (A1C) and alpine grassland (C06–C09).

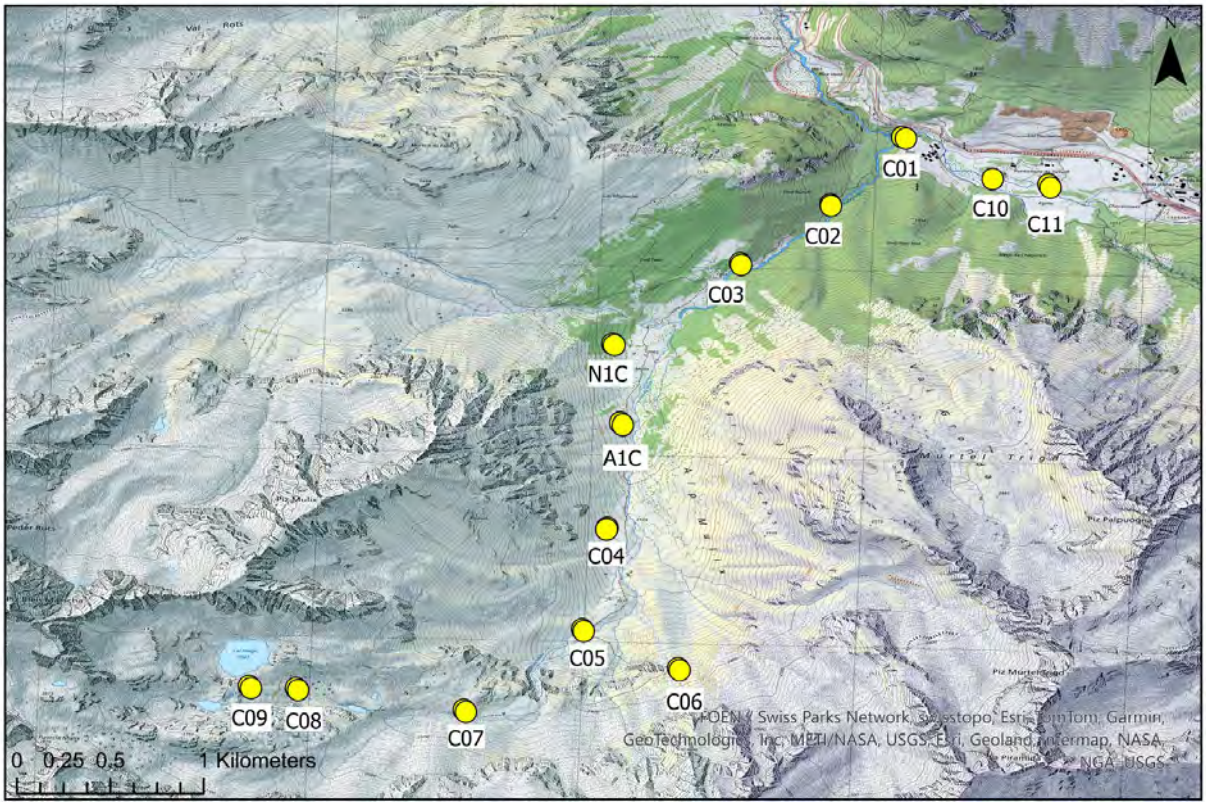

Figure 1. Study area in the Mulix Valley, Preda CH, with all the plot-locations and plot-ID's along the permanent transect (Federal Office of Topography swisstopo, 2024).

Floodplain sites were located at lower elevations with partial tree cover and high gravel content, while subalpine forests exhibited dense vegetation and variable deadwood abundance. Heathland plots and subalpine grasslands occurred at intermediate elevations with sparse woody vegetation and moderate stoniness. Alpine grassland plots were situated at the highest elevations, dominated by low herbaceous cover and rocky substrates (Table 1).

Table 1. Research plots with elevation and vegetation type and land cover characteristics (* for plots with loggers)

Plot	Elevation, m a.s.l	Vegetation type	Land cover characteristics
A1C	2023.5	Subalpine grassland	40% vegetation; 60% rocks, stones; No trees and deadwoods
C01*	1709	Subalpine forest	55-60% vegetation, 10% deadwood, 8% stones and rocks
C02	1801	Subalpine forest	85% vegetation; 7% deadwood, 7% stones
C03	1962	Subalpine forest	85-90% vegetation; 8% stones, 3% deadwoods
C04*	2095	Subalpine heathland	75% vegetation, 30% stones, No trees; 5% deadwoods
C05	2201	Subalpine heathland	75-80% vegetation; No trees; 20% stones, rocks; 4% deadwood
C06*	2310	Alpine grassland	95% vegetation; 30% gravel; No trees
C07*	2404	Alpine grassland	90% vegetation; 20% stones and gravels, 10% deadwood; No trees
C08	2531	Alpine grassland	60-65% vegetation; 30-35% stones, rocks, gravels, No trees and deadwoods
C09*	2592	Alpine grassland	65% vegetation; 35% stones, gravels, rocks; No trees and deadwoods
C10	1706	Floodplain	50% vegetation; 55% gravels; Trees present; 7% deadwood
C11	1713	Floodplain	80% vegetation; Trees and deadwood present; 5% gravels
N1C*	2021	Subalpine forest	80% vegetation; 7% stones and rocks; 20% deadwoods

Field sampling

For this project, we sampled only the 10 m² subplots within each permanent 100 m² plot following the standardized EDGG methodology for assessing grassland diversity across spatial scales (Dengler et al., 2016). The 10 m² subplots were consistently located at the north-western and south-eastern corners of each permanent plot, resulting in a total of 26 subplots. The elevation and vegetation type as well as the land cover characteristics of each plot are listed in **Fehler! Verweisquelle konnte nicht gefunden werden.**.

For the study of the time series we only identified vascular plants. The sampling method we used is shoot-presence (Greig-Smith, 1983). With this method, all plants that are at least partially within the plot are counted, including those whose roots are outside the plot but whose flowers extend into it. The coverage we estimated in a group discussion for each species in the plot after sampling several species of a plot. For tree-layer, shrub-layer and herb-layer we estimated the coverage separately. We assigned the layers as follows (Müller-Dombois & Ellenberg, 1974): Herb-layer <0.5 m; Shrub-layer 0.5 – 5 m; Tree-layer >5 m.

Of the six loggers that remained operational and were not lost to theft or natural disturbances, data were successfully retrieved in August 2025. We used temperature measurements from the underground and air sensors to compare mean temperatures with logger data collected in 2019/2020.

Data cleaning

First of all data that didn't match our criteria, means plots from different sites than the permanent plots and plot sizes different than 10 m^2 have been removed from our data. Also some changes in layer labels had to be done due to different labels in the data from previous years. Then data from 2019 – 2023 and also from this year's sampling was organized and cleaned by detecting errors and inaccuracies in species identification (Boch et al., 2022) followed by combining or deleting taxa. The cleaning we did first for the new data (only 2025). The cleaned species list we then merged with the data from previous years and the cleaning we conducted repeatedly, following the same rules (and also aggregating some of the new data again if there was a reason, such as the occurrence of another species that could be aggregated with this year's species). We detected the following types of errors and inaccuracies:

1. identification of the same taxon to different levels of accuracy, like "cf" – conferatur, "aggr." – aggregatio, subspecies/species identification; these taxa were merged
2. misidentifications due to an observer's error or identification only to the genus/family level that could be corrected/clarified by comparing with the vegetation data of previous years
3. misidentifications or identification only to the genus/family level that could not be corrected/clarified by comparing with the vegetation data of previous years had to be removed from the analysis
4. synonymous terms or spelling mistakes

After the cleaning process, we summarized all taxon corrections and evaluated them to quantify the frequency and types of adjustments made during data harmonization. Then we merged the two cleaned tables of 2019 – 2023 and 2025 into one table using R. The R code we used considered the overlay of the different vegetation layers and thus calculated the cover ratio of a species per subplot.

We subsequently transformed the dataset into a wide format to facilitate further analysis in Vegedaz (Küchler, 2024). The rearrangement we did using the function pivot_wider from the tidyr-package (Wickham et al., 2024) in R.

Using Vegedaz, it was possible for us to efficiently obtain information for all plots, including species-related values and mean indicator values with minimal effort. Afterwards we supplemented the table obtained with information adding about vegetation type manually using Excel.

We retained the number 3 corrections (only identified on genus level) for the Vegedaz analyses. For the calculation of mean indicator values, these entries were not considered automatically by Vedadaz, as genus-level identifications are excluded from these computations. Regarding species richness, we assumed that when both an undetermined taxon and a determined species of the same genus occurred within the same plot, the observer intended to record distinct taxa. Therefore, we treated the undetermined and determined species as separate entries in such cases.

Statistical analyses

For the statistical analyses, species-related values and mean indicator values were first quantified for all sampling plots. These variables were then visualized using boxplots to assess temporal variation (2019–2025) across the five vegetation types, addressing research question 1. To address research question 2, we applied linear mixed-effects models (LMMs). Research question 3 was examined using correlation analyses.

Species-related values

We quantified species richness, species turnover as well as some of the most widely used diversity indices for alpha-diversity like Shannon index, Shannon evenness, and Simpson index (Shannon, 1948; Simpson, 1949; Thukral, 2017) at subplot level (10 m^2). These indices show different types of alpha- diversities. Shannon index is related to the concept of uncertainty and Shannon evenness describes how evenly individuals are distributed among different species in an environment. Simpson index is a measurement of probability, lower diversity increases the likelihood that two randomly chosen individuals belong to the same species (Pielou, 1966). Species richness is defined as the total number of species present within a given subplot (Dengler, 2024). Species turnover as a measurement of beta diversity quantifies the compositional changes in species between two time points and can be calculated using the following formulation (adapted from Dengler, 2024):

$$Species\ turnover = \frac{Sappeared + Sdisappeared}{Stotal}$$

$S_{appeared}$ = Total number of species appeared at time t2 compared to time t1

$S_{disappeared}$ = Total number of species disappeared at time t2 compared to time t1

S_{total} = total species richness across the two time points, calculated as: $S_{total} = S_{t1} + S_{t2} - S_{shared}$

(S_{t1} = Species richness at time t1; S_{t2} = Species richness at time t2; S_{shared} = Number of species common to both years, t1 and t2)

This equation provides a standardized measure of species compositional change, capturing both species gains and losses between two temporal observations.

For the calculation of species turnover, we assigned a value of 1 for the presence of a species and 0 for its absence in the Excel file. The total number of appeared, disappeared, and common (shared) species was calculated by comparing each year with its preceding year (for example, 2020 was compared with 2019, and 2025 was compared with 2023). For each subplot and each species, we subtracted the earlier year's value from the later year's value (e.g., 2025 – 2023). A positive value (1 – 0 = 1) indicated the appearance of a species in 2025, a negative value (0 – 1 = –1) indicated its disappearance, and a zero value (1 – 1 = 0) indicated a common or shared species. Finally, we calculated the total number of positive, negative, and zero values for each subplot and year. All calculations were performed using R version 4.5.1 (R Core Team, 2025). Once these data were obtained, we applied the equation above to calculate species turnover. We obtained cover-based species-related values (Shannon Index, Shannon Evenness, and Simpson Index) by using Vegedaz, a program for recording and evaluating vegetation surveys.

Mean indicator values

Cover-based mean indicator values from Landolt (1977), and recently reviewed by Ivanova & Zolotova (2023) such as air temperature, light, soil moisture and CSR strategies (competitors, stress-tolerant, and ruderals) by Grime (1977) were estimated using Vegedaz as suggested by Büchler et al. (2020).

Linear mixed-effects models (LMMs)

Linear mixed-effects models were used to examine whether the vegetation types differed in species-related values and mean indicator values during the period 2019-2025. The model included vegetation type, year, and the vegetation type × year interaction as fixed effects, and random effects to account for the hierarchical structure of the sampling design. Specifically, random intercepts were specified as *(1 | plot_id / subplot_id)*, allowing subplot identity to be nested within plot identity. The models were fitted using the **lmer()** function from the *lme4* package (Bates et al., 2015; Cuesta Núñez et al., 2023). Model assumptions (normality, homoscedasticity, and independence of residuals) were checked visually using diagnostic plots.

Correlation analyses

To evaluate the relationships between abiotic conditions and community characteristics, we conducted correlation analyses assessing the extent to which soil temperature and air temperature influence species richness and species turnover. Pearson's correlation coefficients were calculated to quantify the strength and direction of these associations.

Results

Patterns and frequency of taxon corrections

We evaluated total of 733 taxa for potential corrections. Among these, we corrected 206 entries (28.1%), while the remaining 72% required no changes. The analysis revealed that type 1 corrections (merging of taxa identified at different taxonomic resolutions such as cf. and aggr.) were by far the most frequent, accounting for approximately two-thirds (66%) of all modifications. Type 3 corrections, corresponding to misidentifications or insufficiently identified taxa, represented around 25%, whereas types 2 and 4 (clarified misidentifications and spelling/synonym corrections, respectively) occurred only occasionally (7% and 2%). The distribution of correction types is shown in Figure 2.

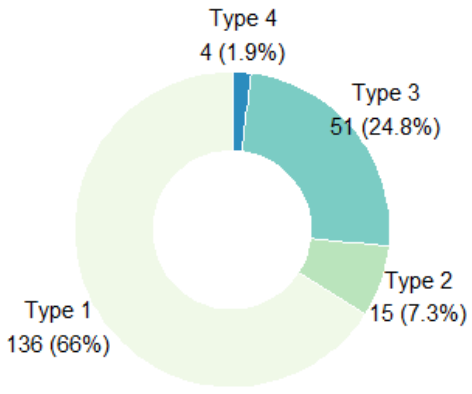

Figure 2. Absolute and relative frequencies of the applied taxon corrections.

The taxa most frequently affected by corrections were *Juniperus communis subsp. alpina* and *Pinus mugo subsp. uncinate*, each with five corrected entries (aggregation to the species level). Other taxa with multiple corrections included *Dryopteris expansa*, *Vaccinium gaultherioides*, and several others. Overall,

the dataset indicates that most corrections were concentrated within a small number of taxa and largely involved merging of taxa identified at different levels of precision.

Occurrence of vegetation species

A total of 345 vascular plant species were recorded at subplot level during the period from 2019–2025. The most frequently occurring species across subplots were *Vaccinium myrtillus* and *Homogyne alpina*, with *V. myrtillus* exhibiting particularly high cover values, reaching up to 64% in certain subplots (Appendix 1. Species occurrence results, Table 1). Both species were present in approximately 60% of all subplots, indicating their dominance within the study area. In total, 126 subplots were surveyed across the study period (26 subplots per year in 2019, 2020, 2021, and 2025; 22 plots in 2023, resulting in 126 total subplots). Of the 345 recorded species, 91 species (26.3%) were observed only once; that is, in a single subplot throughout the entire monitoring period, highlighting a substantial proportion of rare or infrequently occurring taxa within the vegetation community. In contrast, 95 species were recorded in 2–5 subplots, and 52 species occurred in 6–10 subplots. Species with moderate frequency were less common, with 57 species found in 11–20 subplots and 18 species in 21–30 subplots. Only a small fraction of species exhibited widespread distribution, including 12 species recorded in 31–40 subplots, 6 species in 41–50 subplots, 8 species in 51–60 subplots, and 6 species in more than 60 subplots.

Temporal changes in species-related values (Research question 1)

Over the period from 2019 to 2025, species richness and turnover varied notably across the five ecosystem types (Figure 3). Floodplains consistently exhibited the highest species richness, ranging from approximately 44 to 48 species, outperforming other ecosystems, while subalpine forests maintained the lowest richness at around 15 to 16 species. Alpine grasslands, subalpine grasslands, and subalpine heathlands displayed intermediate richness levels, generally between 25 and 43 species. Across all ecosystems, species richness remained relatively stable over time, with only minor fluctuations. In terms of species turnover, values were generally moderate, ranging from 0.3 to 0.6. The turnover values can range between 0 and 1, a high turnover means there are only few shared species between years, a low value indicates many shared species (Ferreira, 2018; Koleff & Gaston, 2002). Subalpine forests experienced the highest turnover, around 0.55, indicating greater temporal changes in species composition. Conversely, alpine and subalpine grasslands had lower turnover values, between 0.3 and 0.42, reflecting more stable communities. Floodplains, despite their high species richness, showed moderate turnover around 0.5 to 0.54. Overall, these patterns suggest that ecosystems with high species richness, like floodplains, do not necessarily experience high turnover, whereas subalpine forests, with low richness, undergo more dynamic changes in species composition. Alpine and subalpine grasslands, with moderate richness and low turnover, represent relatively stable communities over time.

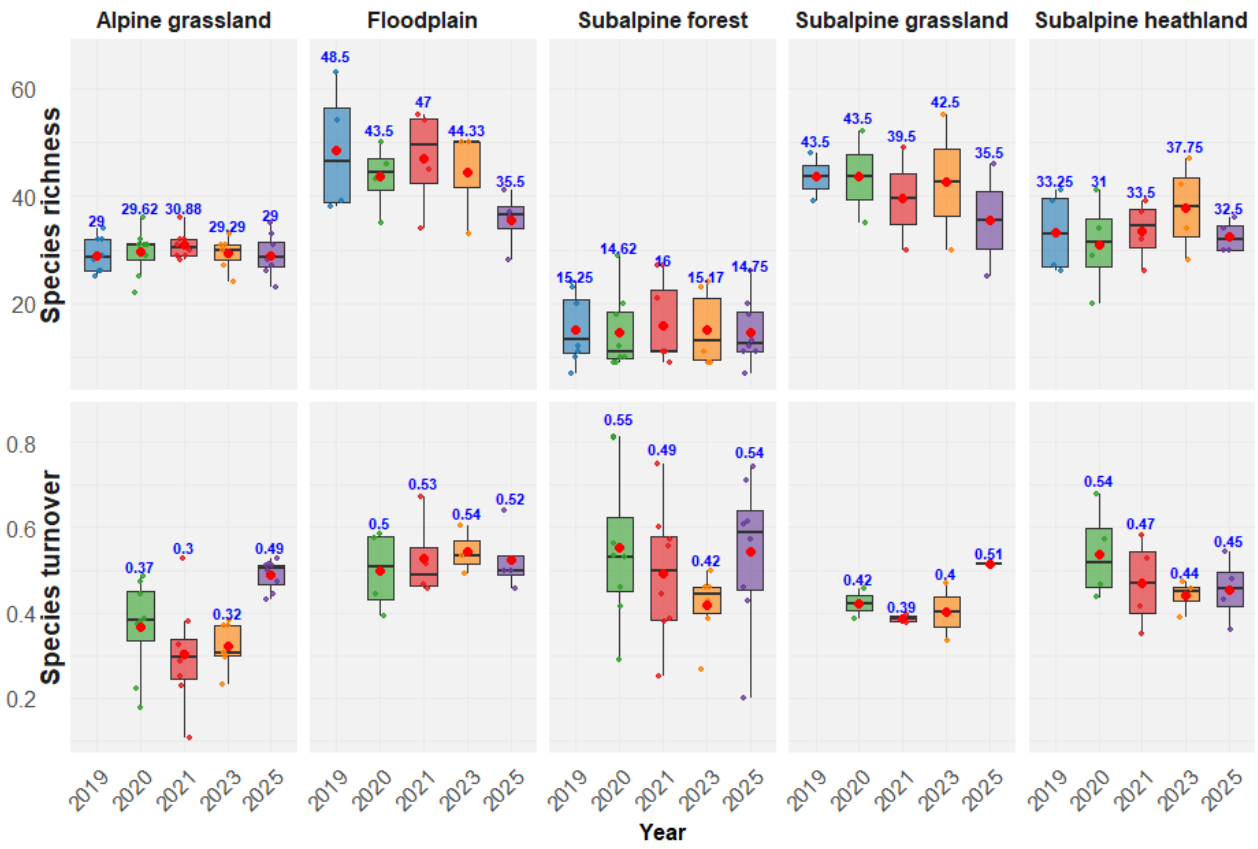

Figure 3. Temporal changes in species richness and species turnover across vegetation types, from 2019 to 2025.

Floodplains show a high number of disappeared species for 2019-2025. They also exhibit a high number of appeared species for 2019-2023. However, the number of appeared species drops sharply in 2025. Together, these patterns indicate a high overall species turnover in floodplain habitats. Subalpine and alpine grasslands exhibit more stable communities with gradual compositional changes. Shared species remain relatively consistent, indicating that while species turnover occurs, core community structure persists over time in most habitats (see Figure 4).

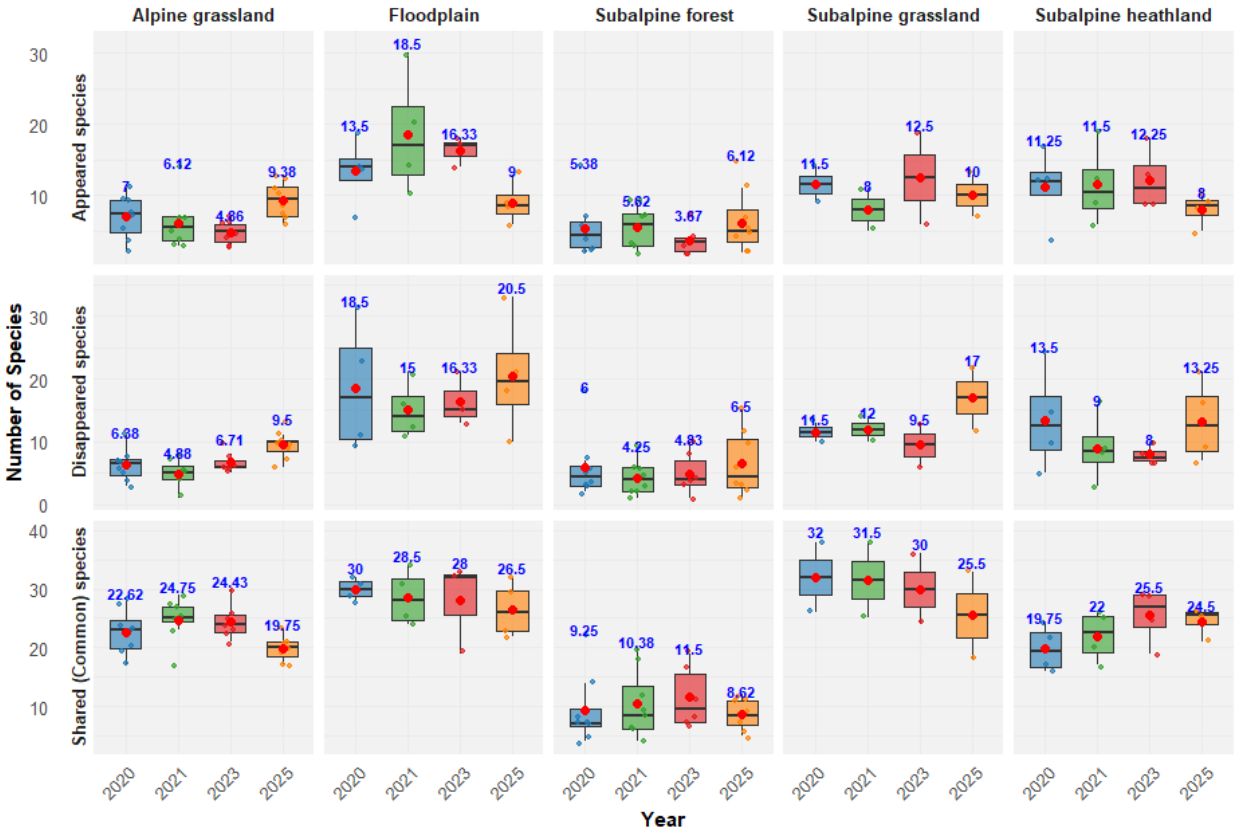

Figure 4. Temporal changes in appeared species, disappeared species, and shared species across vegetation types, from 2019 to 2025.

Across the five ecosystems from 2019 to 2025, subalpine grasslands consistently exhibit the highest diversity and evenness, indicating stable, balanced communities, while subalpine forests show the lowest diversity and evenness, reflecting dominance by a few species and potential vulnerability. Floodplains are relatively diverse but slightly less even, suggesting some dominant species, whereas alpine grasslands and subalpine heathlands display moderate diversity and evenness with minor year-to-year fluctuations (see Figure **5**). Overall, diversity patterns are largely stable over time, with subalpine grasslands emerging as the most robust and subalpine forests the least diverse ecosystems.

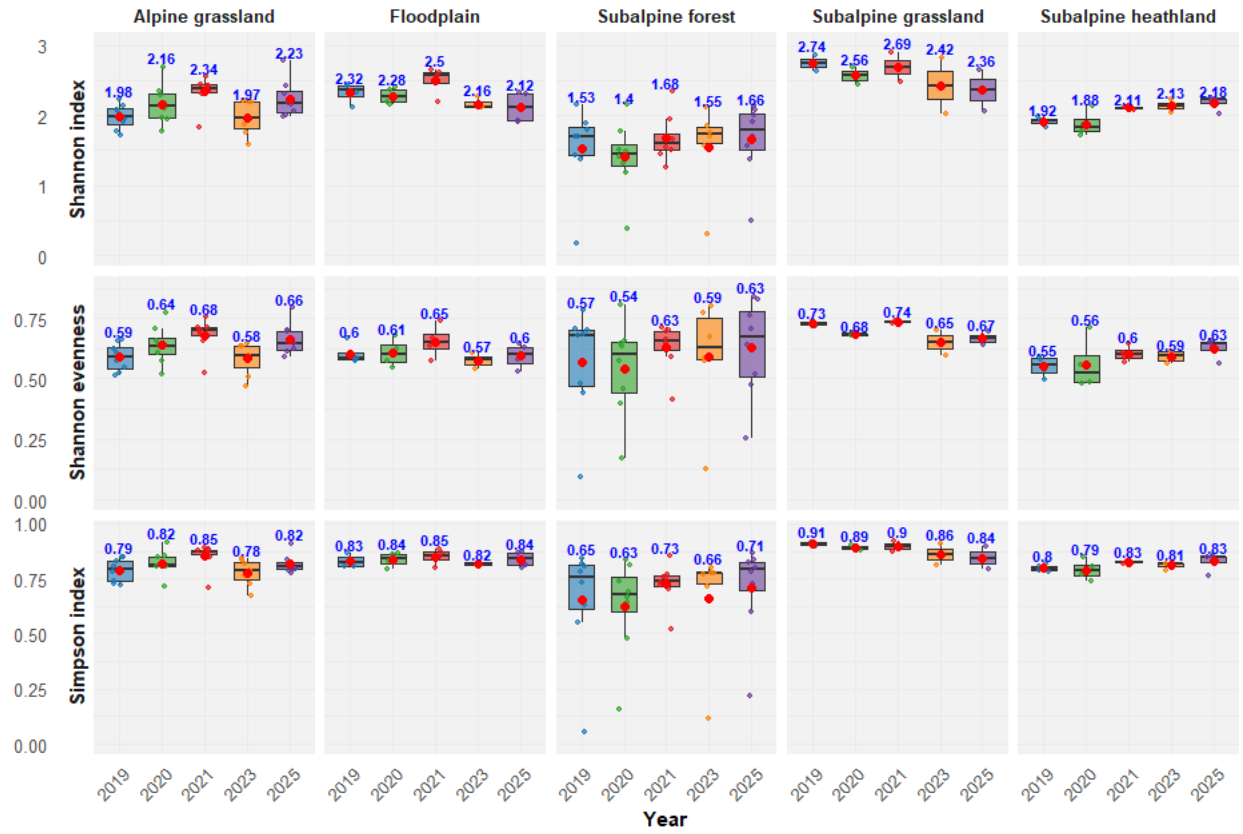

Figure 5. Temporal changes in Shannon index, Shannon evenness, and Simpson index across vegetation types, from 2019 to 2025.

Temporal changes in mean indicators values across vegetation types (Research question 1)

From 2019 to 2025, the five ecosystem types exhibited relatively stable environmental conditions if you look at the ecological indicator values (Figure 6). Floodplains were the warmest and wettest ecosystems, while alpine and subalpine grasslands got the highest mean light number but had lower soil moisture. Subalpine forests were cooler, shaded, and moderately moist, reflecting canopy effects, whereas subalpine heathlands were cooler, moderately exposed to light, and moderately dry. Overall, air temperature, light, and soil moisture showed only minor year-to-year variation across these ecosystems.

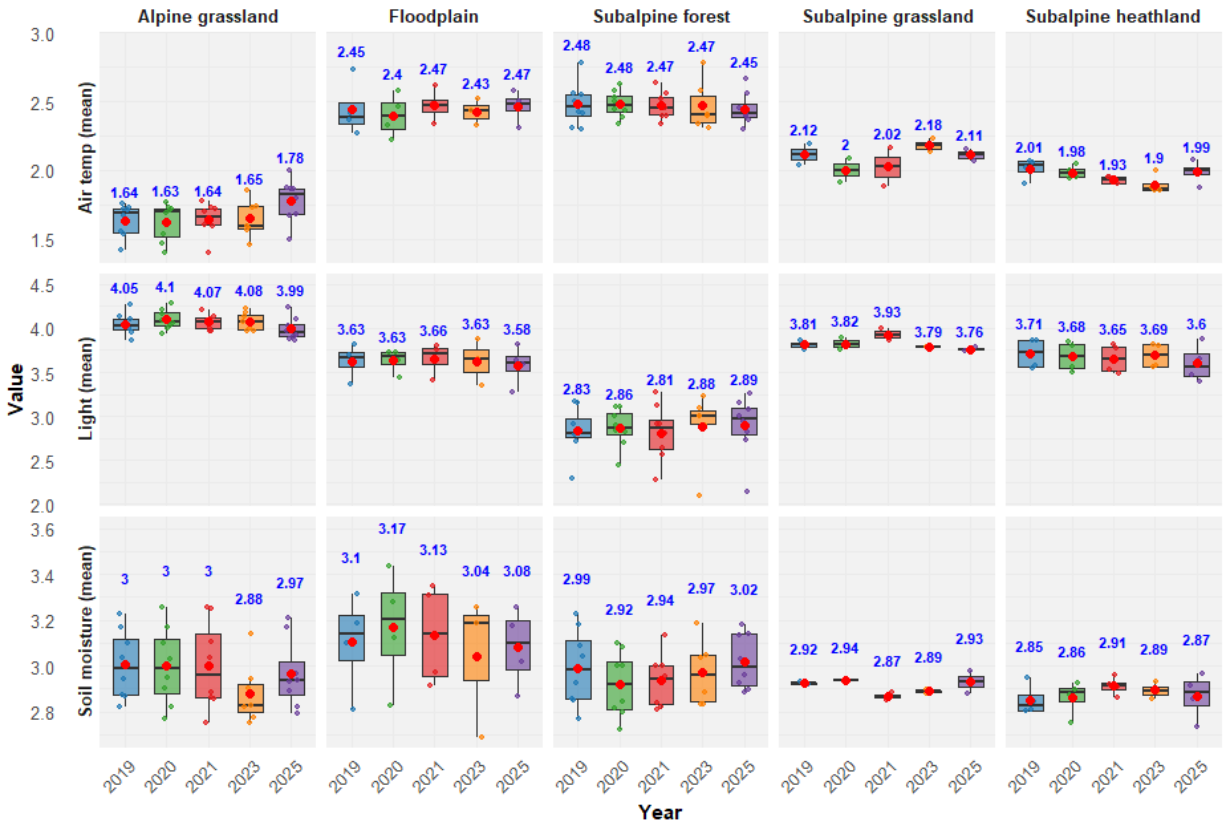

Figure 6. Temporal variation in mean air temperature, mean light, and mean soil moisture across vegetation types, from 2019 to 2025.

Across all habitats, stress-tolerant (S) strategies dominated throughout the study period (2019–2025), reflecting the generally harsh alpine and subalpine conditions. Competitors (C) values were moderate but tended to be higher in subalpine forest and grassland communities, suggesting greater resource availability and competitive interactions in these more productive environments. Ruderal (R) strategies remained consistently low in most habitats, with slightly elevated values in floodplain sites, likely linked to periodic disturbance. Temporal variation in all three strategies was limited, indicating relative functional stability across years (see Figure 7). However, subtle increases in competitive and ruderal components in certain habitats after 2023 may signal early responses to environmental change or shifting disturbance regimes.

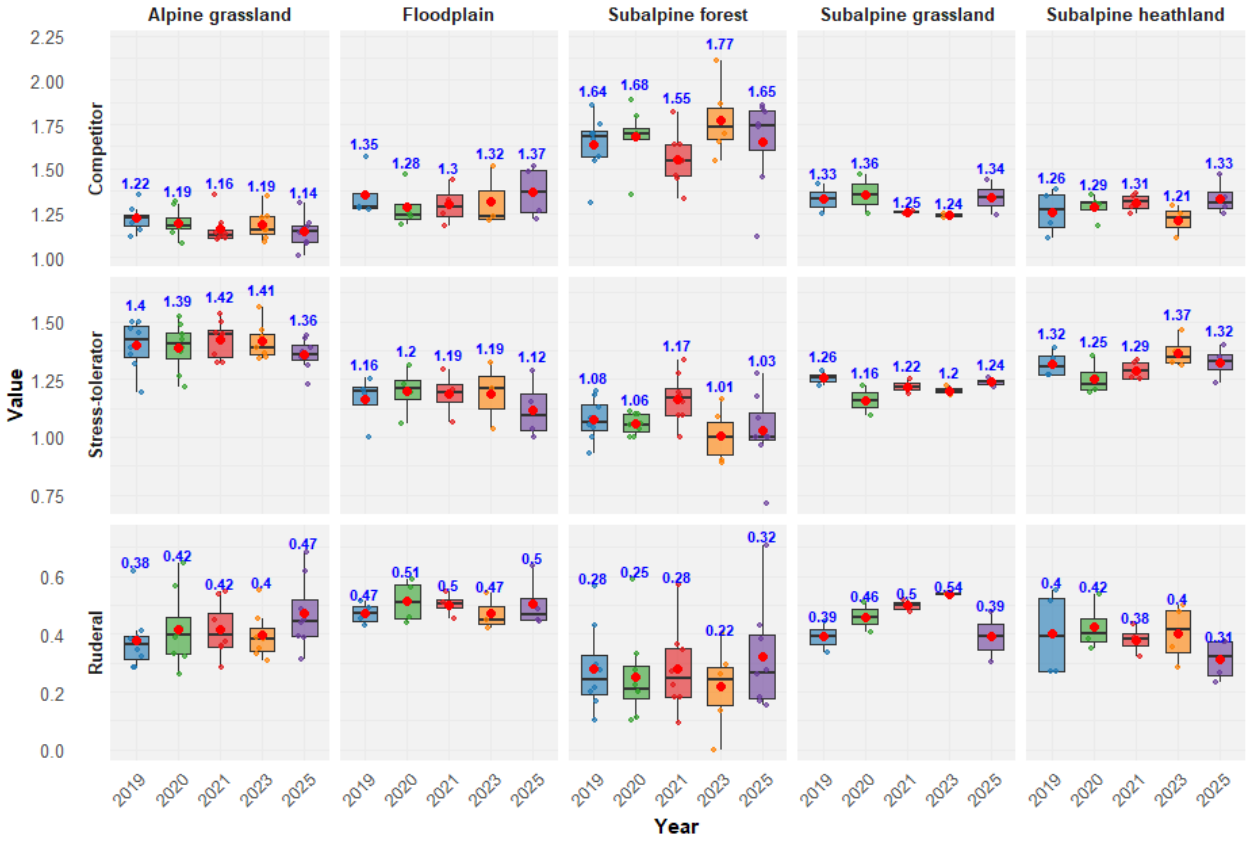

Figure 7. Temporal variation in CSR strategies across vegetation types, from 2019 to 2025.

Statistical Analysis of Differences Among Vegetation Types in Species-Related and Mean Indicator Values (Research question 2)

Linear mixed-effects models revealed significant differences among vegetation types for several response variables (Figure 8 & Figure 9). Species richness ($p = 0.0008$, $R^2_m = 0.697$, $R^2_c = 0.899$), Shannon diversity index ($p = 0.037$, $R^2_m = 0.464$, $R^2_c = 0.751$), competitiveness ($p = 0.0012$, $R^2_m = 0.657$, $R^2_c = 0.872$), stress tolerance ($p = 0.0005$, $R^2_m = 0.665$, $R^2_c = 0.836$), mean air temperature ($p = 0.00003$, $R^2_m = 0.872$, $R^2_c = 0.954$), and mean light availability ($p = 0.0003$, $R^2_m = 0.817$, $R^2_c = 0.959$) all showed significant variation among vegetation types.

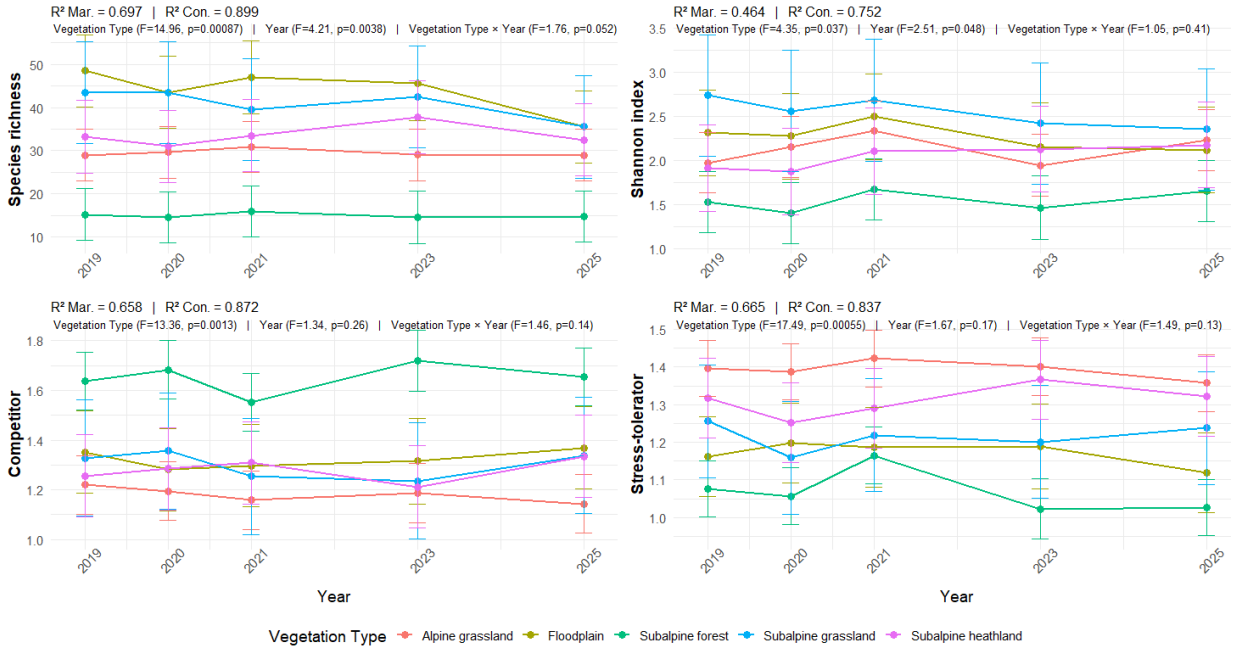

Figure 8. Linear mixed model (LMM) results for four variables: species richness, Shannon index, competitor, and stress-tolerator. Marginal (R^2 Mar) and conditional (R^2 Con) R^2 values, along with F- and p-values for the effects of vegetation type, year, and their interaction, are shown above each panel. Vegetation types are color-coded as follows: Alpine grassland (red), Floodplain (yellow-green), Subalpine forest (green), Subalpine grassland (blue), and Subalpine heathland (magenta).

We detected significant temporal variation across years for species richness ($p = 0.0003$) and the Shannon diversity index ($p = 0.012$). We found significant vegetation type × year interactions for the ruderal ($p = 0.010$), mean air temperature ($p = 0.045$), and mean soil moisture ($p = 0.007$), indicating that temporal trends differed among vegetation types for these variables (Figure 9). In contrast, we detected no significant differences for species turnover, Shannon evenness, or Simpson diversity index (all $p > 0.05$; Appendix 2, Table 2).

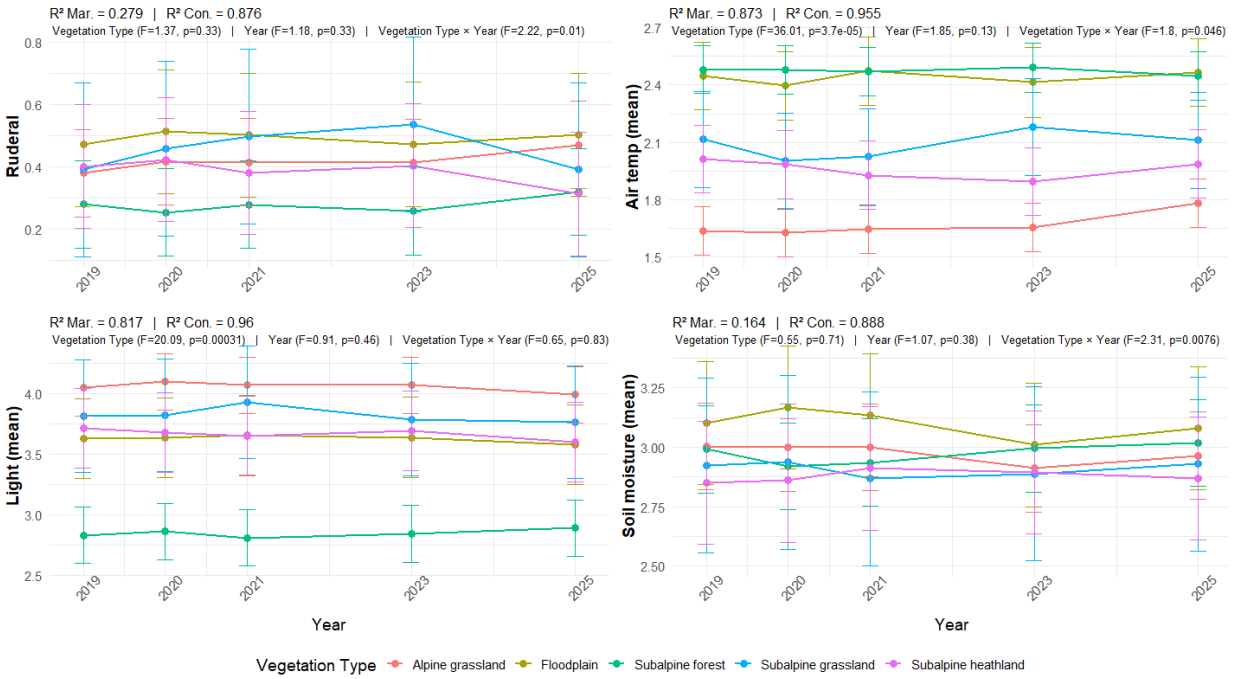

Figure 9. Linear mixed model (LMM) results for four mean indicator variables: ruderal species proportion, air temperature, light availability, and soil moisture. Marginal (R^2 Mar) and conditional (R^2 Con) R^2 values, along with F- and p-values for the effects of vegetation type, year, and their interaction, are shown above each panel.

Relationships between mean soil and air temperature and species richness and turnover (Research question 3)

Based on analysis of logger data from six plots recorded in 2020 and 2025, we did not find any influence of mean soil or mean air temperature on species richness or species turnover. However, there was a strong positive correlation between mean air temperature and mean soil temperature (r = 0.615, p = 0.0023) (Figure 10).

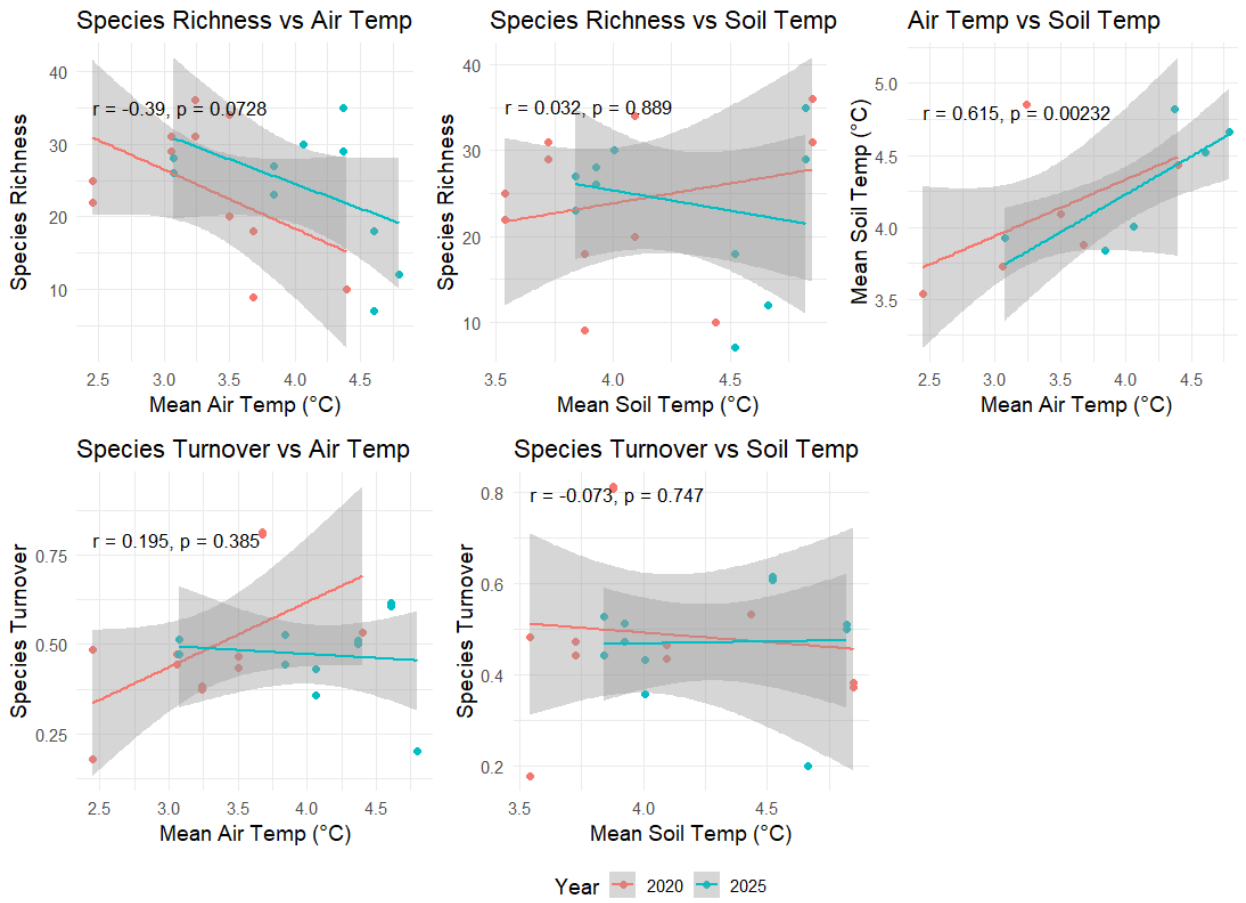

Figure 10. Relationships between air temperature (mean) and soil temperature (mean) and species richness and species turnover based on 2020 and 2025 logger data. Species richness and turnover are shown against mean air and soil temperatures obtained from loggers. Points are colored by year, with linear regression lines, 95% confidence intervals, and Pearson correlation coefficients (r) with p-values.

Discussion

Our study aimed to monitor vegetation changes along an elevational gradient in the subalpine Mulix Valley between 2019 and 2025, focusing on vegetation types, species-related values, and mean indicator values. Main results are discussed in this section according to the respective research questions.

Changes in species-related values and mean indicator values across different vegetation types

Species richness and turnover varied among the five vegetation types studied. Floodplains supported the highest species richness throughout the entire sampling period (2019–2025), whereas subalpine forests exhibited the lowest. Alpine and subalpine grasslands and heathlands showed intermediate richness, which remained relatively stable over time. In 2025, mean species richness was highest in floodplains and subalpine grasslands, yet both vegetation types showed a decline compared to 2023. Plot C10 in the floodplain exhibited markedly lower species richness, thereby reducing the overall mean richness of floodplain plots in 2025 (Figure 3). This reduction is likely due to hydrological alteration caused by the Albula River, which began partially flowing through the plot after 2023. The impact was particularly evident in the southwestern subplot. While the hydrological disturbance explains the localized decline in C10, the overall high species richness of the floodplain vegetation can be attributed to broader ecological factors. Dengler (2024) identified pH and microrelief as the major ecological factors driving high species

richness in the Preda floodplain, consistent with the shift from acidic toward base-rich soils observed in this area. Higher richness may additionally be associated with comparatively higher soil moisture levels relative to other vegetation types (Figure 7). In contrast, the reduced species richness observed in the subalpine forest plots is likely driven by low light availability at the forest floor, as dense canopy cover strongly limits the proportion of photosynthetically active radiation reaching the understory. Dormann et al. (2020) demonstrated that understorey plant species richness in temperate forests increases markedly with light transmittance, identifying light availability as the primary determinant of herb-layer diversity. Grasslands and heathlands showed moderate richness and low turnover, indicating relatively stable and well-adapted communities typical for undisturbed subalpine landscapes (Grime, 1977; Häberlin & Dengler, 2025). Additionally, natural disturbances affected other sites, such as plot A1C, where debris deposition from slope movements over the past six years has buried much of the original plot area, thereby affecting species richness in the subalpine grassland. Overall, species turnover was moderate but reached its highest values in subalpine forests, indicating greater temporal variation in species composition, while grassland communities were comparatively stable. These patterns suggest that high species richness does not necessarily correspond to high turnover or high Shannon index (Figure 3 and Figure 5). Floodplains, despite their high richness, displayed only moderate turnover, whereas subalpine forests, with lower richness, experienced pronounced compositional change (species turnover). Enhanced soil moisture, in combination with increased microsite heterogeneity and periodic disturbance, may create a greater diversity of ecological niches and facilitate species coexistence within these habitats. Further investigation is required to quantify the relative contributions of these factors to the observed richness patterns.

Cover-based diversity indices (Shannon index, Shannon evenness, and Simpson index) and mean indicator values (CSR strategies, light availability, air temperature, and soil moisture) remained largely stable throughout the six-year observation period, although differences were evident among vegetation types. While minor interannual fluctuations were detected, most of these indicators showed no consistent temporal trends. These findings suggest that short-term changes in subalpine vegetation are limited, reflecting the slow community dynamics and strong environmental filtering characteristic of alpine and subalpine ecosystems (Pauli et al., 2012; Steinbauer et al., 2018).

Differences among vegetation types in terms of species-related values and mean indicator values

Significant differences in species richness and Shannon index among vegetation types and years confirm the strong role of habitat and microclimatic conditions in shaping community structure. Significant differences in competitive and stress strategies between vegetation types are particularly noteworthy. These findings can be at least partially attributed to differences in land cover characteristics among the vegetation types (see land cover characteristics in Table 1), as soil gravel content significantly affects soil carbon and nitrogen concentrations, which in turn influence vegetation composition (De Baets et al., 2013; Meersmans et al., 2012; Qin et al., 2015). Also, the soil nutrient availability affects CSR strategies. Especially stress tolerance and competitiveness of species are affected by the environmental gradient of soil nutrient and water availability (Yu et al., 2022). Also the state of the succession can vary slightly between different sites and so the CSR strategies can thus begin to change as well as the influence of various types of disturbance on species pool in early succession which influences the strategies in ongoing succession (Buma et al., 2017; Zhang et al., 2024). A further reason for different numbers in competitiveness and stress-tolerance among vegetation types can be the elevational gradient and its influence on species composition (Haq et al., 2024).

The significant interaction between vegetation type and year for the ruderal strategy may be explained by interannual differences in disturbance intensity, as ruderal species are typically associated with disturbance regimes (Negreiros et al., 2014). This hypothesis cannot be confirmed due to the lack of information on the disturbance regimes of the plots and potential variations in cultivation practices.

Influence of soil temperature and air temperature in species richness and species turnover

Microclimatic measurements supported the expected temperature decrease with elevation. However, relationships between temperature indicators and vegetation metrics were weak. This indicates that plant community responses may be buffered by site-specific factors such as slope, shading, soil variability, or species' longevity (Zellweger et al., 2024).

Problems, limitations, and future outlooks

The quality of long-term ecological data is crucial for detecting subtle vegetation changes. The resampling and data management protocols were consistent across years, providing a reliable basis for temporal comparisons. In our field surveys, we, like other groups, encountered a wide variety of species throughout the 2019 - 2025 period, many of which appeared only sporadically. Incorrect identifications are a potential source of error that must be avoided. To minimize this, we followed the standardized EDGG subplot methodology (Dengler et al., 2016) and carefully re-examined any uncertain specimens, including determination using a microscope and standard identification literature, ensuring reliable species identifications throughout the study. This particularly concerned finds that we could not assign to a common species. By regularly consulting various assessments and carefully checking all rare species, misidentifications can be ruled out.

The method used for data cleaning is based on the method used in previous years. If the data cleaning is not documented thoroughly, the method used varies and data sets are with more entries, it would not be possible to do the time consuming manual data cleaning and it could be a relevant source of errors and influences the results (Zizka et al., 2019). By carefully determining the types and thoroughly documenting the cleaning process, errors in data cleaning can be neglected. Our dataset required relatively few taxonomic corrections, and most adjustments involved harmonizing taxonomic resolution rather than correcting misidentifications. Nevertheless, the partial loss of temperature loggers between sampling campaigns limited the continuity of microclimate data. Such logistical challenges are common in alpine fieldwork and highlight the importance of redundancy and clear metadata for maintaining data integrity in future surveys (Boch et al., 2022). The short six-year observation period also constrains the detection of long-term trends, as vegetation responses to climate change in alpine systems often unfold over decades (Pauli et al., 2012; Steinbauer et al., 2018).

Despite these limitations, the Mulix Valley transect provides a valuable long-term framework for monitoring biodiversity and microclimate interactions in subalpine ecosystems. Continued resampling of these permanent plots will be essential to assess whether the observed short-term stability persists or gives way to directional change under ongoing warming. Combining vegetation data with high-resolution microclimate modelling, soil parameters, and functional traits could help to disentangle biotic and abiotic drivers of vegetation dynamics. Moreover, linking local monitoring efforts such as this one with broader national and international initiatives, such as GLORIA or the Swiss Biodiversity Monitoring program, will enhance our ability to detect regional patterns of alpine biodiversity change and to inform conservation and management strategies in mountain environments.

Acknowledgments

We would like to take this opportunity to thank Dr. Olha Chusova, who supported us throughout the summer school and was always available to answer any questions we had afterwards. We would also like to thank our second supervisor and organizer of the Summer School Biodiversity Monitoring 2025, Prof. Dr. Jürgen Dengler, for his valuable advice and effort to ensure we can gain valuable experience and acquire knowledge during the Summer School.

References

Bates, D., Mächler, M., Bolker, B., & Walker, S. (2015). Fitting Linear Mixed-Effects Models Using lme4. Journal of Statistical Software, 67, 1–48. https://doi.org/10.18637/jss.v067.i01

Begert, M., & Frei, C. (2018). Long-term area-mean temperature series for Switzerland—Combining homogenized station data and high resolution grid data. International Journal of Climatology, 38(6), 2792–2807. https://doi.org/10.1002/joc.5460

Boch, S., Küchler, H., Küchler, M., Bedolla, A., Ecker, K. T., Graf, U. H., Moser, T., Holderegger, R., & Bergamini, A. (2022). Observer-driven pseudoturnover in vegetation monitoring is context-dependent but does not affect ecological inference. Applied Vegetation Science, 25(3), e12669. https://doi.org/10.1111/avsc.12669

Büchler, M.-O., Billeter, R., & Dengler, J. (2020). Optimal site conditions for dry grasslands of high conservation value in the canton of Zurich, Switzerland. TUEXENIA, 40, 527546. https://doi.org/10.14471/2020.40.021

Buma, B., Bisbing, S., Krapek, J., & Wright, G. (2017). A foundation of ecology rediscovered: 100 years of succession on the William S. Cooper plots in Glacier Bay, Alaska. Ecology, 98(6), 1513–1523. https://doi.org/10.1002/ecy.1848

Cuesta Núñez, J., Romero, M. A., Ocampo Reinaldo, M., González, R., Magurran, A., & Svendsen, G. M. (2023). Species turnover drives functional turnover with balanced functional nestedness in a Patagonian demersal assemblage. Journal of Sea Research, 196, 102452. https://doi.org/10.1016/j.seares.2023.102452

De Baets, S., Meersmans, J., Vanacker, V., Quine, T. A., & Van Oost, K. (2013). Spatial variability and change in soil organic carbon stocks in response to recovery following land abandonment and erosion in mountainous drylands. Soil Use and Management, 29(1), 65–76. https://doi.org/10.1111/sum.12017

Dengler, J. (2024). Report from the 5th Master Summer School “Biodiversity Monitoring”, Preda, Switzerland, 14–25 August 2023. Institute of Natural Resource Sciences (IUNR), Zurich University of Applied Sciences (ZHAW).

Dengler, J., Boch, S., Filibeck, G., Chiarucci, A., Dembicz, I., Guarino, R., Henneberg, B., Janišová, M., Marcenò, C., Naqinezhad, A., Polchaninova, N., Vassilev, K., & Biurrun, I. (2016). Assessing plant diversity and composition in grasslands across spatial scales: The standardised EDGG sampling methodology. Bulletin of the Eurasian Dry Grassland Group, 32, 13–30.

Dengler, J., Janišová, M., Török, P., & Wellstein, C. (2014). Biodiversity of Palaearctic grasslands: A synthesis. Agriculture, Ecosystems & Environment, 182, 1–14. https://doi.org/10.1016/j.agee.2013.12.015

Dolezal, J., Dvorsky, M., Kopecky, M., Liancourt, P., Hiiesalu, I., Macek, M., Altman, J., Chlumska, Z., Rehakova, K., Capkova, K., Borovec, J., Mudrak, O., Wild, J., & Schweingruber, F. (2016). Vegetation dynamics at the upper elevational limit of vascular plants in Himalaya. Scientific Reports, 6(1), 24881. https://doi.org/10.1038/srep24881

Elliott, T., Thompson, A., Klein, A., Albert, C., Eisenhauer, N., Jansen, F., Schneider, A., Sommer, M., Straka, T., Settele, J., Sporbert, M., Tanneberger, F., & Mupepele, A. (2023). Abandoning grassland management negatively influences plant but not bird or insect biodiversity in Europe. Conservation Science and Practice, 5(10), e13008. https://doi.org/10.1111/csp2.13008

Federal Office of Topography swisstopo. (2024, January 11). Swiss Map Raster 10. Swisstopo.Admin.Ch. https://www.swisstopo.admin.ch/de/landeskarte-swiss-map-raster-10#Swiss-Map-Raster-10---Download

Ferreira, J. D. (2018). The drivers of species turnover (p. 26) [Introductury Research Essay]. Sverige Landbruksuniversitet SLU.

Gottfried, M., Pauli, H., Futschik, A., Akhalkatsi, M., Barančok, P., Benito Alonso, J. L., Coldea, G., Dick, J., Erschbamer, B., Fernández Calzado, M. R., Kazakis, G., Krajči, J., Larsson, P., Mallaun, M., Michelsen, O., Moiseev, D., Moiseev, P., Molau, U., Merzouki, A., … Grabherr, G. (2012). Continent-wide response of mountain vegetation to climate change. Nature Climate Change, 2(2), 111–115. https://doi.org/10.1038/nclimate1329

Greig-Smith, P. (1983). Quantitative Plant Ecology. University of California Press.

Grime, J. P. (1977). Evidence for the Existence of Three Primary Strategies in Plants and Its Relevance to Ecological and Evolutionary Theory. The American Naturalist, 111(982), 1169–1194.

Häberlin, K. E. R., & Dengler, J. (2025). Recent biodiversity changes in grasslands across elevational bands in Switzerland. Basic and Applied Ecology, 87, 29–37. https://doi.org/10.1016/j.baae.2025.05.003

Haq, A., Ullah, H., Ullah, I., Badshah, L., & Ahmad, S. (2024). Vegetation Dynamics along the Altitudinal Gradient. https://doi.org/10.5772/intechopen.114309

Ioan, S., Roseo, F., & Brambilla, M. (2025). Mountain ecosystem services under a changing climate: A global perspective. Ecosystem Services, 73, 101732. https://doi.org/10.1016/j.ecoser.2025.101732

IPBES. (2019, May 4). Global assessment report on biodiversity and ecosystem services of the Intergovernmental Science-Policy Platform on Biodiversity and Ecosystem Services (E. Brondizio, S. Diaz, J. Settele, & H. T. Ngo, Eds.; Version 1). IPBES secretariat. https://doi.org/10.5281/ZENODO.3831673

Ivanova, N., & Zolotova, E. (2023). Landolt Indicator Values in Modern Research: A Review. Sustainability, 15, 9618. https://doi.org/10.3390/su15129618

Koleff, P., & Gaston, K. J. (2002). The relationships between local and regional species richness and spatial turnover. Global Ecology and Biogeography, 11(5), 363–375. https://doi.org/10.1046/j.1466-822x.2002.00302.x

Körner, C. (2004). Mountain Biodiversity, Its Causes and Function. AMBIO: A Journal of the Human Environment, 33(sp13), 11. https://doi.org/10.1007/0044-7447-33.sp13.11

Körner, C. (2007). The use of 'altitude' in ecological research. Trends in Ecology & Evolution, 22(11), 569–574. https://doi.org/10.1016/j.tree.2007.09.006

Kotlarski, S., Gobiet, A., Morin, S., Olefs, M., Rajczak, J., & Samacoïts, R. (2023). 21st Century alpine climate change. Climate Dynamics, 60(1–2), 65–86. https://doi.org/10.1007/s00382-022-06303-3

Küchler, M. (2024). VEGEDAZ (Version Version 2024) [Computer software]. https://www.wsl.ch/en/services-produkte/vegedaz/

Meersmans, J., Martin, M. P., De Ridder, F., Lacarce, E., Wetterlind, J., De Baets, S., Le Bas, C., Louis, B. P., Orton, T. G., Bispo, A., & Arrouays, D. (2012). A novel soil organic C model using climate, soil type and management data at the national scale in France. Agronomy for Sustainable Development, 32(4), 873–888. https://doi.org/10.1007/s13593-012-0085-x

Müller-Dombois, D., & Ellenberg, H. (1974). Aims and Methods of Vegetation Ecology. https://www.researchgate.net/publication/259466952_Aims_and_Methods_of_Vegetation_Ecology

Negreiros, D., Le Stradic, S., Fernandes, G. W., & Rennó, H. C. (2014). CSR analysis of plant functional types in highly diverse tropical grasslands of harsh environments. Plant Ecology, 215(4), 379–388. https://doi.org/10.1007/s11258-014-0302-6

Pauli, H., Gottfried, M., Dullinger, S., Abdaladze, O., Akhalkatsi, M., Alonso, J. L. B., Coldea, G., Dick, J., Erschbamer, B., Calzado, R. F., Ghosn, D., Holten, J. I., Kanka, R., Kazakis, G., Kollár, J., Larsson, P., Moiseev, P., Moiseev, D., Molau, U., … Grabherr, G. (2012). Recent Plant Diversity Changes on Europe's Mountain Summits. Science, 336(6079), 353–355. https://doi.org/10.1126/science.1219033

Pepin, N. C., Arnone, E., Gobiet, A., Haslinger, K., Kotlarski, S., Notarnicola, C., Palazzi, E., Seibert, P., Serafin, S., Schöner, W., Terzago, S., Thornton, J. M., Vuille, M., & Adler, C. (2022). Climate Changes and Their Elevational Patterns in the Mountains of the World. Reviews of Geophysics, 60(1), e2020RG000730. https://doi.org/10.1029/2020RG000730

Pielou, E. C. (1966). The measurement of diversity in different types of biological collections. Journal of Theoretical Biology, 13, 131–144. https://doi.org/10.1016/0022-5193(66)90013-0

Qin, Y., Yi, S., Chen, J., Ren, S., & Ding, Y. (2015). Effects of gravel on soil and vegetation properties of alpine grassland on the Qinghai-Tibetan plateau. Ecological Engineering, 74, 351–355. https://doi.org/10.1016/j.ecoleng.2014.10.008

Shannon, C. E. (1948). A mathematical theory of communication. The Bell System Technical Journal, 27(3), 379–423. https://doi.org/10.1002/j.1538-7305.1948.tb01338.x

Simpson, E. H. (1949). Measurement of diversity. Nature, 163, 688.

Spörri, M., El Benni, N., Mack, G., & Finger, R. (2023). Spatio-temporal dynamics of grassland use intensity in Switzerland. Regional Environmental Change, 23(1), 23. https://doi.org/10.1007/s10113-022-02023-w

Steinbauer, M. J., Grytnes, J.-A., Jurasinski, G., Kulonen, A., Lenoir, J., Pauli, H., Rixen, C., Winkler, M., Bardy-Durchhalter, M., Barni, E., Bjorkman, A. D., Breiner, F. T., Burg, S., Czortek, P., Dawes, M. A., Delimat, A., Dullinger, S., Erschbamer, B., Felde, V. A., … Wipf, S. (2018). Accelerated increase in plant species richness on mountain summits is linked to warming. Nature, 556(7700), 231–234. https://doi.org/10.1038/s41586-018-0005-6

Theurillat, J.-P., & Guisan, A. (2001). Potential Impact of Climate Change on Vegetation in the European Alps: A Review. Climatic Change, 50(1–2), 77–109. https://doi.org/10.1023/A:1010632015572

Thukral, A. (2017). A review on measurement of Alpha diversity in biology. Agricultural Research Journal, 54, 1. https://doi.org/10.5958/2395-146X.2017.00001.1

Vetaas, O. R. (2021). Mountain biodiversity and elevational gradients. Frontiers of Biogeography, 13(3). https://doi.org/10.21425/F5FBG54146

Weber, D., Schwieder, M., Ritter, L., Koch, T., Psomas, A., Huber, N., Ginzler, C., & Boch, S. (2024). Grassland-use intensity maps for Switzerland based on satellite time series: Challenges and opportunities for ecological applications. Remote Sensing in Ecology and Conservation, 10(3), 312–327. https://doi.org/10.1002/rse2.372

Wickham, H., Vaughan, D., Girlich, M., Ushey, K., Software, P., & PBC. (2024). tidyr: Tidy Messy Data (Version 1.3.1) [Computer software]. https://cran.r-project.org/web/packages/tidyr/index.html

Wild, J., Kopecký, M., Macek, M., Šanda, M., Jankovec, J., & Haase, T. (2019). Climate at ecologically relevant scales: A new temperature and soil moisture logger for long-term microclimate measurement. Agricultural and Forest Meteorology, 268, 40–47. https://doi.org/10.1016/j.agrformet.2018.12.018

Yu, J., Hou, G., Zhou, T., Shi, P., Zong, N., & Sun, J. (2022). Variation of plant CSR strategies across a precipitation gradient in the alpine grasslands on the northern Tibet Plateau. The Science of the Total Environment, 838(Pt 3), 156512. https://doi.org/10.1016/j.scitotenv.2022.156512

Zellweger, F., Sulmoni, E., Malle, J. T., Baltensweiler, A., Jonas, T., Zimmermann, N. E., Ginzler, C., Karger, D. N., De Frenne, P., Frey, D., & Webster, C. (2024). Microclimate mapping using novel radiative transfer modelling. Biogeosciences, 21(2), 605–623. https://doi.org/10.5194/bg-21-605-2024

Zhang, Y., Meiners, S. J., Meng, Y., Yao, Q., Guo, K., Guo, W.-Y., & Li, S. (2024). Temporal dynamics of Grime's CSR strategies in plant communities during 60 years of succession. Ecology Letters, 27(6), e14446. https://doi.org/10.1111/ele.14446

Zizka, A., Silvestro, D., Andermann, T., Azevedo, J., Duarte Ritter, C., Edler, D., Farooq, H., Herdean, A., Ariza, M., Scharn, R., Svantesson, S., Wengström, N., Zizka, V., & Antonelli, A. (2019). CoordinateCleaner: Standardized cleaning of occurrence records from biological collection databases. Methods in Ecology and Evolution, 10(5), 744–751. https://doi.org/10.1111/2041-210X.13152

Appendices

Appendix 1. Species occurrence results

Table 1. The 10 most common species in all the 126 subplots sampled from 2019 - 2025.

Vegetation species	Frequency of occurrence in a subplot	Maximum % of cover in a subplot
Vaccinium myrtillus	76 (60%)	64
Homogyne alpina	75 (59.5%)	25
Potentilla aurea	65 (51.5%)	17
Campanula scheuchzeri	63 (50%)	3
Polygonum viviparum	63 (50%)	3,4
Vaccinium vitis-idaea	61 (48.4%)	30
Leontodon helveticus	60 (47.6%)	12
Anthoxanthum odoratum aggr.	59 (46.8%)	25
Carex sempervirens	57 (45.2%)	28
Ranunculus montanus aggr.	56 (44.4%)	5

Appendix 2. Results of Linear Mixed-Effects Models (LMM)

Table 2. Results of Linear Mixed-Effects Models Testing Differences Among Vegetation Types, Years, and Their Interaction for Species-Related and Mean Indicator Values

Response Variable	Independent variables(factors)	Sum Sq	Mean Sq	NumDF	DenDF	F Value	Pr(>F)	R^2 Mar.	R^2 Cond.
Species richness	Vegetation type	974.89	243.72	4	0.02	14.96	0.0008***	0.696	0.899
	Year	274.58	68.64	4	80.24	4.21	0.0003***		
	Vegetation type × Year	458.58	28.66	16	80.26	1.75	0.0519		
	Residuals	1341.21	13.68		98.0				
Species turnover	Vegetation type	0.085	0.021	4	7.87	2.37	0.139	0.322	0.568
	Year	0.069	0.023	3	59.22	2.58	0.061		
	Vegetation type × Year	0.142	0.011	12	59.31	1.32	0.227		
	Residuals	0.608	0.007		77.0				
Shannon Index	Vegetation type	1.123	0.280	4	7.926	4.34	0.037*	0.464	0.751
	Year	0.649	0.162	4	80.95	2.51	0.047*		
	Vegetation type × Year	1.091	0.068	16	81.01	1.054	0.411		
	Residuals	5.736	0.058		98.0				
Shannon evenness	Vegetation type	0.006	0.001	4	7.95	0.235	0.910	0.104	0.681
	Year	0.061	0.015	4	81.16	2.34	0.061		
	Vegetation type × Year	0.050	0.003	16	81.24	0.487	0.946		
	Residuals	0.595	0.006		98.00				
Simpson index	Vegetation type	0.048	0.012	4	7.933	1.425	0.310	0.235	0.675
	Year	0.029	0.007	4	92.96	0.868	0.486		
	Vegetation type × Year	0.040	0.002	16	92.97	0.301	0.995		
	Residuals	0.794	0.008		98.00				
Competitor	Vegetation type	0.394	0.098	4	7.98	13.36	0.0012***	0.657	0.872
	Year	0.039	0.009	4	79.82	1.33	0.263		
	Vegetation type × Year	0.172	0.010	16	79.84	1.46	0.135		
	Residuals	0.611	0.006		98.00				
Stress-tolerator	Vegetation type	0.323	0.080	4	7.87	17.49	0.0005***	0.665	0.836
	Year	0.030	0.007	4	80.13	1.66	0.165		
	Vegetation type × Year	0.109	0.006	16	80.16	1.48	0.126		
	Residuals	0.387	0.003		98.00				

Response Variable	Independent variables(factors)	Sum Sq	Mean Sq	NumDF	DenDF	F Value	Pr(>F)	R^2 Mar.	R^2 Cond.
Ruderal	Vegetation type	0.016	0.004	4	7.98	1.36	0.326	0.278	0.876
	Year	0.014	0.003	4	79.62	1.17	0.326		
	Vegetation type × Year	0.109	0.006	16	79.65	2.22	0.010*		
	Residuals	0.258	0.002		98.00				
Mean air temperature	Vegetation type	0.912	0.228	4	7.97	36.00	0.00003***	0.872	0.954
	Year	0.046	0.0117	4	80.41	1.852	0.126		
	Vegetation type × Year	0.182	0.0113	16	80.45	1.795	0.045*		
	Residuals	0.537	0.005		98.0				
Mean light	Vegetation type	0.952	0.238	4	7.99	20.08	0.0003***	0.817	0.959
	Year	0.043	0.010	4	80.16	0.908	0.463		
	Vegetation type × Year	0.123	0.007	16	80.19	0.650	0.832		
	Residuals	0.986	0.010		98.0				
Mean soil moisture	Vegetation type	0.008	0.002	4	7.98	0.549	0.705	0.164	0.888
	Year	0.016	0.004	4	79.83	1.065	0.379		
	Vegetation type × Year	0.144	0.009	16	79.86	2.308	0.007**		
	Residuals	0.327	0.003		98.0				

Significance codes: * $p < 0.05$, ** $p < 0.01$, *** $p < 0.001$.

Pr(>F) = The p-value corresponding to the F-statistic

Sum Sq = Sum of squares (Total variation in the response variable explained by each independent variable (factor))

Mean Sq = Mean square = Sum Sq / NumDF

NumDF = Numerator degrees of freedom = The number of categories or levels minus one for each factor

DenDF = Denominator degrees of freedom = The degrees of freedom for the error term (residuals)

The F-Value (F-statistic) or F = Mean Sq (independent variables or effect) / Mean Sq (Residuals)

R^2 Mar. = Marginal R-squared = The proportion of variance explained by fixed effects only (e.g., vegetation type, year).

R^2 Cond. = Conditional R-squared = The proportion of variance explained by both fixed and random effects (if any).

Scale dependence of plant species richness and diversity indices in European alpine and lowland vegetation communities

Katharina Genucchi, Svitlana Kyiak, Anders Larsen, Felix Vissing, Anna Wiewiorowska

Abstract

Biodiversity metrics are known to be scale dependent, with species richness increasing reliably with sampling area. However it remains understudied how diversity and evenness indices respond to the same spatial scaling of sampling area. The aim of this study is to test how various biodiversity indices scale across different grain sizes and whether these patterns are consistent across different ecosystems. We analysed vascular plant communities from diverse alpine and subalpine habitats in the Alps, Preda, Switzerland and from the semi-natural lowland grasslands near Białowieża, Poland. Data was collected using standardized EDGG nested-plot sampling (Dengler et al., 2016) in 3 plot sizes 0.1, 1 and 10 m² recording all species based on shoot presence. We calculated a range of biodiversity indices and modelled their responses to plot size using generalised linear mixed models. Our study reveals that species richness, Simpson's diversity index(1-D), inverse Simpson index(1/D) and Shannon index (H') all significantly increase with plot size for Preda and Bialowieża sites, however Pielou's evenness (J') only scaled significantly in Preda. Although all diversity metrics responded to plot size, fixed effects of area explained little variation, whereas random effects reflecting local environmental heterogeneity accounted for most of the variance. Species-area relationships (SAR) followed power law scaling for Preda, indicated by higher local z-values from 0.1 to 1 m² than from 1 to 10 m², however this was not the case in Białowieża where z-values were similar between all sizes. Our results demonstrate that diversity indices differ in their scale dependence and that one therefore, should be cautious when comparing across grain sizes. Simpson's diversity index was the least affected by grain size and thus seems to be the most robust biodiversity metric when comparing between plot sizes.

Keywords

Biodiversity, biodiversity indices, evenness, plot size, scale dependence, species-area relationship, vegetation monitoring

Introduction

Biodiversity is declining globally, as consistently demonstrated, and acknowledged in scientific research (Ceballos et al., 2015; Dirzo & Raven, 2003; Widmer et al., 2025). It is essential to measure biodiversity in order to monitor decline and change and to understand the impact of both natural and anthropogenic ecological factors on biodiversity (Chase & Knight, 2013; Reutimann et al., 2023; Widmer et al., 2025). It is also important for making informed and sustainable management decisions to mitigate the decline (Buzhdygan et al., 2025; Rahmanian et al., 2019, 2023) and for comparing biodiversity of different habitats and regions (Dembicz et al., 2021; Moradi et al., 2020).

For a comprehensive understanding of biodiversity, various measures must be taken into account, as one alone does not adequately describe biodiversity (Bonar et al., 2011; Gotelli & Chao, 2013; Wilsey et al., 2005). Species richness weights all species equally, regardless of their frequency (Bonar et al., 2011; Gotelli & Chao, 2013) while evenness describes how evenly individuals are distributed across the different species (Smith & Wilson, 1996) and diversity combines both richness and evenness (Maurer & McGill, 2011).

It is also important to consider that biodiversity patterns are scale dependent (Kallimanis et al., 2008; Storch et al., 2007). Patterns and processes in nature often depend on the scale of observation, with different mechanisms acting at different scales (Legendre & Legendre, 2012). Therefore, conclusions drawn at one spatial scale cannot necessarily be applied to others, requiring careful consideration when working across scales. Nevertheless, many biodiversity studies neglect the scale dependency by focusing on one single plot size and leaving the scale-dependent mechanisms of biodiversity drivers largely unresolved (Buzhdygan et al., 2025; Dengler, 2009). This limited understanding of how biodiversity patterns and processes change across spatial scales reduces the applicability of local findings to broader ecological and conservation contexts (Barton et al., 2013; Chase et al., 2019; Ladouceur et al., 2023).

The scale dependence of species richness is well researched (Chase et al., 2018). The Species Area Relationship (SAR) is strongly scale dependent and is overall best described by the power law. For most cases a constant z-value can be assumed if species were recorded by shoot presence (Dembicz et al., 2021; Dengler et al., 2020; Zhang et al., 2021). Therefore, species richness from plots of different sizes is not directly comparable (Portier et al., 2022). Unfortunately, up until now very little is known about how diversity and evenness indices respond to spatial scaling, representing an important gap for comparable biodiversity assessments across habitats and studies.

The aim of this study is to investigate how different measurements of taxonomic plant diversity vary with spatial scale and environmental context across contrasting alpine and lowland ecosystems. Using standardised nested-plot data (0.1, 1 and 10 m^2) from Preda (Switzerland) and Białowieża (Poland), we assessed patterns in species richness and diversity indices (Shannon index, Simpson's diversity index (1-D), inverse Simpson index (1/D), and Pielou's evenness). We did this to explore scale-dependent changes in richness and evenness and compare these changes between regions that differ in climate and elevation.

We address the following questions:

1. How do species richness and diversity indices change with increasing plot size, and do they reveal scale-dependent shifts in community evenness?
2. Are spatial diversity patterns consistent between alpine and lowland regions, or do environmental gradients lead to distinct scaling relationships?

We expect all biodiversity metrics to increase with grain size, but with varying sensitivity depending on how strongly they weigh evenness or dominance. Shannon and inverse Simpson indices are expected to level off more gradually than species richness, reflecting differences in species' relative abundances. Pielou's evenness is expected to slightly decline as less abundant plants appear with increasing grain size.

Methods

Study sites

Our study uses data from 2 regions, representing alpine and lowland regions.

Alpine study area: Data was collected around Preda (Canton of Grisons, Eastern Switzerland) from 18-25 August 2025. Our plots were located around the Sonnenhof field station in Preda and in the nearby valleys Val Zavretta (base-rich bedrock) and Val Mulix (acidic bedrock). The area comprises alpine and subalpine vegetation types, including grasslands, heathlands, wetlands, forest patches, and open scree. Our plots spanned an elevational gradient from approximately 1700 to 2600 m a.s.l., covering a wide range of site conditions from floodplains and scree vegetation. In total, we gathered data from 42 nested plots (totalling 126 subplots) across this site (Figure 1.).

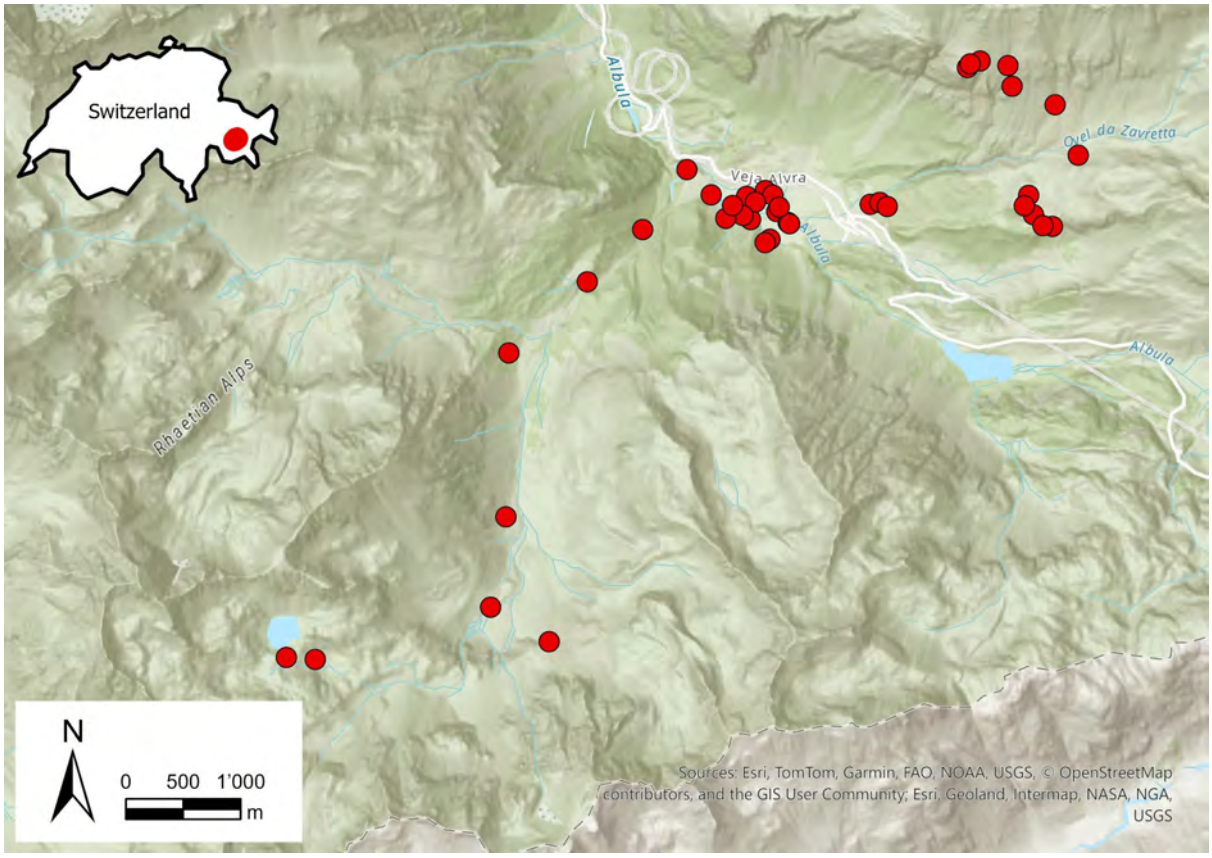

Figure 1. Sampling area around Preda (Canton of Grisons, Switzerland) in the Albula Valley. Val Mulix is in the Southwest, Val Zavretta in the Northeast of Preda. The red dots indicate a nested plot each.

Lowland study area: The lowland grassland data used in our study was collected during the 4th & 6th Summer School "Biodiversity Monitoring" held near the village of Białowieża in the Podlaskie Voivodeship, eastern Poland in August 2022 and 2024. The plots were situated in semi-natural grasslands at the edge of the Białowieża National Park, a UNESCO World Heritage Site that represents the last remaining temperate lowland primeval forest in Europe (Falinski, 2012; UNESCO World Heritage Convention, 2025). The surrounding landscape consists of traditionally managed and gradually abandoned meadows, interspersed with shrub patches and forest edges, reflecting long-term transitions in land use (Dembicz & Dengler, 2023). In total, 17 permanent triplets (57 nested plots, totalling 171 subplots) were surveyed

(Figure 2.), each representing a gradient in management intensity from regularly mown to recently abandoned and long-term abandoned grasslands undergoing woody encroachment (Dembicz & Dengler, 2023, 2025).

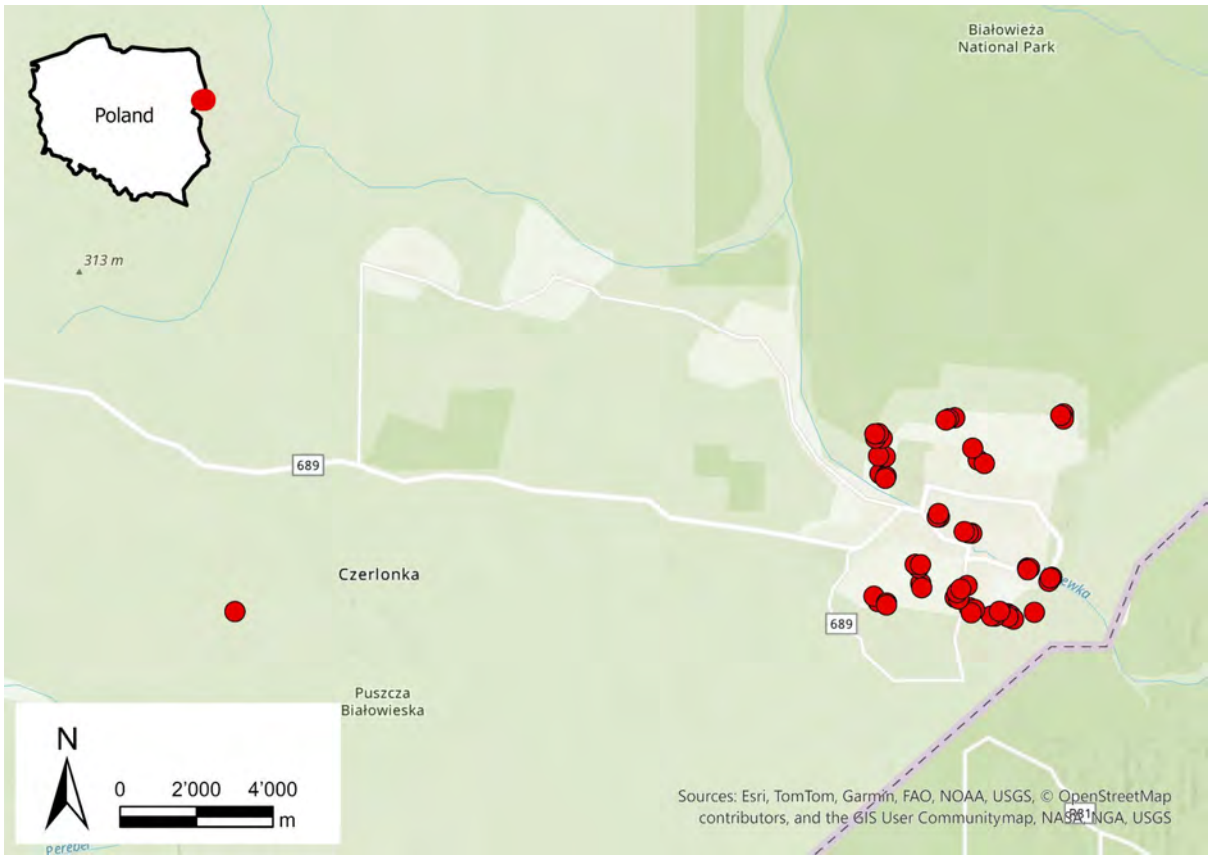

Figure 2. Sampling area around Białowieża (Podlaskie Voivodeship, Poland). The red dots indicate a nested plot each. Note that the dots that are very close together form a triplet.

Field sampling

For the sampling in Preda we used a reduced version of the standardised EDGG nested sampling methodology (Dengler et al., 2016) with subplot sizes of 0.1, 1 and 10 m², placing the smaller subplots in the north-west corner of the corresponding 10 m² plot. We used FlorApp (Info Flora, 2025) to record the shoot presence of all vascular plants and estimated the percentage cover per species in all subplots (Dengler et al. 2016). To enable resampling in future surveys, north-west corners were georeferenced with GPS and marked by burying a magnet for long-term monitoring.

In Białowieża, plots were surveyed using the same nested design and protocol as in Preda (Dengler et al., 2016). Each site formed a triplet of grasslands under different management (mown, recently abandoned, woody encroached). Vegetation and soil data were recorded with identical procedures, ensuring full comparability between regions (Dembicz & Dengler, 2023).

Data analysis

We carried out all statistical analyses in R version 4.4.0 (R Core Team, 2024).

We calculated species richness as the number of taxa with non-zero cover values per plot. We calculated diversity indices using the vegan package (Oksanen et al., 2025), including the Shannon index (H'), Simpson's diversity index (1-D), inverse Simpson index (1/D) and Pielou's evenness (J' = H' / log S).

We fitted models with *glmmTMB* (Brooks et al., 2017) including plot as a random intercept in Preda and triplet/plot as a random intercept in Białowieża to account for the nested sampling design and plot size as a fixed effect in both locations. We examined model residuals for overdispersion, outliers and overall fit using *DHARMa* (Hartig et al., 2024).

We analysed each index separately to test for differences among plot sizes (0.1, 1 and 10 m²). We modeled richness with poisson distribution. We modeled Shannon and inverse Simpson indices values with Gaussian GLMMs, as their distributions were approximately normal. Simpson's diversity index, bounded between 0 and 1, was analysed using beta regression (family = beta_family). We tested if the model is a better fit after applying the Smithson–Verkuilen transformation $(y \times (N - 1) + 0.5) / N$ to correct boundary values or with zero-inflation accounted for. We chose the models with zero-inflation as they provided better AIC values. Pielou's evenness was also analysed using beta regression, but without transformation. The zeros in Pielou's evenness model were removed. Model fit was evaluated using DHARMa residual diagnostics. We performed pairwise post-hoc comparisons between plot sizes using *emmeans* (Lenth et al., 2025) with Tukey correction for multiple testing.

To evaluate the species–area relationship (SAR), we calculated local z-values according to Zhang et al. (2021) for two grain sizes and then used a paired t-test to check if there is any significant difference in z-values among grain sizes.

Results

Change in biodiversity indices with changing plot size in Preda

In Preda all biodiversity metrics changed with increasing plot sizes (Figure 3.). For species richness the estimated marginal means increased from 9.52 (95% CI [7.83, 11.6]) in 0.1 m^2 plots, to 16.36 (95% CI [13.58, 19.7]) in 1 m^2 plots and to 24.83 (95% CI [20.69, 29.8]) in 10 m^2 plots. Pairwise Tukey-adjusted comparisons indicated that all of the plot sizes differed significantly ($p < 0.0001$) (Figure 3.A). For Simpson's diversity index the estimated marginal means were: 0.686 for 0.1 m^2 plots (95% CI [0.627, 0.739]), 0.728 for 1 m^2 plots (95% CI [0.673, 0.777]) and 0.776 for 10 m^2 plots (95% CI [0.726, 0.820]). There was a significant increase in index value between 0.1 and 10 m^2 plots (Tukey adjusted $p<0.0001$) and 1 and 10 m^2 plots (Tukey adjusted $p=0.025$). However, there were no significant differences between plot sizes of 0.1 and 1 m^2 (Tukey adjusted $p=0.089$) (Figure 3.B). For Shannon index the estimated marginal means increased from 1.49 (95% CI [1.32, 1.66]) in 0.1 m^2 plots, to 1.78 (95% CI [1.60, 1.95]) in 1 m^2 plots and to 1.94 (95% CI [1.77, 2.11]) in 10 m^2 plots. All pairwise Tukey-adjusted comparisons showed that the differences are significant ($p < 0.0001$ for difference between 0.1 m^2 and other plot sizes, $p=0.025$ for difference between 1 and 10 m^2 plots) (Figure 3.C). For inverse Simpson index the estimated marginal means were: 4.01 for 0.1 m^2 plots (95% CI [3.31, 4.71]), 4.58 for 1 m^2 plots (95% CI [3.88, 5.27]) and 5.40 for 10 m^2 plots (95% CI [4.70, 6.10]). There was a significant increase in index value between 0.1 and 10 m^2 plots (Tukey adjusted $p<0.0001$) and 1 and 10 m^2 plots (Tukey adjusted $p=0.017$). However, there were no significant differences between plot sizes of 0.1 and 1 m^2 (Tukey adjusted $p=0.143$) (Figure 3.D). For Pielou's evenness there was significant decrease in estimated marginal means between 0.1 m^2 (0.698, 95% CI [0.641, 0.732]) and other plot sizes (1 m^2: 0.632, 95% CI [0.583, 0.678], 10 m^2: 0.603, 95% CI

[0.553,0.652], Tukey adjusted p=0.028 for difference between 0.1 m^2 and 1 m^2 and p=0.0005 for difference between 0.1 m^2 and 10 m^2). There were no significant differences in evenness value between 1 and 10 m^2 (Tukey adjusted p=0.422) (Figure 3.E).

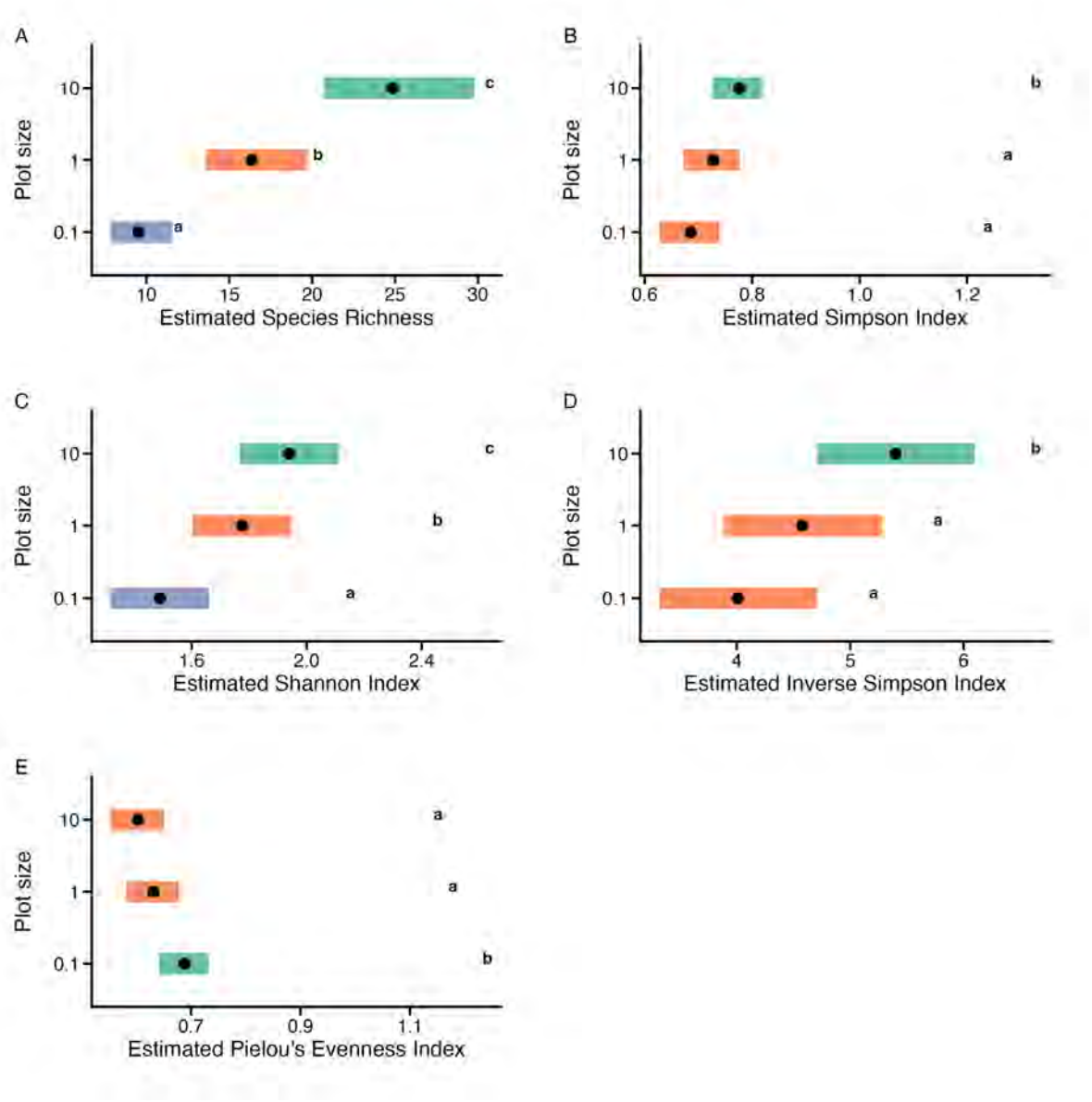

Figure 3. Estimated marginal means (± 95% CI) for each of the biodiversity metric models in Preda, with letters indicating statistically different groups from post-hoc pairwise comparisons. A - Plot size effect on species richness, B - Plot size effect on Simpson's diversity index, C- Plot size effect on Shannon index, D - Plot size effect on inverse Simpson index, E - Plot size effect on Pielou's evenness.

Even though all models showed significant differences between plot sizes, they differed in how much of the variance was explained by the fixed effect (plot size). The species richness model explained a moderate part of the variance through fixed effect (R^2m = 0.296). The model for Simpson's diversity index explained a very low part of the variance through fixed effect (R^2m = 0.008). The models for the other metrics explained a low part of the variance through fixed effect (Table 1).

Table 1. Conditional and marginal R^2 values for all mixed-effects models for biodiversity metrics in Preda

Metric	Conditional R^2	Marginal R^2
Species richness (S)	0.907	0.296
Simpson's diversity index (1-D)	0.131	0.008
Shannon index (H')	0.768	0.097
Inverse Simpson index (1/D)	0.662	0.058
Pielou's evenness (J')	0.925	0.076

Change in biodiversity indices with changing plot size in Białowieża

In Białowieża all of the biodiversity metrics, except Pielou's evenness, increased with increasing plot sizes (Figure 4.). For species richness the estimated marginal means increased from 9.57 (95% CI [7.97, 11.5]) in 0.1 m^2 plots, to 14.46 (95% CI [12.11, 17.3]) in 1 m^2 plots and 23.28 (95% CI [19.59, 27.7]) in 10 m^2 plots. Pairwise Tukey-adjusted comparisons indicated that all plot sizes differed significantly ($p < 0.0001$) (Figure 4.A). For Simpson's diversity index the estimated marginal means increased from 0.679 (95% CI [0.625, 0.729]) in 0.1 m^2 plots, to 0.749 (95% CI [0.701, 0.791]) in 1 m^2 plots and 0.805 (95% CI [0.763, 0.841]) in 10 m^2 plots. Pairwise Tukey-adjusted comparisons indicated that all plot sizes differed significantly ($p \leq 0.0001$) (Figure 4.B). For Shannon index the estimated marginal means increased from 1.49 (95% CI [1.31, 1.68]) in 0.1 m^2 plots, to 1.80 (95% CI [1.62, 1.90]) in 1 m^2 plots and 2.09 (95% CI [1.91, 2.28]) in 10 m^2 plots. Pairwise Tukey-adjusted comparisons indicated that all plot sizes differed significantly ($p < 0.0001$) (Figure 4.C). For inverse Simpson index the estimated marginal means increased from 3.89 (95% CI [2.95, 4.82]) in 0.1 m^2 plot, to 4.92 (95% CI [3.98, 5.85]) in 1 m^2 plots and 6.22 (95% CI [5.29, 7.16]) in 10 m^2 plots. Pairwise Tukey-adjusted comparisons indicated that all plot sizes differed significantly ($p \leq 0.0002$) (Figure 4.D). For Pielou's evenness there was no significant difference between the plot sizes (all Tukey adjusted $p>0.8$) (Figure 4.E).

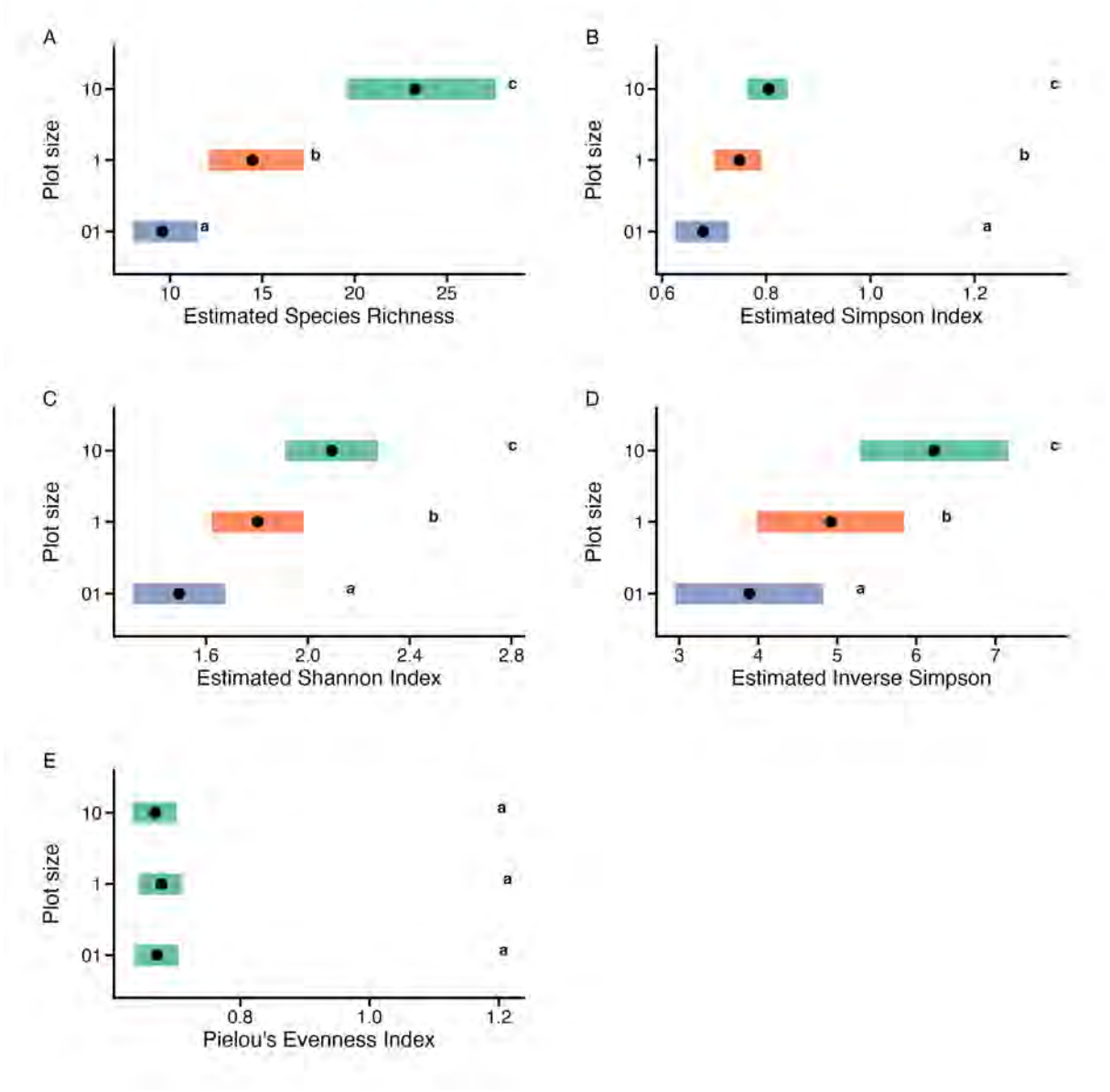

Figure 4. Estimated marginal means (± 95% CI) for each of the biodiversity metric models in Białowieża, with letters indicating statistically different groups from post-hoc pairwise comparisons. A - Plot size effect on species richness, B - Plot size effect on Simpson's diversity index, C - Plot size effect on Shannon index, D - Plot size effect on inverse Simpson index, E - Plot size effect on Pielou's evenness.

Even though all models, except the Pielou's evenness model, showed significant differences between plot sizes, they differed in how much of the variance was explained by the fixed effect (plot size). The species richness model (R^2m = 0.38), Shannon index model (R^2m = 0.174) and inverse Simpson index model (R^2m = 0.112) explained a moderate part of the variance through fixed effect. The model for Simpson's diversity index explained a very low part of the variance through fixed effect (R^2m = 0.016) (Table 2).

Table 2. Conditional and marginal R^2 values for all mixed-effects models for biodiversity metrics in Białowieża

Metric	Conditional R^2	Marginal R^2
Species richness (S)	0.837	0.38
Simpson's diversity index (1-D)	0.105	0.016
Shannon index (H')	0.849	0.174
Inverse Simpson index (1/D)	0.773	0.112
Pielou's evenness (J')	insignificant	insignificant

Local z-values in Preda and in Białowieża

Local mean z-values in Preda were higher between 0.1 and 1 m^2 plots (0.268 ± 0.149) than between 1 and 10 m^2 plots (0.149 ± 0.103; paired t-test: t = -4.0309, df = 41, p = 0.0002) (Figure 5). Indicating that the scaling function for species richness is a power function. In Białowieża this pattern was not observed. The difference between 0.1 and 1 m^2 plots and between 1 and 10 m^2 plots was not statistically significant (paired t-test: t = 0.8583, df = 56, p = 0.3944).

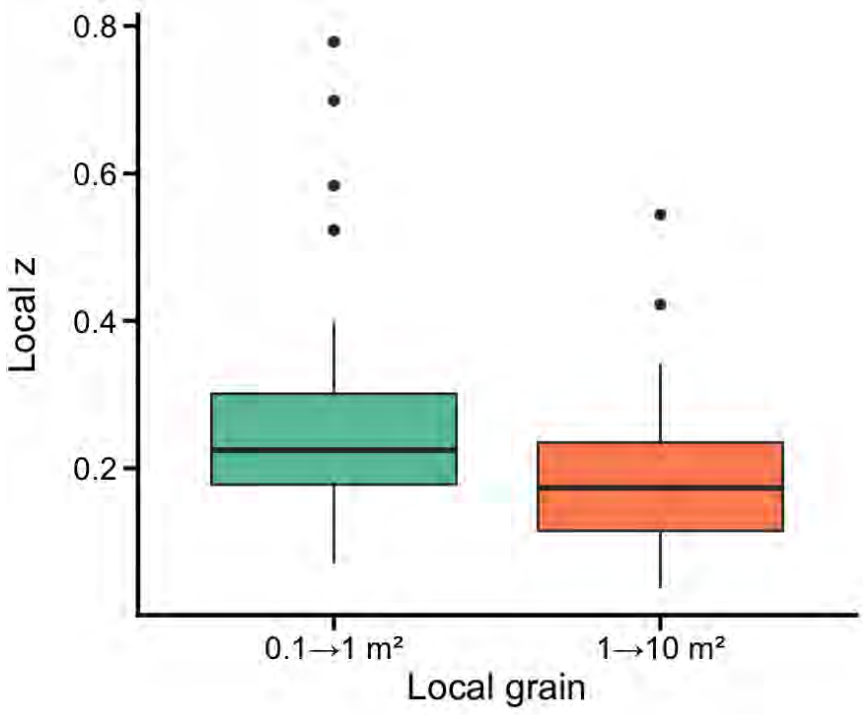

Figure 5. Local z-values for two grain sizes, representing the difference between the largest and medium plots and the difference between medium and smallest plots in Preda.

Discussion

Overall tendencies

Our results for species richness are well aligned with existing research regarding species-area relationships. Our data shows a significant growth of species richness with area, which was already

described by Storch et al. (2007). The mean z-value in both study sites is in line with expected results for vascular plants in palearctic grasslands, 0.26 +- 0.11 (Dengler et al., 2020).

Site differences between Białowieża and Preda

In Preda, the species–area relationship followed the expected power-law form described by Arrhenius (1921), with a significant difference between local z-values for different grain sizes indicating that richness increased with area as predicted by power law. This also aligns with the view that heterogeneity in substrate, slope, and soil depth enhances fine-scale taxonomic turnover in alpine grasslands (Blank-Pachlatko et al., 2019; Häberlin & Dengler, 2025). The largest difference in species richness from 0.1 m² to 1 m² indicates that the majority of species turnover occurs within the smallest spatial interval. This pattern aligns with the ecospace framework, which predicts diminishing returns of area-based sampling once major abiotic gradients are captured at fine resolution (Brunbjerg et al., 2017).

In Białowieża the difference between local z-values describing the rate of species accumulation was not significant, suggesting that the relationship may deviate from a strict power-law relationship. The weak and non-significant scaling observed in Białowieża might stem from the fact that these sites were selected along a management gradient rather than a spatial heterogeneity gradient. Mown, recently abandoned and woody-encroached grasslands differ more in vegetation structure and competitive hierarchies than in micro-scale environmental variation (Dembicz et al., 2021). Thus, the fact that the Białowieża sampling regiment was not originally designed for analysing spatial scaling might be the reason behind the non-significant result regarding the power law.

Taxonomic diversity

Values for Simpson's diversity, Shannon and inverse Simpson indices were different across grain sizes both for Białowieża and Preda. Even though the differences were mostly significant, the variation in the data can only be explained to a limited extent by the grain size. The low marginal but high conditional R^2 values across models indicate that plot size alone explains less of the variation in species richness and diversity indices than the random effects related to site identity. This supports the interpretation that local environmental heterogeneity, rather than sampling area itself, shapes community diversity in both regions (Dengler et al., 2020). The limited explanatory power of area is expected but may also reflect methodological constraints from observations being based on shoot presence. Because shoot presence records any part of a plant crossing the plot boundary, and the perimeter-to-area ratio is largest at the smallest plot size (0.1 m²), species richness can be inflated (Zhang et al., 2021). Rooted presence would not cause the same flattening of the SAR slope, which is why plots using different recording techniques should not be directly compared (Cancellieri et al., 2017). This effect may also help explain the pattern observed for the Simpson's diversity and inverse Simpson indices in Preda, where the smallest grain sizes (0.1 m² and 1 m²) did not differ significantly from each other, but both differed from the 10 m² plots.

Diversity indices

The very low marginal R^2 for Simpson's diversity index (Preda = 0.008; Białowieża < 0.02) indicates that plot size explained almost none of the variation in diversity. This suggests that variation in Simpson's diversity is primarily driven by local productivity, disturbance regimes and management history rather than area per se (Häberlin & Dengler, 2025; Moog et al., 2005; Widmer et al., 2025). In both regions, dominant grasses and sedges maintain high cover across all grain sizes, resulting in minimal changes to community evenness with increasing area.

Finally, the slight decline in evenness (Pielou's J') across spatial grains in Preda suggests that the additional species recorded in larger plots were mainly rare or spatially restricted taxa. This pattern is consistent with random colonization and fine-scale habitat filtering rather than any major restructuring of community composition (Pärtel et al., 2019). However, even where taxonomic scaling is weak or scaling patterns were not found, as in Białowieża, functional or phylogenetic differentiation may still occur, indicating that subtle ecological processes could be overlooked when focusing solely on taxonomic species diversity. Investigating such multidimensional aspects of diversity would be a valuable next step for understanding how scale influences community organization in contrasting ecosystems. When analyzing these dimensions of diversity, one could investigate whether similar scale saturation occurs for functional or phylogenetic diversity, which may respond differently to spatial expansion.

Conclusions, limitations, and future studies

A limitation of this study is its focus on vascular plants. Including other taxonomic groups such as bryophytes and terricolous lichens could alter the observed scale dependency of diversity. Extending future research to a wider range of taxonomic groups, vegetation types, geographical gradients and spatial scales would help determine whether the patterns observed here are consistent across ecosystems (Kallimanis et al., 2008).

Beyond taxonomic diversity, functional and phylogenetic diversity should also be included to obtain a more complete understanding of biodiversity scaling. Functional traits, defined as morpho-physio-phenological characteristics that affect fitness indirectly through their influence on growth, reproduction, and survival (Violle et al., 2007), may exhibit their own scale dependence (Rahmanian et al., 2019). Phylogenetic diversity, which reflects the evolutionary relationships among species within a community (Flynn et al., 2011), can reveal hidden scaling patterns that are not captured by purely taxonomic or functional metrics. Describing how such dimensions of diversity scale, as has been done for species richness (Zhang et al., 2021), could provide new insights into the mechanisms shaping biodiversity patterns across spatial scales.

Our findings support earlier research showing that local heterogeneity and sampling design, rather than area alone, govern biodiversity scaling in European grasslands (Dengler et al., 2020; Zhang et al., 2021). Scale dependence in the indices analysed here was modest but consistent: nearly all diversity metrics were influenced by plot size, yet Simpson's diversity index was least affected. This indicates that Simpson's diversity index provides a reliable measure for comparing alpha-diversity between plots of differing or uncertain size, whereas species richness and Shannon index remain more sensitive to area.

These results highlight that accounting for spatial scale is essential for meaningful biodiversity assessments. Plot size matters, but not equally for all indices. Recognising which metrics are most and least scale dependent will strengthen both theoretical understanding and the practical monitoring of biodiversity across habitats, regions and time.

References

Arrhenius, O. (1921). Species and Area. Journal of Ecology, 9(1), 95–99. https://doi.org/10.2307/2255763

Barton, P. S., Cunningham, S. A., Manning, A. D., Gibb, H., Lindenmayer, D. B., & Didham, R. K. (2013). The spatial scaling of beta diversity. Global Ecology and Biogeography, 22(6), 639–647. https://doi.org/10.1111/geb.12031

Blank-Pachlatko, J., Wyttenbach, M., & Dengler, J. (2019). Alpine grassland vegetation at Gornergrat (Canton of Valais, Switzerland): Vegetation mapping for environmental planning. Palaearctic Grasslands - Journal of the Eurasian Dry Grassland Group, 43, 23–37. https://doi.org/10.21570/EDGG.PG.43.23-37

Bonar, S. A., Fehmi, J. S., & Mercado-Silva, N. (2011). An overview of sampling issues in species diversity and abundance surveys. In A. E. Magurran & B. J. McGill (Eds.), Biological diversity: Frontiers in measurement and assessment (pp. 11–24). Oxford University Press.

Brooks, M. E., Kristensen, K., Benthem, K. J. van, Magnusson, A., Berg, C. W., Nielsen, A., Skaug, H. J., Mächler, M., & Bolker, B. M. (2017). glmmTMB Balances Speed and Flexibility Among Packages for Zero-inflated Generalized Linear Mixed Modeling. The R Journal, 9(2), 378–400. https://doi.org/10.32614/RJ-2017-066

Brunbjerg, A. K., Bruun, H. H., Moeslund, J. E., Sadler, J. P., Svenning, J.-C., & Ejrnæs, R. (2017). Ecospace: A unified framework for understanding variation in terrestrial biodiversity. Basic and Applied Ecology, 18, 86–94. https://doi.org/10.1016/j.baae.2016.09.002

Buzhdygan, O., Baldauf, S., Borovyk, D., Vynokurov, D., Ladouceur, E., Chusova, O., Iemelianova, S., Budzhak, V., Tietjen, B., Bezrodnova, O., Bezsmertna, O., Chorney, I., Dembicz, I., Dengler, J., Didukh, Y., Janišová, M., Khodosovtsev, O., Kucher, O., Moysiyenko, I., … Kuzemko, A. (2025). Scale-Dependent Effects of Plant Diversity Drivers Across Different Grassland Habitats in Ukraine. Ecology and Evolution, 15(2). https://doi.org/10.1002/ece3.70941

Ceballos, G., Ehrlich, P. R., Barnosky, A. D., García, A., Pringle, R. M., & Palmer, T. M. (2015). Accelerated modern human-induced species losses: Entering the sixth mass extinction. Science Advances, 1(5). https://doi.org/10.1126/sciadv.1400253

Chase, J. M., & Knight, T. M. (2013). Scale-dependent effect sizes of ecological drivers on biodiversity: Why standardised sampling is not enough. Ecology Letters, 16(1), 17–26. https://doi.org/10.1111/ele.12112

Chase, J. M., McGill, B. J., McGlinn, D. J., May, F., Blowes, S. A., Xiao, X., Knight, T. M., Purschke, O., & Gotelli, N. J. (2018). Embracing scale-dependence to achieve a deeper understanding of biodiversity and its change across communities. Ecology Letters, 21(11), 1737–1751. https://doi.org/10.1111/ele.13151

Chase, J. M., McGill, B. J., Thompson, P. L., Antão, L. H., Bates, A. E., Blowes, S. A., Dornelas, M., Gonzalez, A., Magurran, A. E., Supp, S. R., Winter, M., Bjorkman, A. D., Bruelheide, H., Byrnes, J. E. K., Cabral, J. S., Elahi, R., Gomez, C., Guzman, H. M., Isbell, F., … O'Connor, M. (2019). Species richness change across spatial scales. Oikos, 128(8), 1079–1091. https://doi.org/10.1111/oik.05968

Dembicz, I., & Dengler, J. (2023). Report from the Master Summer School "Biodiversity Monitoring", Białowieża, Poland, 15–25 August 2022.

Dembicz, I., & Dengler, J. (2025). Report from the 6th Master Summer School "Biodiversity Monitoring", Białowieża, Poland, 16–27 August 2024.

Dembicz, I., Dengler, J., Gillet, F., Matthews, T. J., Steinbauer, M. J., Bartha, S., Campos, J. A., De Frenne, P., Dolezal, J., García-Mijangos, I., Guarino, R., Güler, B., Kuzemko, A., Naqinezhad, A., Noroozi, J., Peet, R. K., Terzi, M., & Biurrun, I. (2021). Fine-grain beta diversity in Palaearctic open vegetation: Variability within and between biomes and vegetation types. Vegetation Classification and Survey, 2, 293–304. https://doi.org/10.3897/VCS/2021/77193

Dengler, J. (2009). A flexible multi-scale approach for standardised recording of plant species richness patterns. Ecological Indicators, 9(6), 1169–1178. https://doi.org/10.1016/j.ecolind.2009.02.002

Dengler, J., Boch, S., Filibeck, G., Chiarucci, A., Dembicz, I., Guarino, R., Henneberg, B., Janišová, M., Marcenò, C., Naqinezhad, A., Polchaninova, N. Y., & Biurrun, I. (2016). Assessing plant diversity and composition in grass- lands across spatial scales: The standardised EDGG sampling methodology. Bulletin of the Eurasian Grassland Group, 32, 13–30.

Dengler, J., Matthews, T. J., Steinbauer, M. J., Wolfrum, S., Boch, S., Chiarucci, A., Conradi, T., Dembicz, I., Marcenò, C., García-Mijangos, I., Nowak, A., Storch, D., Ulrich, W., Campos, J. A., Cancellieri, L., Carboni, M., Ciaschetti, G., De Frenne, P., Dolezal, J., … Biurrun, I. (2020). Species–area relationships in continuous vegetation: Evidence from Palaearctic grasslands. Journal of Biogeography, 47(1), 72–86. https://doi.org/10.1111/jbi.13697

Dirzo, R., & Raven, P. H. (2003). Global State of Biodiversity and Loss. Annual Review of Environment and Resources, 28, 137–167. https://doi.org/10.1146/annurev.energy.28.050302.105532

Falinski, J. B. (2012). Vegetation dynamics in temperate lowland primeval forests: Ecological studies in Białowieza forest (Vol. 8). Springer Science & Business Media.

Flynn, D. F. B., Mirotchnick, N., Jain, M., Palmer, M. I., & Naeem, S. (2011). Functional and phylogenetic diversity as predictors of biodiversity–ecosystem-function relationships. Ecology, 92(8), 1573–1581. https://doi.org/10.1890/10-1245.1

Gotelli, N. J., & Chao, A. (2013). Measuring and Estimating Species Richness, Species Diversity, and Biotic Similarity from Sampling Data. In S. A. Levin (Ed.), Encyclopedia of biodiversity (2. ed, Vol. 5, pp. 195–211). Elsevier Inc. https://doi.org/10.1016/B978-0-12-384719-5.00424-X

Häberlin, K. E. R., & Dengler, J. (2025). Recent biodiversity changes in grasslands across elevational bands in Switzerland. Basic and Applied Ecology, 87, 29–37. https://doi.org/10.1016/j.baae.2025.05.003

Hartig, F., Lohse, L., & leite, M. de S. (2024). DHARMa: Residual Diagnostics for Hierarchical (Multi-Level / Mixed) Regression Models (Version 0.4.7) [Computer software]. https://cran.r-project.org/web/packages/DHARMa/index.html

Info Flora. (2025, November 11). Daten melden. Info Flora. https://www.infoflora.ch/de/mitmachen/daten-melden.html

Kallimanis, A. S., Halley, J. M., Vokou, D., & Sgardelis, S. P. (2008). The scale of analysis determines the spatial pattern of woody species diversity in the Mediterranean environment. Plant Ecology, 196(1), 143–151. https://doi.org/10.1007/s11258-007-9341-6

Ladouceur, E., Isbell, F., Clark, A. T., Harpole, W. S., Reich, P. B., Tilman, G. D., & Chase, J. M. (2023). The recovery of plant community composition following passive restoration across spatial scales. Journal of Ecology, 111(4), 814–829. https://doi.org/10.1111/1365-2745.14063

Legendre, P., & Legendre, L. (2012). Numerical ecology (3d English edition). Elsevier.

Lenth, R. V., Piaskowski, J., Banfai, B., Bolker, B., Buerkner, P., Giné-Vázquez, I., Hervé, M., Jung, M., Love, J., Miguez, F., Riebl, H., & Singmann, H. (2025). emmeans: Estimated Marginal Means, aka Least-Squares Means (Version 2.0.0) [Computer software]. https://cran.r-project.org/web/packages/emmeans/index.html

Maurer, B. A., & McGill, B. J. (2011). Measurement of species diversity. In A. E. Magurran & B. J. McGill (Eds.), Biological diversity: Frontiers in measurement and assessment (pp. 55–65). Oxford University Press.

Moog, D., Kahmen, S., & Poschlod, P. (2005). Application of CSR-and LHS-strategies for the distinction of differently managed grasslands. Basic and Applied Ecology, 6(2), 133–143.

Moradi, H., Fattorini, S., & Oldeland, J. (2020). Influence of elevation on the species-area relationship. Journal of Biogeography, 47(9), 2029–2041. https://doi.org/10.1111/jbi.13851

Oksanen, J., Simpson, G. L., Blanchet, F. G., Kindt, R., Legendre, P., Minchin, P. R., O'Hara, R. B., Solymos, P., Stevens, M. H. H., Szoecs, E., Wagner, H., Barbour, M., Bedward, M., Bolker, B., Borcard, D., Borman, T., Carvalho, G., Chirico, M., Caceres, M. D., … Weedon, J. (2025). vegan: Community Ecology Package (Version 2.7-2) [Computer software]. https://cran.radicaldevelop.com/web/packages/vegan/index.html

Pärtel, M., Carmona, C. P., Zobel, M., Moora, M., Riibak, K., & Tamme, R. (2019). DarkDivNet – A global research collaboration to explore the dark diversity of plant communities. Journal of Vegetation Science, 30(5), 1039–1043. https://doi.org/10.1111/jvs.12798

Portier, J., Zellweger, F., Zell, J., Asensio, I. A., Bosela, M., Breidenbach, J., Seben, V., Wueest, R. O., & Rohner, B. (2022). Plot size matters: Toward comparable species richness estimates across plot-based inventories. Ecology and Evolution, 12(6), e8965. https://doi.org/10.1002/ece3.8965

R Core Team. (2024). R: A Language and Environment for Statistical Computing (Version 4.4.0) [Computer software]. R Foundation for Statistical Computing. https://www.R-project.org/

Rahmanian, S., Hejda, M., Ejtehadi, H., Farzam, M., Memariani, F., & Pyšek, P. (2019). Effects of livestock grazing on soil, plant functional diversity, and ecological traits vary between regions with different climates in northeastern Iran. Ecology and Evolution, 9(14), 8225–8237. https://doi.org/10.1002/ece3.5396

Rahmanian, S., Nasiri, V., Amindin, A., Karami, S., Maleki, S., Pouyan, S., & Borz, S. A. (2023). Prediction of Plant Diversity Using Multi-Seasonal Remotely Sensed and Geodiversity Data in a Mountainous Area. Remote Sensing, 15(2), 387. https://doi.org/10.3390/rs15020387

Reutimann, P., Billeter, R., & Dengler, J. (2023). Effects of grazing versus mowing on the vegetation of wet grasslands in the northern Pre-Alps, Switzerland. Applied Vegetation Science, 26(1), e12706. https://doi.org/10.1111/avsc.12706

Smith, B., & Wilson, J. B. (1996). A Consumer's Guide to Evenness Indices. Oikos, 76(1), 70–82. https://doi.org/10.2307/3545749

Storch, D., Marquet, P. A., & Brown, J. H. (Eds.). (2007). Scaling biodiversity. Cambridge University Press.

UNESCO World Heritage Convention. (2025). Białowieża Forest. UNESCO World Heritage Convention. https://whc.unesco.org/en/list/33/

Violle, C., Navas, M.-L., Vile, D., Kazakou, E., Fortunel, C., Hummel, I., & Garnier, E. (2007). Let the concept of trait be functional! Oikos, 116(5), 882–892. https://doi.org/10.1111/j.0030-1299.2007.15559.x

Widmer, S., Riedel, S., Babbi, M., Herzog, F., Wohlgemuth, T., Kessler, M., & Dengler, J. (2025). One Century of Change: Stronger Diversity Decline in Lowland Than in Mountain Grasslands in Central Europe. Global Change Biology, 31(10), e70529. https://doi.org/10.1111/gcb.70529

Wilsey, B. J., Chalcraft, D. R., Bowles, C. M., & Willig, M. R. (2005). Relationships among indices suggest that richness is an incomplete surrogate for grassland biodiversity. Ecology, 86(5), 1178–1184. https://doi.org/10.1890/04-0394

Zhang, J., Gillet, F., Bartha, S., Alatalo, J. M., Biurrun, I., Dembicz, I., Grytnes, J., Jaunatre, R., Pielech, R., Van Meerbeek, K., Vynokurov, D., Widmer, S., Aleksanyan, A., Bhatta, K. P., Campos, J. A., Czortek, P., Dolezal, J., Essl, F., García-Mijangos, I., … Dengler, J. (2021). Scale dependence of species–area relationships is widespread but generally weak in Palaearctic grasslands. Journal of Vegetation Science, 32(3), e13044. https://doi.org/10.1111/jvs.13044

Beyond vascular plants: cryptogams improve community-weighted mean predictions of soil pH in Alpine ecosystems

Dunin Karwicki and Bartosz Norek, University of Warsaw under the supervision of Marcin Mazurkiewicz

Abstract

Vegetation-based soil pH predictions using ecological indicator values traditionally rely on vascular plants alone, yet bryophytes and lichens also respond to soil acidity gradients. We tested whether taxonomic completeness in community-weighted mean calculations improves bioindication accuracy across diverse Alpine ecosystems. We sampled vegetation at three spatial scales (0.1, 1, and 10 m²) across an elevational gradient in the Swiss Alps encompassing grasslands, forests, heaths, and wetlands, comparing 45 model combinations varying in taxonomic scope (vascular plants only vs all taxa including cryptogams), EIVE version (1.0 vs 1.5), weighting type, and plot size using cross-validated predictions. Linear mixed-effects models revealed that taxonomic scope was the only significant predictor of soil pH prediction accuracy (likelihood ratio test: $\chi^2 = 6.39$, $p = 0.011$), while weighting type, plot size, and EIVE version showed no significant effects. Including bryophytes and lichens reduced prediction error by 8.5% (Cohen's $d = 0.09$) and increased average species richness per plot by 35%, with effects consistent across plot sizes but strongest at small spatial scales (11.7% improvement at 0.1 m² vs 4.8% at 10 m²). Complete taxonomic inventories including cryptogams provide measurably more accurate soil pH predictions across diverse Alpine ecosystems, supporting the investment of additional field time for bryophyte and lichen identification when precise environmental characterization is required.

Keywords

Alpine ecosystems, bioindication, bryophytes, community-weighted mean, cryptogams, ecological indicator values, EIVE, lichens, soil pH prediction, taxonomic completeness

Introduction

Accurately estimating soil reaction plays a crucial role in ecological monitoring, habitat assessment, and vegetation classification. Direct soil measurements provide reliable data but are often logistically demanding in long-term or large-scale monitoring programs. Ecological indicator value (EIV) systems provide a powerful alternative: they infer environmental conditions from species composition, allowing efficient and non-destructive environmental assessment (Landolt et al., 2010; Chytrý et al., 2020).

Recent studies (Ostrowski et al., 2025) evaluated several EIV systems and demonstrated that plant-based predictions of soil pH can match measured values with high accuracy, while noting that methodological decisions - such as indicator system, plot size, taxonomic scope, and CWM (community weighted-mean) weighting - substantially affect model outcomes. Their work signified the need for a more formal statistical evaluation of the factors that contribute the most to predictive power.

Several EIV databases are available currently. With the example set by Landolt (*Flora Indicativa*, 1977), many authors subsequently produced their own tables, which are often specialised in a given region or

taxonomic group. The most famous values were produced by Ellenberg for vascular plants (Ellenberg, 1992) and nowadays they are the benchmark. Vascular plants understandably received the most attention, gaining values for Switzerland (Dengler et al., 2023), Czechia (Chytry et al., 2018, Tichy et al., 2023), Sweden (Tyler et al., 2021), the UK (Hill et al., 1999) and even Poland (Zarzycki et al., 2002). There are, however, also solely bryological publications with more careful consideration of moss biology (van Zuijlen et al., 2023), and even values for certain lichens (Szczepańska, 2010), though work still needs to be done.

Recent methodological syntheses also highlight the conceptual foundations of CWM approaches and their limitations, calling for careful evaluation of weighting choices and taxonomic scope when CWMs are used as predictors of environmental gradients (Muscarella et al. 2016; Lepš 2023). In sum, by pairing a comprehensive model comparison with mixed-effects inference and cross-validated prediction, the current analysis aims to identify which of these methodological decisions has the greatest impact on model performance, thereby offering practical recommendations for improving indicator-based soil assessments in biodiversity monitoring programs. (see also Ostrowski et al. 2025 on EIV calculation choices). Therefore, three questions arise, which we plan to answer in this report: 1. Are previous studies correct in their assumptions about scale and weighing type not having an effect on the model? 2. Is the addition of bryophytes and lichens truly worth the time and effort, does it enhance predictive power? 3. What combination of parameters for a CWM model has the best ecological justification and highest predictive power?

Methods

Study area

Fieldwork was conducted in the Alpine region of subalpine Mulix Valley, a north-facing Valley in the Swiss Alps near Preda, Switzerland, encompassing an elevational gradient between 1750 and 2650 m a. s. l. The study area represents typical inner-alpine valley systems characterized by continental climate and diverse communities encompassing grasslands, forests, heaths, and wetlands. This high habitat diversity is driven by the complex local geology, where basic, limestone-derived soils meet acidic soils originating from the region's silicate-rich gneiss formations. This juxtaposition creates a sharp gradient, fostering distinct calcareous, acidic, and intermediate community types.

Vegetation sampling

We employed a nested-plot design adopting a simplified version of the standardized vegetation sampling protocol widely used in grassland biodiversity research (Dengler et al. 2016). At each one of 42 sampling locations, we established nested square plots (126 total) of three grain sizes: 0.1 m² (31.6 × 31.6 cm), 1 m² (100 × 100 cm), and 10 m² (316 × 316 cm). The smallest plot was positioned in one corner of the 1 m² plot, which in turn occupied one corner of the 10 m² plot. This hierarchical arrangement allowed us to assess scale-dependent patterns in species composition and diversity while minimizing within-site heterogeneity.

In each plot, we recorded the complete species composition of all vascular plants, bryophytes, and lichens using the shoot presence method (Dengler et al. 2016). Species presence was determined by the occurrence of above-ground vegetative or reproductive shoots within the plot boundaries, including rooted individuals and those rooting outside but with shoots present within the plot. For each species, we

visually estimated percentage cover in percentages, using a fine-grained scale, with measurements as low as 0.001% cover.

Species identification and taxonomic standardization

Initial species identification in the field was conducted using the SwissFlora mobile application (Info Flora 2024), which provides comprehensive coverage of the Swiss flora with distribution data. This ensured rapid and reliable determination of most species in situ. Difficult or critical taxa were photographed and collected as specimens for later determination in the laboratory.

The species that could not be reliably identified in field, were collected and morphologically and anatomically analyzed using standard microscope techniques and bryophyte identification keys and atlases (Hedenäs & Bisang, 2004; Smith, 2004; Hedenäs & Hallingbäck, 2014; Lüth, 2019).

Following initial identification, all species names were standardized and harmonized to the Euro+Med PlantBase taxonomic framework (Euro+Med 2006), which serves as the authoritative checklist for the European flora. This taxonomic standardization was essential to ensure compatibility with the European Indicator Values for Ellenberg (EIVE) database (Tichý et al. 2023), which provides ecological indicator values calibrated to the Euro+Med taxonomy. We used the EIVE system in two versions: EIVE 1.0 (Dengler et al. 2023), which provides indicator values exclusively for vascular, and an unpublished version of EIVE 1.5, which extends coverage to include bryophytes and lichens.

The taxonomic scope of our sampling allowed us to explicitly test whether including cryptogams (bryophytes and lichens) in community-weighted mean calculations improves soil pH predictions compared to using vascular plants alone – a question of practical importance given the additional field time required for complete bryophyte and lichen inventories.

Soil sampling and pH measurement

At each sampling location, we collected soil samples from the upper 10 cm of the mineral soil level, testing the combination of 3 separate cores for each nested plot. Samples were air-dried, sieved to <2 mm, and 10g of the sample was mixed with 25 g of distilled water and analyzed for pH. Soil pH measurements serve as the response variable for evaluating the predictive performance of vegetation-based indicator values.

Community-weighted mean calculations

For each plot and taxonomic configuration, we calculated community-weighted mean (CWM) of soil reaction values using EIVE indicator values. When multiple records of the same species occurred within a plot, each in a separate layer (herbs, shrubs, trees), we combined cover values probabilistically using the formula (Fischer et al. 2015): combined cover = $1 - \prod(1 - c_i/100) \times 100$, where c_i represents individual cover percentages. This approach accounts for the possibility that cover estimates may partially overlap.

We tested multiple weighting approaches, among them presence weighting (unweighted mean of indicator values), following recent evidence that simple presence-based methods often outperform cover-weighted approaches (Ostrowski et al. 2025). The CWM for each plot was calculated as: $CWM = \Sigma(R_i) / n$, where R_i is the EIVE pH indicator value for species i and n is the number of species in the plot.

Statistical analysis

All analyses were conducted in R version 4.5.1 (R Core Team 2025). We evaluated pH prediction accuracy by comparing predicted pH values (from CWM calculations) against measured soil pH values using cross-

validated predictions. For each plot-size and taxonomic configuration, we employed leave-one-out cross-validation for samples with n < 5 observations and 5-fold cross-validation for larger samples. Prediction accuracy was quantified as squared prediction error, which was log-transformed [log(1 + error)] to meet model assumptions.

We compared taxonomic configurations using linear mixed-effects models (LMMs) with the lme4 package (Bates et al. 2015). Our primary model included taxonomic scope (vascular plants only vs all taxa including bryophytes and lichens) and plot size (0.1, 1.0, 10.0 m^2) as fixed effects, with a random intercept for plot ID to account for repeated measurements across plot sizes. Models were fit using maximum likelihood estimation. Model comparison used likelihood ratio tests, and estimated marginal means were computed using the emmeans package (Lenth 2024). Effect sizes were quantified using Cohen's d via the effectsize package (Ben-Shachar et al. 2020). The significance threshold was set at $\alpha = 0.05$.

Results

General mixed model

The general mixed model with all parameters as fixed effects significantly outperformed a null (intercept-only) model (LR $\chi^2 = 13.7$, df = 8, p =0.09). The intraclass correlation coefficient (ICC = 0.821) indicated that 82.1% of variance in prediction error was attributable to differences between plots, justifying the mixed-model approach.

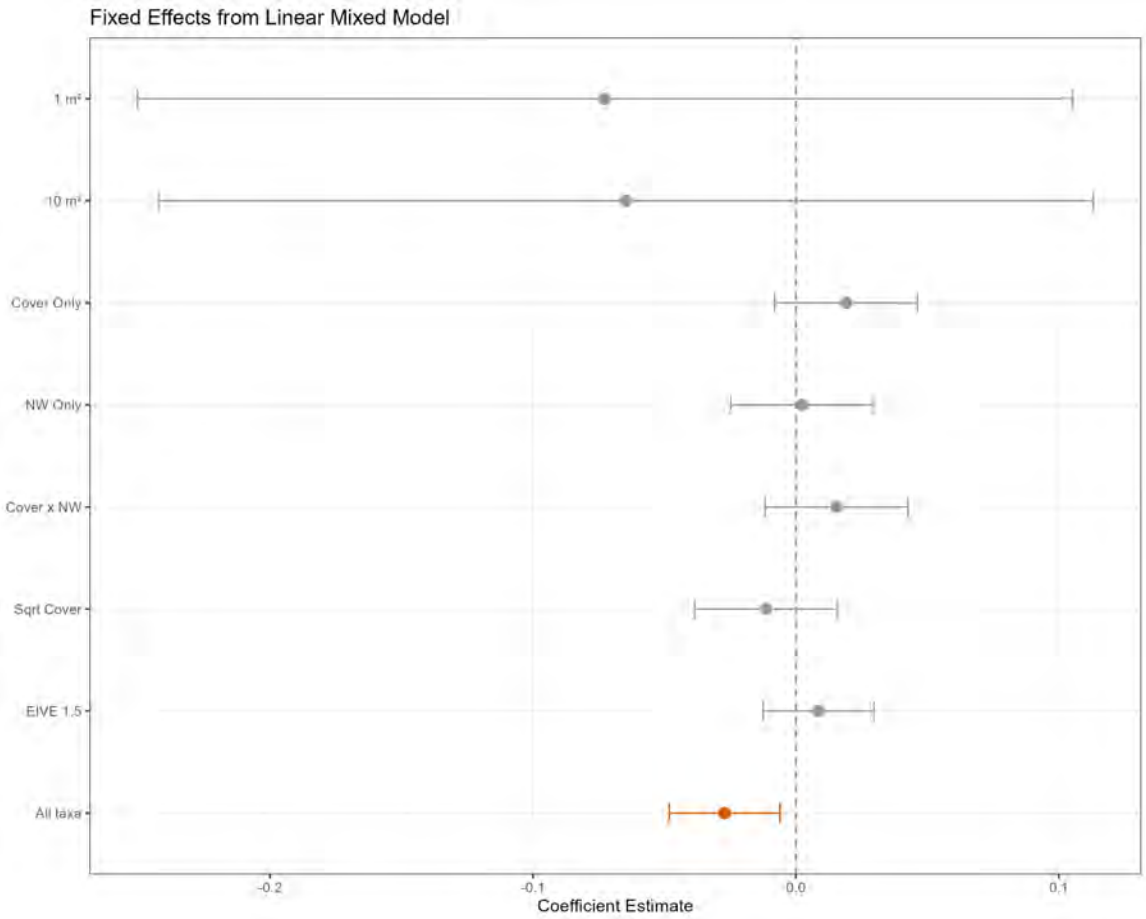

Figure 1. Fixed-effect estimates from the linear mixed model predicting pH accuracy (log-transformed squared error). Points show coefficient estimates with 95% confidence intervals. Negative coefficients indicate better performance (lower prediction error). Orange points indicate statistically significant effects ($p < 0.05$). Reference levels: plot size - 0.1 m² plots, EIVE system - EIVE 1.0, taxonomic group type - vascular species only (EIVE 1.5) , weighting type - presence weighting.

Taxonomic group type focused mixed-effects model

Based on the results of general mixed-effects model (Figure 1), we ran a focused mixed-effects model comparing vascular-only versus all taxa (vascular + bryophytes + lichens), which revealed a significant effect of taxonomic completeness on pH prediction accuracy (likelihood ratio test: $\chi^2 = 6.39$, df = 1, $p = 0.011$). Including cryptogams reduced prediction error by 8.5% compared to using vascular plants alone (Figure 2). This effect was consistent across all three plot sizes (0.1, 1.0, and 10.0 m²), though the magnitude varied slightly with grain size (Figure 4). Effect size analysis confirmed this was a meaningful improvement: Cohen's d = 0.09, indicating a small but practically relevant effect.

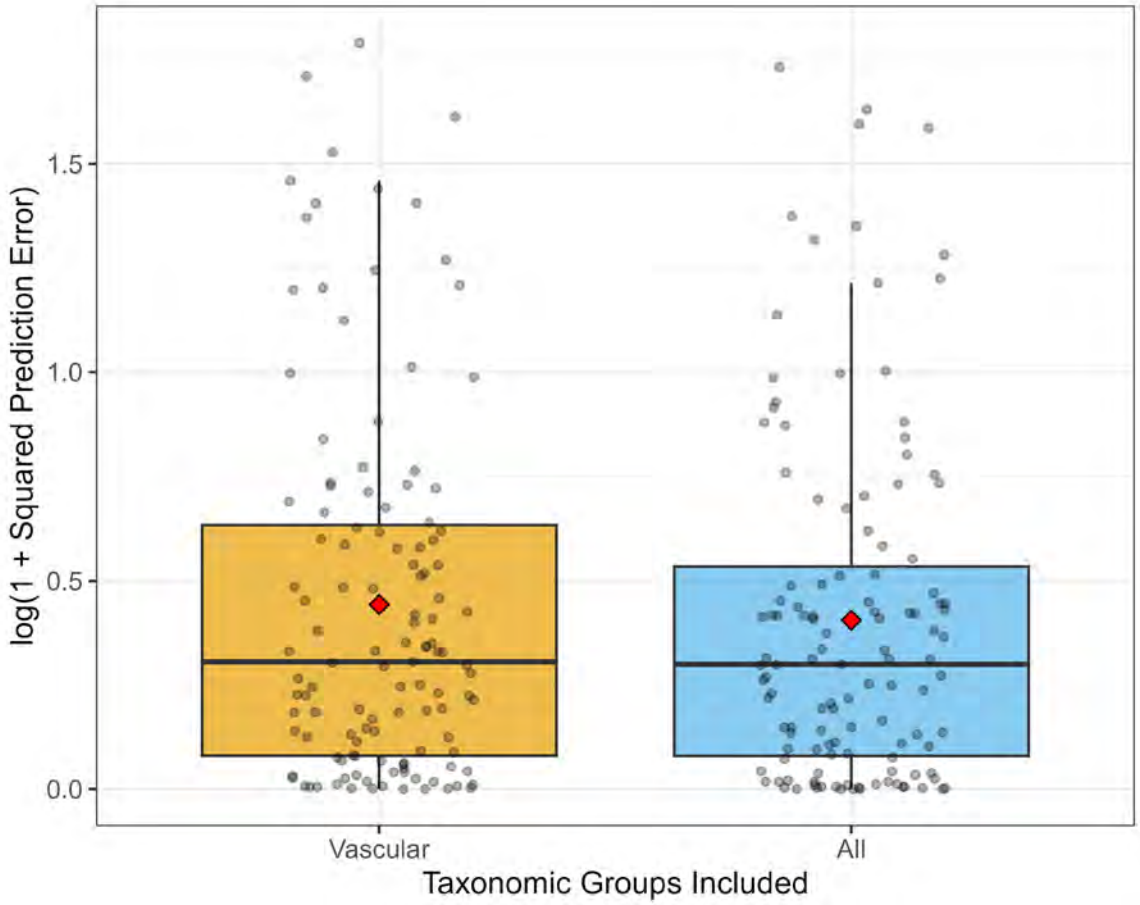

Figure 2. Effect of taxonomic completeness on pH prediction accuracy. Boxplots show log-transformed squared prediction errors for vascular plants only (orange) versus all taxa including bryophytes and lichens (blue). Lower values indicate better prediction accuracy. Red diamonds indicate means. Including cryptogams significantly improved accuracy by 8.5%.

Species richness by taxonomic scope

Including cryptogams substantially increased the species pool available for CWM calculations. Across all plots, vascular plant richness averaged 19.0 species per plot (SD = 13.1, range: 1-63), while total richness when including bryophytes and lichens averaged 25.6 species per plot (SD = 15.7, range: 1-74), representing a 35% increase in species numbers (Figure 3).

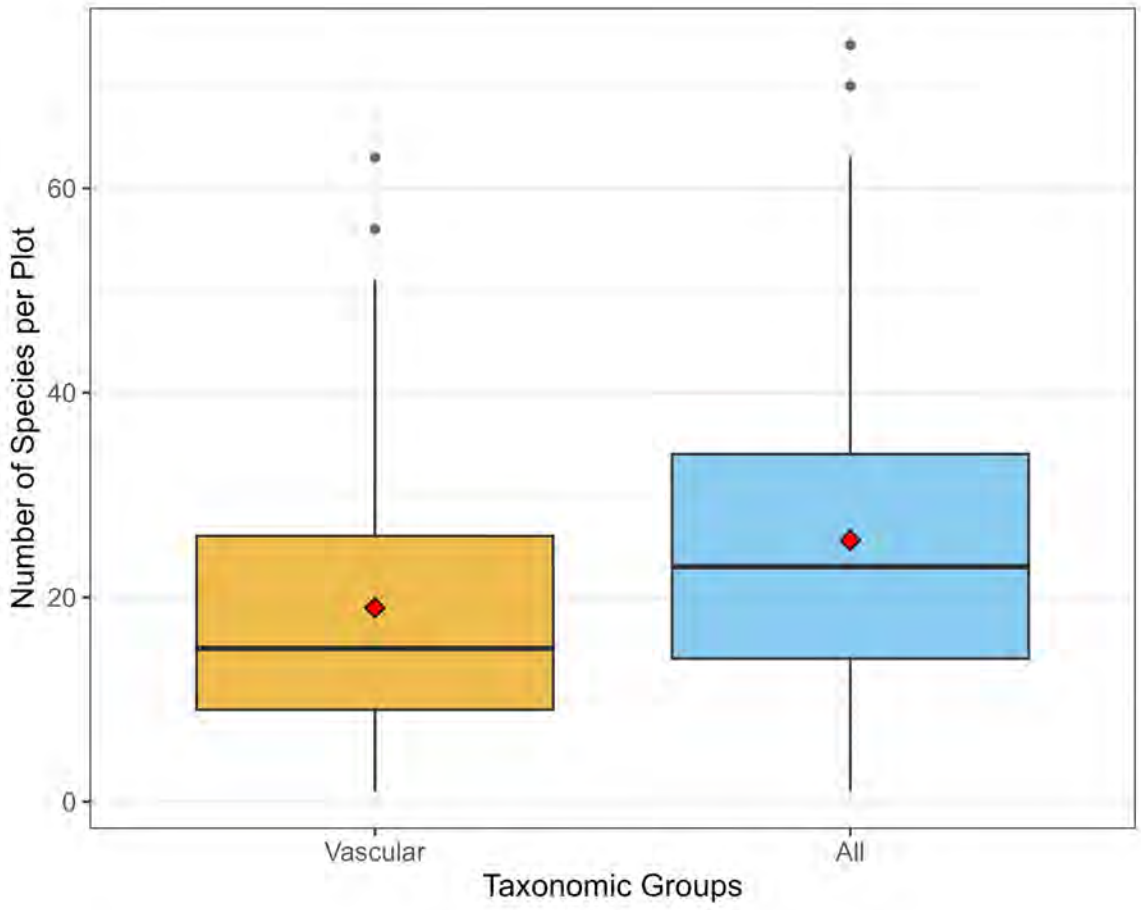

Figure 3. Species richness comparison between taxonomic scopes. Including bryophytes and lichens increased average species richness per plot by 35% (from 19.0 to 25.6 mean species), contributing to more robust community-weighted mean estimates. Diamonds represent means.

Mixed effects of plot size and taxonomic group type

The improvement of mean error when comparing the models with vascular only taxa and all taxa was decreasing with plot size. The size of the effect was the largest for the smallest plot size, at 0.1 m² the benefit of including all taxa was 11.7%, (MAE 0.482 → 0.426) at 1.0 m² it was slightly smaller at 8.6% (MAE 0.412 → 0.382) and for the largest plot of 10 m² the size of the effect was only 4.8% (MAE 0.430 → 0.409).

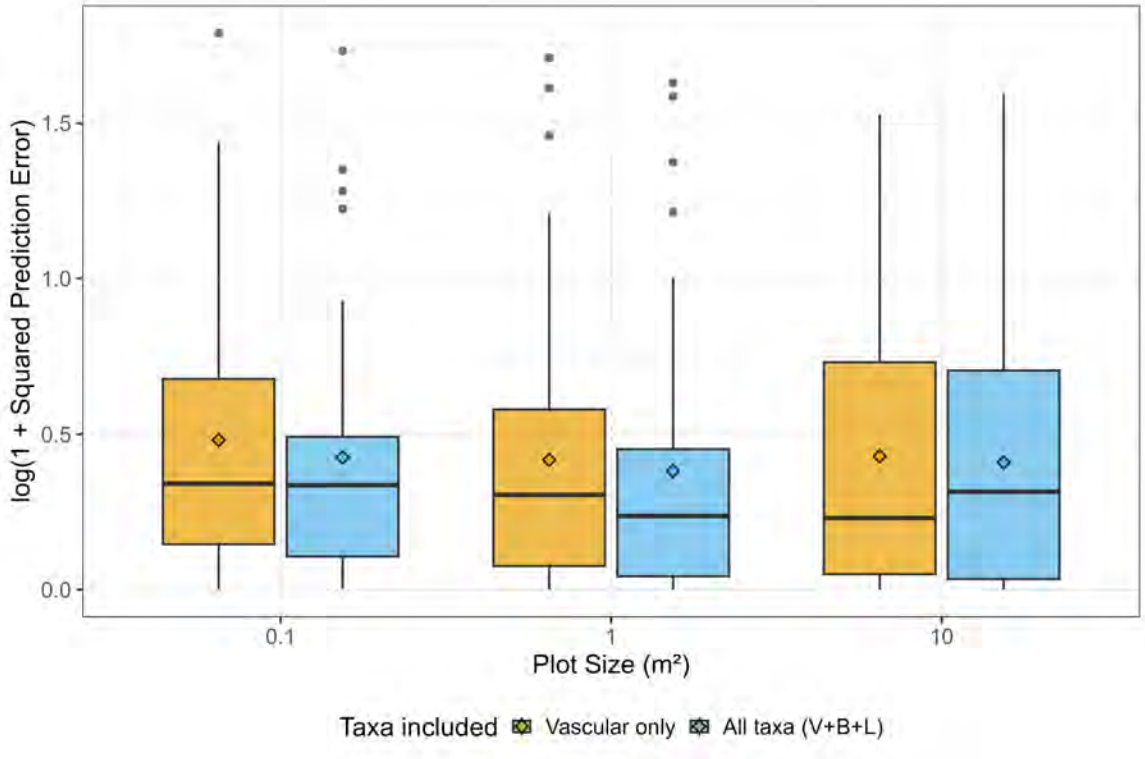

Figure 4. Taxonomic effect across plot sizes. The benefit of including cryptogams was consistent across all three spatial grains (0.1, 1.0, and 10.0 m²), with blue boxes (all taxa) consistently showing lower prediction errors than orange boxes (vascular only) at each plot size. Diamonds represent means.

Discussion

Obtained results provide clear evidence that complete taxonomic inventories, that is including bryophytes and lichens, improve the accuracy of vegetation-based soil pH predictions in Alpine grasslands. This finding has important practical implications: while cryptogam identification requires additional field time and taxonomic expertise, the 8.5% improvement in prediction accuracy justifies this investment for studies where precise environmental characterization is important.

Our analytical approach differs fundamentally from that of Ostrowski et al. (2025) in how we quantified the performance of different bioindication scenarios. While Ostrowski used Pearson correlation coefficients *r* to directly compare mean EIV predictions against measured environmental variables across different weighting schemes and EIV systems, we employed linear mixed-effects models with cross-validated predictions to assess prediction error. This distinction is important: correlation coefficients measure the strength of linear association but do not directly quantify prediction accuracy, whereas our approach using squared prediction error explicitly evaluates how well CWM values predict actual soil pH when applied to new data. The cross-validation framework we employed provides a more rigorous test of predictive performance by avoiding overfitting and estimating out-of-sample error. Furthermore, our use of mixed-effects models allowed us to account for the nested structure of our data (multiple plot sizes within each sampling location), which would not be captured by simple correlational analysis.

The consistency of the cryptogam effect across plot sizes (0.1-10 m²) is particularly noteworthy, as it suggests that the value of including these taxa is not an artifact of sampling scale. Furthermore, the effect decreased with plot size, which correlates well with larger increase in species richness after including cryptogams in the smaller plots. Whether working at fine grains typical of detailed community studies, or

larger grains used in rapid assessment protocols, bryophytes and lichens contribute meaningful information about soil conditions. This result aligns with the "wisdom of the crowd" principle (Ostrowski et al. 2025), which states that predictions based on larger species assemblages tend to be more reliable because individual species' idiosyncrasies average out. Cryptogams are not simply adding noise to the signal – they are responding to the same environmental gradients as vascular plants, and their inclusion makes the community-level signal more robust. The 35% increase in species numbers when including bryophytes and lichens provides a larger ecological "sample size" for estimating plot-level pH conditions.

The weighting scheme exerted no significant effect on prediction error, which is in agreement with (Ostrowski et al., 2025). These patterns support earlier findings that overly emphasizing dominant species can obscure environmental signals carried by less abundant but ecologically specialized taxa (Bruelheide, 2000). This means that for predicting pH, mere presence plays a larger role than exact cover percentage, and therefore more time can be spent on searching for additional small plant species.

The differences among plot sizes were minimal, with no significant effect on model accuracy. This is in agreement with prior results, that even small plots retain sufficient environmental signal for pH prediction (Ostrowski et al., 2025).

Similarly, no meaningful reduction of error came from using EIVE 1.5 over EIVE 1.0, confirming no detectable difference between versions under mixed-effects modelling. This suggests that either version may be used reliably for soil reaction estimation based only on vascular plants. This could, though, be proven false by updating EIVE 1.5 to encompass more species and their aggregates.

The high intraclass correlation coefficient (ICC = 0.821) indicates that more than 80% of variation in prediction error was attributable to between-plot differences. This highlights the considerable ecological heterogeneity characteristic of the chosen plots, given the Alpine region where microtopography, soil texture, and hydrological differences strongly structure plant communities (Dolezal et al., 2016; Zellweger et al., 2023). To create a robust model, the ICC needs to be further reduced, as only then studied parameters will be of importance, rather than the choice of plots. This could be done with either an even denser array of plots in the region of the study or with expanding to other cantons of Switzerland, particularly lower grassland-like and near-lake ones, or even the rest of Europe, which is inevitable if EIVE is to become a standard Pan-European toolkit.

To summarise, our findings point to several practical recommendations. Main takeaways are to simply use presence of species (which supports Ostrowski et al., 2025), especially for small plots; include bryophytes and lichens when possible to enhance predictive accuracy; plot size and EIVE version are flexible parameters with minimal impact on model performance, thus time saved on big plots can be transferred to doing more smaller plots, further strengthening the model; mixed-effects models provide an appropriate framework for indicator-based predictions in heterogeneous landscapes.

Overall, ecological indicator systems, when paired with suitable choices of parameters and multi-taxon vegetation data, continue to serve as robust tools for estimating soil pH in monitoring programs.

References

Bates, D., Mächler, M., Bolker, B., & Walker, S. (2015). Fitting linear mixed-effects models using lme4. Journal of Statistical Software, 67, 1–48.

Ben-Shachar, M. S., Lüdecke, D., & Makowski, D. (2020). effectsize: Estimation of effect size indices and standardized parameters. Journal of Open Source Software, 5, 2815.

Bruelheide, H. (2000). A new measure of fidelity and its application to defining species groups. Journal of Vegetation Science, 11, 167–178.

Chytrý, M., Danihelka, J., Kaplan, Z., Pyšek, P., Tichý, L., & Danihelka, J. (2018). Flora and vegetation of the Czech Republic: diversity, distribution patterns, threats, and conservation. Preslia, 90, 1–120.

Chytrý, M., Hennekens, S. M., Jiménez-Alfaro, B., Knollová, I., Dengler, J., Jansen, F., Landucci, F., Schaminée, J. H. J., & Yamalov, S. (2020). Ecoinformatics for large-scale vegetation ecology. Journal of Vegetation Science, 31, 479–491.

Dengler, J., Boch, S., Filibeck, G., Chiarucci, A., Dembicz, I., Guarino, R., Henneberg, B., Janišová, M., Marcenò, C., Naqinezhad, A., Polchaninova, N., Vassilev, K., & Biurrun, I. (2016). Assessing plant diversity and composition in grasslands across spatial scales: the standardized EDGG sampling methodology. Bulletin of the Eurasian Dry Grassland Group, 32, 13–30.

Dengler, J., Jansen, F., Chusová, O., Hüllbusch, E., Nobis, M. P., Van Meerbeek, K., Axmanová, I., Bruun, H. H., Chytrý, M., Guarino, R., Karrer, G., Moeys, K., Raus, T., Steinbauer, M. J., Tichý, L., Tyler, T., Bita-Nicolae, C., Didukh, Y., Diekmann, M., ... Gillet, F. (2023). Ecological Indicator Values for Europe (EIVE) 1.0. Vegetation Classification and Survey, 4, 7–29.

Doležal, J., Kopecký, M., Liancourt, P., Mudrák, O., & Janeček, Š. (2016). Vegetation dynamics at the upper elevational limit of vascular plants in the Himalayas. Plant Ecology & Diversity, 9, 37–48.

Ellenberg, H., Weber, H. E., Düll, R., Wirth, V., Werner, W., & Paulissen, D. (1992). Zeigerwerte von Pflanzen in Mitteleuropa. 2nd ed. Scripta Geobotanica, Göttingen.

Euro+Med. (2006–). Euro+Med PlantBase – the information resource for Euro-Mediterranean plant diversity. http://ww2.bgbm.org/EuroPlusMed/

Fischer, H. S. (2015). On the combination of species cover values from different vegetation layers. Applied Vegetation Science, 18, 169–170.

Hedenäs, L., & Bisang, I. (2004). Key to European Moss Genera. Journal of Bryology, 26, 1–20.

Hedenäs, L., & Hallingbäck, T. (2014). Mosses of Sweden: Keys and Distribution. Swedish Species Information Centre.

Hill, M. O., Mountford, J. O., Roy, D. B., & Bunce, R. G. H. (1999). Ellenberg's Indicator Values for British Plants. Institute of Terrestrial Ecology, Huntingdon.

Info Flora. (2024). SwissFlora. Swiss National Data and Information Centre on the Swiss Flora. https://www.infoflora.ch

Lenth, R. V. (2024). emmeans: Estimated marginal means. R package version 2.0.0. https://cran.r-project.org/package=emmeans

Lepš, J. (2023). Differences in trait–environment relationships: implications for community-weighted mean tests. Journal of Ecology, 111, 1751–1765.

Landolt, E., Bäumler, B., Erhardt, A., Hegg, O., Klötzli, F., Lämmler, W., Nobis, M., Rudmann-Maurer, K., Schweingruber, F. H., Theurillat, J.-P., Urmi, E., Vust, M., & Wohlgemuth, T. (2010). Flora Indicativa: Ecological Indicator Values and Biological Attributes of the Flora of Switzerland and the Alps. Haupt Verlag, Bern.

Lüth, M. (2019). Die Moose Baden-Württembergs. Ulmer Verlag.

Muscarella, R., Galetti, M., & Ribeiro, M. C. (2016). Species traits and community-weighted means predict functional responses to disturbance. Ecology, 97, 1608–1616.

Ostrowski, G., Aicher, S., Mankiewicz, A., Chusova, O., Dembicz, I., Widmer, S., & Dengler, J. (2025). Mean ecological indicator values: use EIVE but no cover-weighting. Vegetation Classification and Survey, 6, 57–67.

R Core Team. (2025). R: A language and environment for statistical computing. R Foundation for Statistical Computing, Vienna. https://www.R-project.org

Smith, A. J. E. (2004). The Moss Flora of Britain and Ireland. 2nd ed. Cambridge University Press.

Szczepańska, K. (2010). Ecological indicator values for selected lichens in northern Poland. Acta Mycologica, 45, 89–100.

Tichý, L., Axmanová, I., Dengler, J., Guarino, R., Jansen, F., Midolo, G., Nobis, M., Van Meerbeek, K., Aćić, S., Attorre, F., Bergmeier, E., Biurrun, I., Bonari, G., Bruelheide, H., Campos, J. A., Čarni, A., Chiarucci, A., Ćuk, M., Ćušterevska, R., & Chytrý, M. (2023). Ellenberg-type indicator values for European vascular plant species. Journal of Vegetation Science, 34, e13168.

Tyler, T., Olsson, P. A., & Thor, G. (2021). Ecological indicator values for Swedish vascular plants. Nordic Journal of Botany, 39, e03101.

van Zuijlen, K., Bergamini, A., Ahonen, I., Afonina, O., Aigoin, D., Aleffi, M., ... Buryová, B. (2023). A comprehensive trait dataset for European bryophytes: the Bryophytes of Europe Traits (BET) initiative. Journal of Bryology, 45, 1–35.

Zarzycki, K., Trzcińska-Tacik, H., Różański, W., Szeląg, Z., Wołek, J., & Korzeniak, U. (2002). Ecological Indicator Values of Vascular Plants of Poland. W. Szafer Institute of Botany, Polish Academy of Sciences, Kraków.

Zellweger, F., De Frenne, P., Lenoir, J., Vangansbeke, P., Verheyen, K., et al. (2023). Microclimate drivers of plant communities in mountain landscapes. Nature Ecology & Evolution, 7, 1129–1138.

From grains to gradients: cross-taxonomic evaluation of EIVE

Nadiia Kapets, Iryna Rabyk & Oksana Tyshchenko

Abstract

Ecological Indicator Values (EIVs) are widely used to infer environmental conditions from plant community composition, yet their accuracy depends on the calibration system, taxonomic scope, and aggregation method. This study aimed to evaluate the performance of the Ecological Indicator Values for Europe (EIVE) versions 1.0 and 1.5 in estimating soil pH.

We analysed the effects of plot size, habitat type, taxonomic composition (vascular plants, bryophytes, lichens), and the unweighted approach on the accuracy of EIVE-based predictions. Particular attention was given to the unweighted approach, as evidence consistently indicates that reducing the influence of dominant species improves the predictive accuracy of indicator values.

Model performance, assessed using Spearman's correlation between measured soil pH and EIVE-based estimates, showed that EIVE 1.0/1.5 combined with the unweighted approach, appropriate grain size, habitat type, and (for EIVE 1.5) multi-taxon datasets provided sufficient accuracy. The EIVE 1.5 reliably reflects soil acidity in most habitats (with correlations up to 0.88 in grasslands) but its accuracy decreases in forests, open habitats, and especially in wetlands, highlighting a strong dependence on habitat type and the need for expanded data collection in hydromorphic systems.

These results highlight substantial improvements in predictive power across methodological configurations.

Overall, EIVE 1.5 emerged as a more reliable cross-taxon system for quantitative bioindication across spatial scales.

Keywords

bioindication, ecological gradients, EIVE, grains, plant community weighting, soil pH, taxonomic scope, spatial scale, vegetation ecology.

Introduction

The concept of Ecological Indicator Values (EIVs) was initiated by Heinrich Ellenberg, who published the system Zeigerwerte der Gefäßpflanzen Mitteleuropas in 1974. This system assigns numerical values to vascular plant species, reflecting their optimal positions along key environmental gradients — such as light, temperature, moisture, soil reaction (pH), and nutrient availability. These values, typically expressed on ordinal scales (mostly 1–9), are not direct measurements but expert-based assessments derived from long-term field observations and ecological experiments (Ellenberg et al. 1991).

Over the following decades, Ellenberg's system became the foundation for regional adaptations across Europe: for the Alps (Landolt et al. 2010), Poland (Zarzycki et al. 2002), Hungary (Borhidi 1995), and Ukraine (Didukh 2011). Although each of these systems successfully captured local ecological specificity, their reliance on different scales, calibration methods, and taxonomic scopes has limited direct interregional comparability.

To overcome these inconsistencies, a new generation of pan-European indicator systems was developed. Tichý et al. (2023) harmonized 13 regional datasets while preserving Ellenberg's original ordinal scaling, providing the first continent-wide synthesis of indicator values. Building on this foundation, Ecological Indicator Values for Europe (EIVE) 1.0 (Dengler et al. 2023) represents the most comprehensive and modern system to date, covering over 14,800 taxa across Europe. It applies continuous scales (0–10) and incorporates both niche position and niche breadth, thereby enabling more precise ecological and macroecological analyses. The updated EIVE 1.5 (Dengler et al., unpublished) further refined these calibrations by improving taxonomic consistency offering enhanced ecological resolution and analytical robustness.

The use of ecological indicator values (EIV) in vegetation ecology has traditionally focused on vascular plants. However, due to the ecological importance of bryophytes—especially in forests, peatlands, and alpine environments—there is growing interest in integrating them into bioindication systems. The first systematic compilation of ecological indicator values for bryophytes was presented by Düll as a dedicated chapter 3 in the volume Zeigerwerte von Pflanzen in Mitteleuropa Düll, 1991). This study assessed the ecological preferences of leafy and liverwort bryophytes in Central Europe along key abiotic gradients such as light, temperature, continentality, humidity, and substrate pH. It marked one of the earliest steps toward integrating cryptogams into indicator systems traditionally focused on vascular plants. A key step in this direction was the study by Simmel et al. (2021), which introduced Ellenberg N-values for over 1,000 bryophyte species in Central Europe, thereby adapting the classical Ellenberg system for non-vascular plant groups. In parallel, Hájek et al. (2020) expanded the scope of ecological indicator systems by integrating both vascular plants and bryophytes into a unified framework. For the first time, ecological optima and tolerances were estimated jointly for both groups using extensive phytosociological datasets. This integration substantially improved the accuracy of soil moisture, particularly in peatland ecosystems, across both regional and continental scales. In 2023, the BET (Bryophytes of Europe Traits) dataset, published by van Zuijlen et al.**,** presented a comprehensive compilation of morphological, functional, and ecological traits for cryptogams. Although not a complete indicator system, this dataset offers a robust foundation for the future standardization of bryophyte-based bioindication. The most recent advance is the integration of cryptogams into the EIVE 1.5 database, which provides indicator values for mosses and liverworts across several key environmental gradients. This enables more comprehensive vegetation analyses**,** particularly in ecosystems where cryptogams serve as dominant or diagnostic species.

Empirical verification has confirmed the effectiveness of these systems (Moeys 2020). In a recent study by Ostrowski et al. (2025), four major ecological indicator systems (Ellenberg, Landolt, Tichý, and EIVE) — were analyzed based on vegetation data from the Swiss Alps. Among them, the EIVE system achieved the highest predictive performance, especially when using unweighted or niche-width-weighted community means, while cover-weighted approaches tended to reduce accuracy. All tested systems exhibited strong relationships with environmental parameters such as soil pH and temperature, confirming their robustness as tools for quantitative bioindication.

Grain size is an essential parameter in field-based botanical research and the calculation of mean ecological indicator values (EIVs). The proper selection of plot size affects not only the number of species recorded but also the accuracy of environmental bioindication.

According to the findings of Ostrowski et al. (2025), larger plots (10 m^2) yield stronger correlations between EIVs and actual environmental parameters such as soil pH or mean annual temperature. This is attributed to the greater representativeness of species composition on larger plots, which helps to smooth out individual indicator inaccuracies and results in more stable mean values.

This effect is directly linked to the concept of the “wisdom of the crowd” (Surowiecki, 2004), which posits that combining numerous independent estimates provides a more accurate result than relying on dominant species alone. In species-rich communities, each species may carry a degree of uncertainty in its indicator value, but increasing the number of species included reduces the impact of such biases.

Furthermore, as noted by Dengler et al. (2008), very small plots (1 m² or less) may overestimate local variability and fail to reflect actual environmental gradients, whereas excessively large plots may obscure fine-scale ecological boundaries. Therefore, grain size should be carefully selected based on the scale of the study, vegetation type, and expected heterogeneity of the habitat. In summary, modern pan-European systems - particularly EIVE 1.0 and EIVE 1.5 - have proven to be highly efficient, versatile, and precise tools that enable reliable cross-taxon comparisons across diverse vegetation types. By integrating expert ecological knowledge with statistically validated indicator values and large vegetation-plot databases, they provide a robust framework for interpreting species–environment relationships across Europe.

However, despite their broad applicability, empirical tests comparing alternative community-weighting approaches and model configurations remain limited.

The aim of this study is to compare the predictive performance of the EIVE 1.0 and 1.5 indicator systems across vascular plants, cryptogams, and combined taxa, and to assess how plot size and taxonomic composition influence the strength of the relationship between CWM-based indicator values and measured soil pH.

Specifically, we addressed the following questions:

(i) How do EIVE 1.0 and EIVE 1.5 differ in their ability to predict soil pH across nested plot sizes (0.1, 1 and 10 m²)?

(ii) How does the performance of EIVE-based pH indication vary among habitat types (forest, grassland, heath, open and wetland) and across spatial grains?

(iii) How reliably does EIVE 1.5 capture soil acidity across taxonomic scopes (vascular plants, cryptogams and all taxa combined) when community-weighted means are calculated using an unweighted approach?

By addressing these questions, our work contributes to improving the methodological reliability of indicator-based vegetation analysis and strengthens the use of EIVE as a unified system for ecological assessment across habitats.

Methods

Study site

The study area is located near Preda, in the canton of Grisons, Switzerland, within the boundaries of Parc Ela – the largest nature park in the country. This region was selected due to its geological heterogeneity, pronounced elevational gradients, and the presence of contrasting bedrock types.

The vegetation cover of Parc Ela develops on diverse geological substrates – from dolomites and marls to gneisses and basalts, which form young, shallow soils with varying carbonate content. The area features mountain coniferous forests (notably with *Picea abies*), subalpine and alpine meadows, heathlands, moist grasslands, and wetland areas. Land use mainly consists of alpine livestock grazing, with localized zones

of disturbance due to trampling and secondary overgrowth. These conditions create high ecological heterogeneity and significantly influence the floristic composition and vegetation structure (Seiler, 2021).

The biodiversity plots were distributed across two side valleys—Val Mulix to the south of Preda and Val Zavretta to the north—as well as within the floodplain zone of the Alvra (Albula) River (Fig. 1).

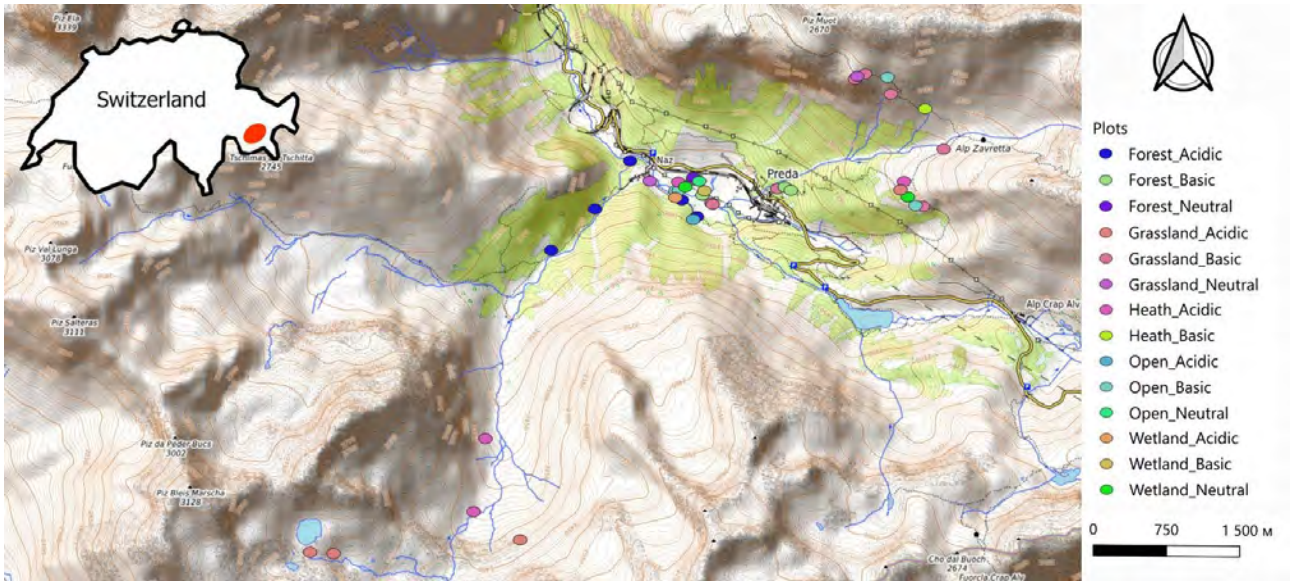

Figure 1. Map of the study area and spatial distribution of the plots (created in QGIS; points of surveyed plots are shown).

The sampling plots covered an elevational range from 1,738 to 2,636 m a.s.l. (Table 1). Val Mulix is situated on unconsolidated morainic deposits formed during the last glacial period and is predominantly underlain by acidic silicate-rich bedrock such as granite or diorite derivatives (Böhlert et al. 2011). In contrast, Val Zavretta is characterized by dolomitic and breccia formations of limestone origin, resulting in a generally alkaline substrate (Makhloufi & Samankassou 2019). The floodplain between these valleys contains a mix of these contrasting lithologies.

This pronounced difference in bedrock composition is expected to be reflected in a strong soil pH gradient: Val Mulix with predominantly acidic conditions and Val Zavretta with base-rich, alkaline soils.

The local climate further confirms the environmental extremity of the site: the mean annual temperature is around 1.9 °C, with average annual precipitation of ~700 mm. The landscape includes a mosaic of floodplains, subalpine forests, heathlands, and subalpine to alpine grasslands, creating a broad array of ecological niches and microhabitats.

In the context of ecological bioindication, soil pH is a central axis in all ecological indicator value (EIV) systems (Diekmann 2003). Many plant species have relatively narrow pH optima and low tolerance for deviations, which makes pH-based indicator values (R-values) a powerful proxy for edaphic conditions (Peppler-Lisbach, 2008). In an environment that encompasses both acidic and base-rich soils, such a broad range of conditions allows for the assessment of a high correlation between species-based indicator values (EIVs) and measured soil pH. This creates ideal conditions for evaluating the predictive power of different EIV systems in alpine conditions.

Field sampling

Field research within the framework of the Biodiversity Monitoring Summer School, organized jointly by the Zurich University of Applied Sciences (ZHAW), the University of Warsaw (UW), and Kherson State University (KSU), was carried out from August 18 to 29, 2025.

In our study, we used high-quality standardised vegetation-plot data from precisely delimited 120 nested square plots of different grain sizes (0.1, 1, and 10 m²; Tab. 1). At each plot, vegetation sampling was conducted following the modified EDGG protocol (Dengler et al. 2016), using standardized record sheets together with digital data collection via the FlorApp application (Schnyder & Stofer 2016). The plots were permanently referenced by the coordinates of the north-west (NW) corner to allow future re-visitation. For each plot, we recorded the plot identifier, date, observer(s), precise GPS coordinates (decimal degrees; NW corner; GPS precision), altitude, slope inclination and aspect, substrate type, and land-use or management category. Additionally, total vegetation cover and the mean height and cover of four structural layers (tree, shrub, herbaceous, and bryophyte/lichen) were measured. All terricolous vascular plants, bryophytes, and lichens visible within the plot were recorded, and their projective cover was estimated separately for each grain size and vegetation layer, applying the shoot-presence and percent-cover recording approach of the EDGG protocol. Supplementary information comprised photographic documentation and free-text remarks. This procedure follows the principles of multi-taxon and multi-scale biodiversity sampling and ensures full compatibility with the GrassPlot database structure (Dengler et al., 2018). Parameters that could not be recorded using the app were noted manually. These included grazing intensity, deadwood cover, gravel cover, soil depth (measured using the rod penetration technique, according to Viro (1952), and microrelief. The plots were established to cover all major subalpine and alpine biotopes of the study area. These include subalpine forests, subalpine grasslands, subalpine heathland, alpine grasslands, floodplain vegetation (including habitat mosaics and floodplain forest), alpine dwarf-shrub habitats above the tree line, open alluvial and rocky vegetation, and wetland habitats associated with the Albula floodplain, springs, and river margins. These biotope categories correspond directly to the habitat types used in our analysis: forest, grassland, heath, open, and wetland.

To analyze soil pH, samples were collected from the top 10 cm of the soil in five randomly selected locations within the 10 m² plots, in four locations within the 1 m² plots, and in two locations within the 0.1 m² plots. The samples were air-dried and sieved. Then, 10 grams of dried sieved soil were mixed with 25 grams of distilled water. After shaking, the mixture was left to stand for one hour for sediment to settle, measured using a portable pH meter (HI991300, Hanna Instruments). Indicator values (EIVE R) were extracted from both EIVE 1.0 (Dengler et al., 2023) and 1.5 (Dengler et al., unpublished).

Species names in the datasets were cross-checked according to the Euro+Med taxonomy (https://europlusmed.org/) for vascular plants and bryophytes; for lichens — Nimis et al. (2018).

Table 1. Three datasets used in this study.

Dataset ID	Indicator	Number of plots	Grain size of plot, m²	Elevational range, m a.s.l.
#1	pH	40	0.1	1738–2636
#2	pH	40	1	1738–2636
#3	pH	40	10	1738–2636

Statistical analyses

Statistical analysis was performed using R (version 4.4.1 (2024-06-14 ucrt) in the RStudio environment (version 2025.09.0+387; Posit team, 2024). Data preprocessing and analysis were performed in R using several core packages, including tidyverse (Wickham et al., 2019) for data manipulation, transformation, and visualization; dplyr and tidyr for filtering, grouping, and restructuring tabular data; ggplot2 and ggpubr for generating graphical outputs; purrr for functional programming workflows; and broom (Wickham, 2016; Robinson et al., 2025; Kassambara, 2025; Wilke, 2025; Wickham & Henry, 2025) for converting linear model results into tidy tabular format. These tools enabled the integration and harmonization of datasets collected in diverse formats and structures. Species names across all datasets were standardized using the mutate() function from the dplyr package to ensure consistency with species naming conventions in the ecological indicator value tables of the EIVE system. An unweighted mean (wi = 1) was calculated for each species. Since the EIVE 1.0 dataset does not include cryptogams (bryophytes and lichens), analyses based on this version relied solely on vascular plant data. For configuration based on the EIVE 1.5, the strength of association between predicted and measured soil pH values was quantified using Spearman's rank correlation coefficient (ρ) to evaluate monotonic relationships. This model is based on the EIVE 1.5 dataset and included different taxonomic group combinations: vascular plants only, bryophytes + lichens, and all taxa combined. Following common practice in indicator-value calibration (Diekmann 2003), we quantified gradient sensitivity using the slope (β_1) of linear models relating community-weighted mean EIVE values to measured soil pH. Linear models were constructed separately for each grain size and vegetation type. For models based on the EIVE 1.0 dataset, which does not include cryptogams, analyses were restricted to vascular plants only. A single model based on the EIVE 1.5 dataset included different taxonomic group combinations: vascular plants only, bryophytes + lichens, and all taxa combined. Model results, including slopes, standard errors, and p-values, were exported as tables. Slopes were visualized in R using ggplot2. The output tables include R^2 and adjusted R^2 values, which are presented in Appendices 1 and 2.

Geographic coordinates of sampling sites were imported into QGIS (version 3.34.13) using the Swiss national coordinate system LV95 (EPSG:2056) and visualized on a base map of Switzerland. This allowed for spatial assessment of site distribution and ecological gradients. Data visualizations were produced using the ggplot2 and cowplot packages, allowing for a clear and comparative presentation of the different calculation approaches within both the EIVE 1.0 and 1.5 systems.

The methodological framework also incorporates the conceptual approaches proposed by Ball et al. (2023), which emphasize the integration of functional trait variability and ecological niche modeling to improve indicator value systems. These concepts offer a broader theoretical basis for interpreting species–environment relationships.

Results

Effectiveness of the EIVE 1.0 and EIVE 1.5 indicator systems in predicting soil acidity across grain sizes

We calculated the Spearman rank correlation coefficient between the EIVE 1.0 and EIVE 1.5 indicator values and the measured pH for three nested plot sizes (Fig. 2).

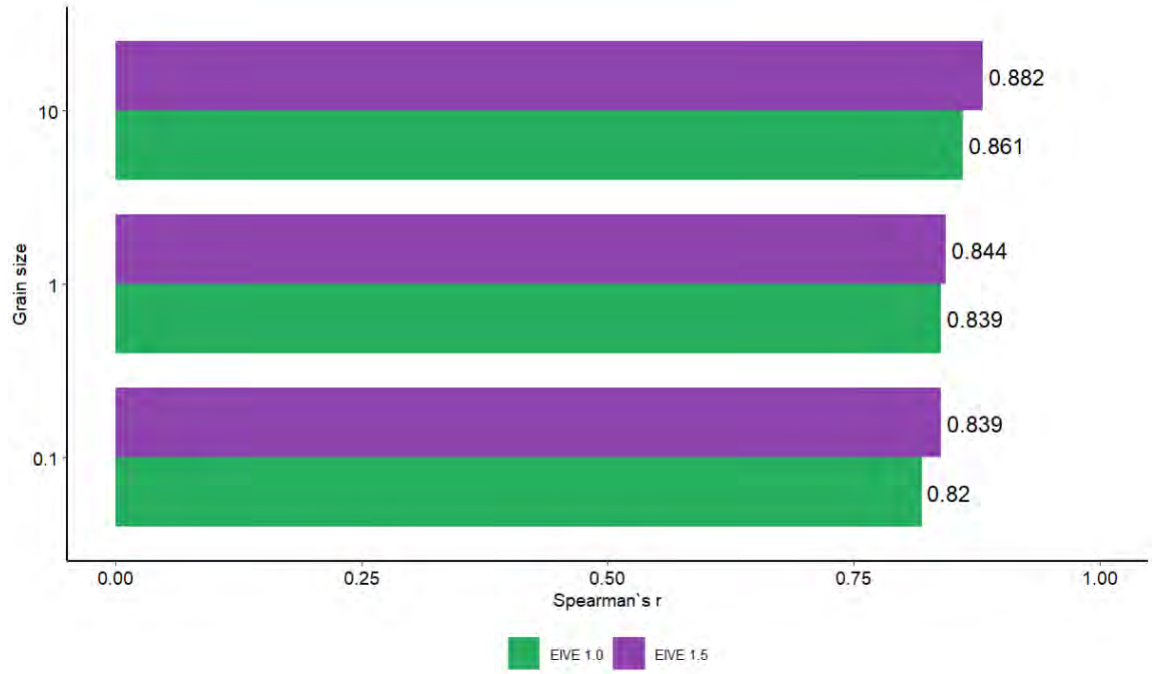

Figure 2. Comparison of EIVE 1.0 and EIVE 1.5 indicator performance in predicting pH across plot grain sizes.

Increasing grain size did not lead to a substantial decline in accuracy, with r_s values remaining within a narrow range of approximately 0.82 to 0.88, suggesting a minimal effect of spatial scale on indicator performance. At the same time, EIVE 1.5 consistently showed slightly higher accuracy compared to EIVE 1.0: the improvement was about 0.01–0.02 at grain sizes 0.1 and 1 and increased to roughly 0.02–0.03 at grain size 10, indicating a small but stable enhancement in agreement with the measured pH.

Effectiveness of the EIVE 1.0 and EIVE 1.5 indicator systems in predicting soil acidity across habitat type

We compared the accuracy of the EIVE 1.0 and EIVE 1.5 indicator values in predicting soil pH across different habitat types (Fig. 3).

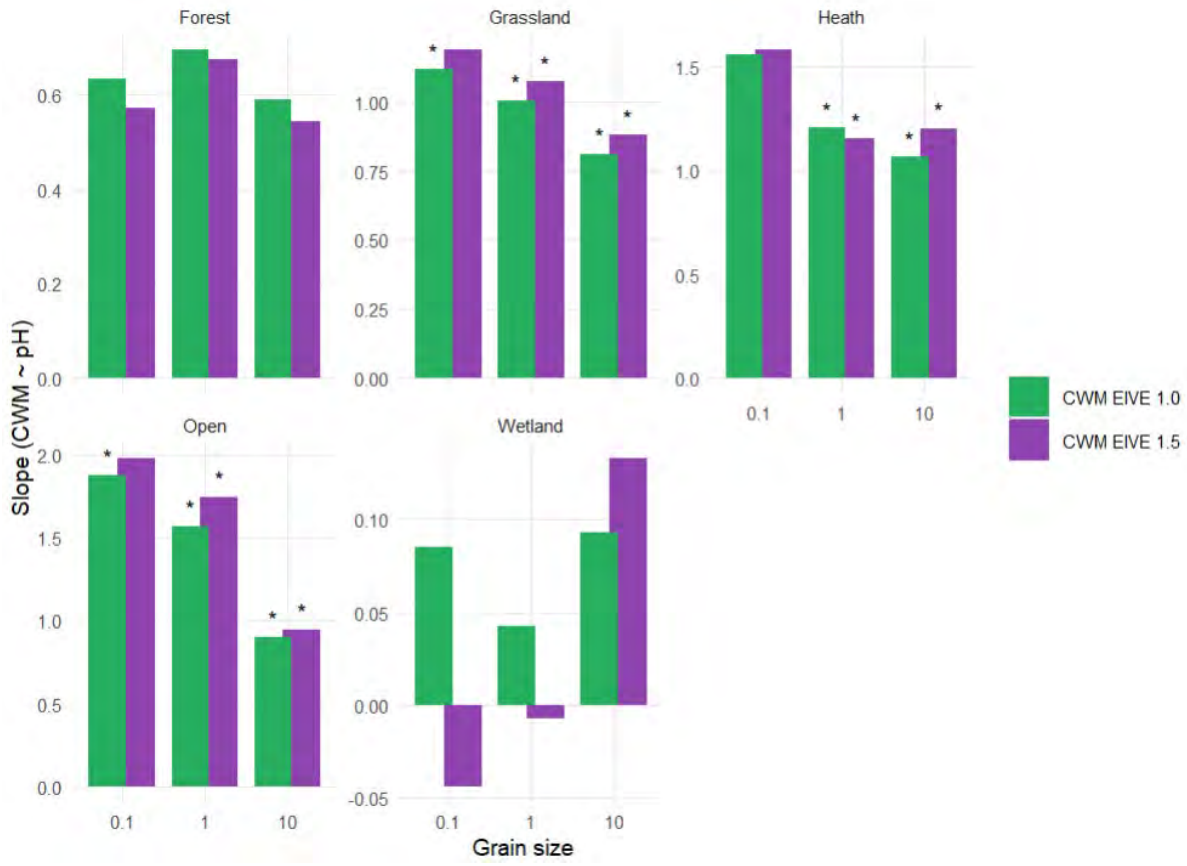

Figure 3. Comparison of CWM15 vs CWM10 slopes (Vascular plants).

The analysis demonstrates how the sensitivity of EIVE 1.0 and EIVE 1.5 indicator values (i.e., the slope of the CWM ~ pH model) for vascular plants changes depending on habitat type and plot size.

The highest and most stable correspondence between indicator values R and soil pH was observed in grasslands: on 0.1 m² plots, the slope was around 1.1–1.2; on 1 m² plots, approximately 0.9–1.0; and on 10 m² plots, about 0.8. In heath, the highest slopes were also at the smallest scale, decreasing to approximately 1.1–1.2 with increasing plot size. Open habitats showed the strongest vegetation response among all habitat types: at 0.1 m², the slope reached 1.9–2.0 but decreased to about 1.0 on 10 m² plots. Forest communities exhibited moderate and relatively stable slopes: 0.6–0.7 on 0.1–1 m² plots, declining to around 0.55 on 10 m² plots.

The weakest and most unstable results were found in wetlands, where slopes were generally very low: around 0.08–0.15 on the smallest plots, dropping to zero or even negative values at 1 m², with a slight increase to approximately 0.20 on 10 m² plots (for EIVE 1.5). In most cases, EIVE 1.5 produced slightly higher slope values, indicating better accuracy—especially on smaller plots—though the difference between the two versions remained minor.

In heath and wetlands, for some plot sizes, the variance of CWM15/CWM10 was very low, and the number of observations was insufficient. For example, in wetlands at a plot size of 1 m², n = 4 and var(CWM15) = 0.0031; at 0.1 m², n = 4 and var(CWM15) = 0.046. In heathlands at 0.1 m², although var(CWM15) = 4.08, the sample size was only n = 5, which is too small for a reliable estimate. Under such conditions, both Spearman and Pearson correlations become unreliable: when variance is low or the sample size is small, correlation values tend to approach zero or become statistically insignificant. In contrast, on larger and

more heterogeneous plots—such as Forest at 0.1 m² (n = 10, cor = 0.638) and Grassland at 0.1 m² (n = 15, cor = 0.832)—both CWM and pH showed sufficient variability, and correlation values were valid. Therefore, the near-zero or unstable correlations observed in heathlands and wetlands at small grain sizes are attributable to low CWM variance and insufficient sample size.

The influence of taxonomic composition on the strength of the CWM–pH relationship across different habitat types

This interpretation is further supported by the comparison of slopes across different taxonomic groups (Fig. 4). The figure shows bar plots of slope values for the linear relationship between community-weighted means (CWM) and soil pH for five habitat types—Forest, Grassland, Heath, Open, and Wetland—and for three combinations of taxonomic groups: L+B (lichens + bryophytes), V (vascular plants), and V+L+B (all groups combined).

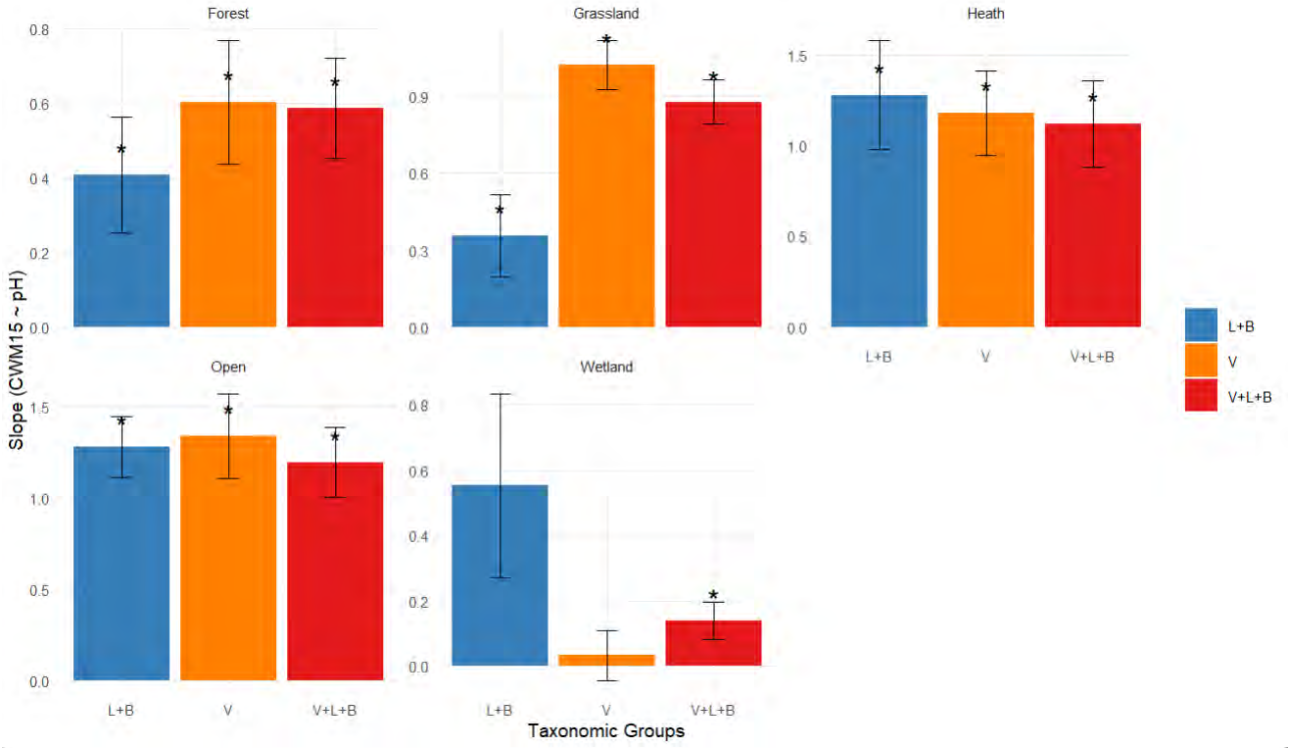

Figure 4. Cwm15 ~ pH: comparison of bryophytes, lichens, and vascular plants across habitat types.

The y-axis represents slope values, while the x-axis indicates the taxonomic groups. Error bars represent standard errors, and asterisks (*) mark statistically significant slopes. In most habitats (e.g., grassland, open, and heath), high and statistically significant slopes were observed across nearly all taxonomic groups, reflecting a strong and consistent CWM–pH relationship. In forest habitats, all groups showed moderate slope values, with significant results for V and V+L+B. By contrast, wetland habitats exhibited generally low and mostly non-significant slopes across all groups, except for V+L+B, which showed a significant but weak relationship.

Discussion

General patterns and reliability of the EIVE system

The results of this study indicate that the EIVE indicator system provides a reasonably accurate approximation of soil acidity across a variety of vegetation types and spatial scales. Consistently high correlation values across all levels (Fig. 2) demonstrate that both versions—EIVE 1.0 and EIVE 1.5—offer relatively reliable predictions of soil pH. All correlations were high and very similar between the two EIVE versions, indicating stable and reliable performance of both indicator systems in predicting pH regardless of plot size. The slight improvement in accuracy observed with EIVE 1.5 reflects improved calibration; however, the overall difference between versions remained minimal. This supports the reliability of both systems and aligns with the concept of indicator values as proxies for species' ecological optima (Diekmann, 2003; Zelený, 2024), especially in contexts where dominance-related biases are minimized.

High and consistent performance in grasslands

Grasslands proved to be the most informative habitat type, where indicator values consistently and accurately reflected actual soil pH values across all spatial scales (Figs. 2–3). This pattern confirms previous findings that reported strong floristic–edaphic relationships in herbaceous vegetation on mineral soils (Diekmann, 2003; Ivanova & Zolotova, 2024). Vascular plants contributed most substantially to the predictive accuracy, whereas lichens and bryophytes played a limited role (Fig. 4), further emphasizing their key role as pH indicators in grasslands.

Weak and unstable indication in wetlands

Wetlands exhibited the lowest and most unstable correlations between indicator values and soil pH (Figs. 3–4). This is consistent with previous assessments highlighting the limited effectiveness of Ellenberg-type indicators in hydromorphic environments (Diekmann, 2003). Likely contributing factors include hydrological variability, peat accumulation, microtopography, and the dominance of cryptogams with broad ecological amplitudes. Additionally, small sample sizes (e.g., n = 4 for some plots) further contributed to statistical instability. Improving calibration in such systems will require greater sampling effort, ideally including multi-year or repeated observations.

Context-dependent role of taxonomic composition

The results clearly show that community taxonomic composition significantly affects indicator accuracy (Fig. 4). In open habitats and heathlands, cryptogams (lichens and bryophytes) provided greater predictive power than vascular plants, which is consistent with their known sensitivity to substrate chemistry and microclimatic variation in oligotrophic or exposed environments (Ivanova & Zolotova, 2024). Probably the unweighted approach proved especially effective in these cases, as low cryptogam cover would otherwise reduce their influence in abundance-weighted methods. In contrast, in grasslands and forests, the pH signal was primarily driven by vascular plants.

Effect of spatial scale on indicator accuracy

A clear scale-dependent pattern was observed in forest habitats, where the strongest correlations occurred on the smallest plots (0.1 m²), and declined on larger plots (Fig. 3). This trend is consistent with meta-analyses showing that vegetation–environment relationships weaken as spatial scale increases

(Dembicz et al., 2025). Larger plots encompass more microsite variability (e.g., light, moisture, soil depth, and litter), which can dilute clear environmental signals such as soil pH. These findings underline that both taxonomic composition and plot-level heterogeneity strongly influence the performance of indicator values, particularly in habitats with low trait variance or limited sample sizes.

EIVE 1.5: improvement without loss of stability

Although the improvements observed in EIVE 1.5 over version 1.0 were modest, the newer version consistently showed slightly higher accuracy, particularly in small plots and habitats with strong vegetation–soil coupling (Figs. 2–3). This likely reflects better estimation of ecological optima and niche widths (Dengler et al., 2023; Ostrowski et al., 2025). Nevertheless, both versions remain suitable for large-scale application when used in ecologically comparable vegetation types.

Methodological considerations and directions for future research

Unweighted approach may increase variability ("noise") in species-rich or gradient-diffuse habitats. For future EIVE calibrations, it is probably advisable to systematically compare unweighted, cover-weighted, and niche-width-weighted means (Zelený, 2024) to identify the most robust approach. Limitations of this study include small sample sizes in certain habitats. To improve robustness, integrating repeated or long-term pH measurements is recommended. Furthermore, this study focused exclusively on soil pH, although the EIVE system also includes gradients of moisture, nutrients, light, and temperature—all of which warrant future evaluation.

Acknowledgments

We express our sincere gratitude to the Institute of ZHAW Natural Resource Sciences (Switzerland), the University of Warsaw (Poland), and Kherson State University (Ukraine). This study was conducted within the framework of the Summer School “Biodiversity Monitoring” 2025. We warmly thank all participants of the Summer School for their valuable contributions to data collection and species identification. Our special thanks go to Marcin Mazurkiewicz for his leadership and continuous support, which were essential for the success of our fieldwork and data processing. We are also deeply grateful to Jürgen Dengler, whose inspiring idea initiated this project and whose insightful guidance and encouragement greatly supported all teams throughout the work. We deeply appreciate the kind support during the ongoing military aggression of the Russian Federation against Ukraine.

References

Ball, J. P., Rosén, E., Dengler, J., & Tälle, M. (2023). From traits to indicators: Advancing ecological assessments using functional trait variability. Ecological Indicators, 148, 110123. https://doi.org/10.1016/j.ecolind.2023.110123

Böhlert, R., Mirabella, A., Plötze, M., & Egli, M. (2011). Landscape evolution in Val Mulix, eastern Swiss Alps—Soil chemical and mineralogical analyses as age proxies. Catena, 87(3), 313–325. https://doi.org/10.1016/j.catena.2011.06.013

Borhidi, A. (1995). Social behaviour types, the naturalness and relative ecological indicator values of the higher plants in the Hungarian flora. Acta Botanica Hungarica, 39, 97–181.

Dembicz, I., Dengler, J., Czarnocka-Cieciura, M., Zaniewski, P. T., Skłodowska, K., & Kozub, Ł. (2025). Drivers of plant and lichen diversity in grasslands on mineral islands surrounded by peatlands (Biebrza Valley, NE Poland). Perspectives in Plant Ecology, Evolution and Systematics, 67, 125870. https://doi.org/10.1016/j.ppees.2025.125870

Dengler, J., Jansen, F., Chusova, O., Hüllbusch, E., Nobis, M. P., van Meerbeek, K., Axmanová, I., Bruun, H. H., Chytrý, M., Guarino, R., Karrer, G., Moeys, K., Raus, T., Steinbauer, M. J., Tichý, L., Tyler, T., Batsatsashvili, K., Bita-Nicolae, C.,

Didukh, Y., … Gillet, F. (2023). Ecological Indicator Values for Europe (EIVE) 1.0. Vegetation Classification and Survey, 4, 7–29. https://doi.org/10.3897/VCS.98324

Dengler, J., Wagner, V., Dembicz, I., García-Mijangos, I., Naqinezhad, A., Boch, S., Chiarucci, A., Conradi, T., Filibeck, G., Guarino, R., Janisová, M., Steinbauer, M., Acíc, S., Acosta, A.T.R., Akasaka, M., Andere-Allers, M., Apostolova, I., Axmanová, I. et al. (2018). GrassPlot – a database of multi-scale plant diversity in Palaearctic grasslands. Phytocoenologia, 48(3), 331–347.

Dengler, J., Boch, S., Filibeck, G., Chiarucci, A., Dembicz, I., Guarino, R., Henneberg, B., Janišová, M., Marcenò, C., Naqinezhad, A., Polchaninova, N. Y., Vassilev, K., & Biurrun, I. (2016). Assessing plant diversity and composition in grasslands across spatial scales: the standardised EDGG sampling methodology. Bulletin of the Eurasian Grassland Group, 32, 13–30.

Dengler, J., Chytrý, M., & Ewald, J. (2008). Phytosociology. In S. E. Jørgensen & B. D. Fath (Eds.), Encyclopedia of ecology (Vol. 4, pp. 2767–2779). Elsevier. https://doi.org/10.1016/B978-008045405-4.00533-4

Didukh, Y. P. (2011). The ecological scales of the species of the Ukrainian flora and their use in synphytoindication. Phytosociocentre, Kyiv.

Diekmann, M. (2003). Species indicator values as an important tool in vegetation ecology. Journal of Vegetation Science, 14, 461–466. https://doi.org/10.1078/1439-1791-00185

Düll, R. (1991) Zeigerwerte von Laub-und Lebermoosen. In: Ellenberg, H., Weber, H., Düll, R., Wirth, V., Werner, W. & Paulissen, D. (Eds.) Zeigerwerte von Pflanzen in Mitteleuropa. Scripta Geobotanica (Vol. 18), 3rd edition. Göttingen: Goltze, 9–166.

Ellenberg, H. (1974). Zeigerwerte mitteleuropäischer Gefäßpflanzen. Scripta Geobotanica, 9, 1–97.

Ellenberg, H., Weber, H. E., Düll, R., Wirth, V., Werner, W., & Paulißen, D. (1991). Zeigerwerte von Pflanzen in Mitteleuropa (2nd ed.). Scripta Geobotanica, 18. Göttingen: Goltze.

Euro+Med PlantBase. (n.d.). European Distributed Institute of Taxonomy – Plant data portal. Retrieved November 15, 2025, from https://www.emplantbase.org/home.html

Hájek, M., Dítě, D., Horsáková, V., Mikulášková, E., Peterka, T., Navrátilová, J., Jiménez-Alfaro, B., Hájková, P., Tichý, L., & Horsák, M. (2020). Towards the pan-European bioindication system: Assessing and testing updated hydrological indicator values for vascular plants and bryophytes in mires. Ecological Indicators, 116, 106527. https://doi.org/10.1016/j.ecolind.2020.106527

Info Flora. (2025). Vegetationsaufnahmen in FlorApp. https://docs.infoflora.ch/de/FlorApp/Vegetationsaufnahmen_Florapp.html

Kassambara, A. (2025) ggpubr: 'ggplot2' based publication ready plots. R package version 0.6.1, https://rpkgs.datanovia.com/ggpubr/.

Landolt, E., Bäumler, B., Erhardt, A., Hegg, O., Klötzli, F., Lämmler, W., Nobis, M., Rudmann-Maurer, K., Schweingruber, F. H., Theurillat, J.-P., Urmi, E., Vust, M., & Wohlgemuth, T. (2010). Flora indicativa: Ökologische Zeigerwerte und biologische Kennzeichen zur Flora der Schweiz und der Alpen. Bern: Haupt.

Makhloufi, Y., & Samankassou, E. (2019). Geochemical constrains on dolomitization pathways of the Upper Jurassic carbonate rocks in the Geneva Basin (Switzerland and France). Swiss Journal of Geosciences, 112(6), Article 50. https://doi.org/10.1007/s00015-019-00350-5

Moeys, K. (2020) Testing a new European system of Ecological Indicator Values for plants: Validatie van het nieuwe Europese systeem voor ecologische indicatorwaarden van planten. Master's thesis, KU Leuven, Leuven.

Nimis PL. Hafellner J, Roux C, Clerc P Mayrhofer H, Martellos S, Bilovitz PO (2018) The lichens of the Alps - an annotated checklist Mvcokevs 31: 1-634. https://doi.org/10.3897/mycokeys.31.23568 2

Ostrowski, A., Nowak, A., Kącki, Z., & Nobis, M. (2025). Evaluation of weighting approaches in phytosociological analysis: implications for ecological indicator value-based modelling. Applied Vegetation Science, 28(1), e12789.

Ostrowski, J. D., Boch, S., Wipf, S., & Walthert, L. (2025). A comparison of ecological indicator value systems for alpine plant communities: Predictive performance and methodological implications. Vegetation Classification and Survey, 6, 45–62. https://doi.org/10.3897/VCS.XXXXX

Peppler-Lisbach, C. (2008). Using species-environment amplitudes to predict pH values from vegetation. Journal of Vegetation Science, 19(4), 437–444. https://doi.org/10.3170/2008-8-18394

Posit team (2024) RStudio: Integrated Development Environment for R. Posit Software, PBC, Boston, MA, USA. http://www.posit.co/.

R Core Team (2024) R: A language and environment for statistical computing. R Foundation for Statistical Computing, Vienna, Austria. https://www.R-project.org/.

Robinson, D., Hayes, A. & Couch, S. (2025) broom: Convert statistical objects into tidy tibbles. R package version 1.0.10, https://doi.org/10.32614/CRAN.package.broom.

Seiler, H.F. (2021) Regionale Typologie der Quellfluren im Parc Ela (Graubünden, Schweiz). Bachelorarbeit, Zürcher Hochschule für Angewandte Wissenschaften, Wädenswil, 1–79.

Simmel, J., Ahrens, M., Poschlod, P. (2021). Ellenberg N values of bryophytes in Central Europe. Journal of Vegetation Science, 32(1), e12957. https://doi.org/10.1111/jvs.12957

Surowiecki, J. (2005) The Wisdom of Crowds: Why the Many Are Smarter Than the Few. Abacus, London. ISBN 978-0349116051.

Tichý, L., Axmanová, I., Dengler, J., Guarino, R., Jansen, F., & 62 others. (2023). Ellenberg-type indicator values for European vascular plant species. Journal of Vegetation Science, 34(1), e13168. https://doi.org/10.1111/jvs.13168

Tichý, L., Chytrý, M., Hennekens, S. M., Jansen, F., Jiménez-Alfaro, B., Knollová, I., Landucci, F., & Schaminée, J. H. J. (2023). Harmonized Ellenberg-type indicator values for vascular plants across Europe. Applied Vegetation Science, 26(1), e12723. https://doi.org/10.1111/avsc.12723

van Zuijlen, K., Nobis, M. P., Hedenäs, L., Hodgetts, N., Calleja Alarcón, J. A., Albertos, B., Bernhardt-Römermann, M., Gabriel, R., Garilleti, R., Lara, F., Preston, C. D., Simmel, J., Urmi, E., Bisang, I., & Bergamini, A. (2023). Bryophytes of Europe Traits (BET) data set: A fundamental tool for ecological studies. Journal of Vegetation Science, 34(2), e13179. https://doi.org/10.1111/jvs.13179

Wickham, H. (2016) ggplot2: Elegant graphics for data analysis. Springer-Verlag, NY, USA.

Wickham, H., Averick, M., Bryan, J. et al. (2019) Welcome to the tidyverse. Journal of Open Source Software, 4, 1686, https://doi.org/10.21105/joss.01686.

Wickham, H. & Henry, L. (2025) purrr: A complete and consistent functional programming toolkit for R. R package version 1.2.0, https://doi.org/10.32614/CRAN.package.purrr.

Wilke, C.O. (2025) cowplot: Streamlined plot theme and plot annotations for 'ggplot2'. R package version 1.2.0, https://wilkelab.org/cowplot/

Zarzycki, K., Trzcińska-Tacik, H., Różański, W., Szeląg, Z., Wołek, J., & Korzeniak, U. (2002). Ecological indicator values of vascular plants of Poland. Kraków: W. Szafer Institute of Botany, Polish Academy of Sciences.

Zelený, D., Helsen, K., & Lee, Y. N. (2024). Extending the CWM approach to intraspecific trait variation: How to deal with overly optimistic standard tests? Oecologia. https://doi.org/10.1007/s00442-024-05568-1

Appendices

The appendices of this document are in the form of an attached files and contain:

1. **Table from R1** (CWM15_CWM10_slopes_by_grain_veg.csv)
2. **Table from R2** (CWM15_slopes_with_R2.csv)
3. **Subsetting** (table_data_FINAL_edOT_NK_OT__with_pH_biotope3.csv)
4. **Script** (VegIII_Script_Final.R)
5. **Figures (**CWM15_slopes_by_habitat_grain.png, Vascular_CWM10_CWM15_vs_pH_by_grain_habitat.png, Vascular_CWM_vs_pH_by_grain.png**)**

Environmental drivers of orthoptera abundance and diversity along an altitudinal gradient in Preda, Switzerland

Patryk Werner, Fabian Rätz, Dylan Derradj

Abstract

Understanding how Orthopteran abundance and species richness responds to elevational and habitat gradients is crucial for predicting biodiversity shifts under changing climatic and land-use conditions. In this study we analysed Orthopteran abundance and species richness in alpine grasslands near Preda (Switzerland) across an altitudinal gradient between 1760 and 2300 m a.s.l. from 2019 to 2025. Data were collected using standardized sweep-net sampling and manual collection. We assessed the effects of elevation, inclination, vegetation structure, cardinal orientation, topography, and land-use type.

Both abundance and species richness declined with increasing elevation. Temporal analyses revealed that this negative elevational trend remained consistent across years, suggesting stable, long-term abiotic control of Orthopteran communities. Environmental variables related to vegetation height and slope positively influenced Orthopteran abundance, whereas microrelief and stone cover had negative effects, reflecting reduced vegetation density and harsher microclimatic conditions at higher sites. Species richness was primarily constrained by elevation and resource availability but increased with total vegetation cover and slope inclination.

Overall, elevation acted as an integrative proxy for abiotic and biotic gradients, primarily temperature and vegetation structure, that are likely to shape Orthopteran abundance and diversity. It indicates that alpine Orthopteran communities are mainly structured by large-scale climatic constraints, with fine-scale habitat heterogeneity mediating their expression. Our findings therefore highlight the importance of structurally diverse habitats and low-intensity management to conserve Orthopteran diversity in alpine ecosystems under ongoing climatic changes.

Keywords

Orthoptera, Alpine grasslands, Altitudinal gradient, GLM, GLMM, Grisons Switzerland

Introduction

Global biodiversity is threatened by the consequences of the climate crisis. Insects, which form the largest taxonomic group, are hit by an alarming decrease in diversity (Fartmann et al. 2022). They play a crucial role in ecosystems as herbivores, pollinators, decomposers, and prey for carnivorous animals. Their loss can therefore trigger chain reactions that disturb entire food webs, especially threatening many insectivorous species. Among insects, Orthoptera (grasshoppers, crickets, and bush crickets) are especially sensitive indicators of environmental change (Fartmann et al. 2022; Marini et al. 2008). Most short-horned grasshoppers (Caelifera) are herbivorous and strongly influence plant community dynamics, while long-horned bush crickets (Ensifera) often act as predators, sometimes specializing on other Orthoptera. This multifunctional role means that shifts in Orthoptera diversity and abundance can impact through multiple levels of the food web (Fartmann et al. 2022).

Abundance and species richness of Orthoptera are closely related to climatic factors, land-use intensity, and vegetation structure. Temperature and habitat composition directly determine their development, mobility, and reproduction, especially for the vulnerable nymphal stages. Land-use change, such as intensification of agriculture or abandonment of traditional pastures, has been identified as one of the main drivers of Orthoptera decline in Europe (Fumy et al. 2021; Fartmann et al. 2022).

Therefore, mountain ecosystems, such as the Swiss Alps, are particularly valuable for studying biodiversity responses to environmental gradients (Sergio and Pedrini 2007). Altitude acts as a natural climate proxy, with temperature, vegetation communities, and land-use changing relatively quickly across the vegetational mosaic of the Alps. This makes altitudinal gradients helpful to simplify how climate and habitat structure shape Orthoptera communities. Despite their ecological importance, data on Orthoptera diversity patterns along alpine gradients remain limited. Long-term and fine-scale studies on the interactions between climate, microhabitat, and land use along these gradients remain scarce, limiting the ability to formulate targeted conservation strategies for alpine biodiversity (König et al. 2024). By addressing these gaps, we expect to generate insights relevant for both ecological research and the adaptive management of mountain ecosystems in the face of ongoing environmental change.

We aim to investigate abundance and diversity of Orthoptera along an altitudinal gradient in Preda (Grisons, Switzerland). By linking species composition to climate, vegetation, and land-use, we want to provide insights into how altitude may affect orthopteran communities. With four years of data (2019, 2021, 2023 and 2025) we want to answer the following questions:

1. How do Orthopteran abundance and species richness vary along the altitudinal gradient?
2. Do patterns of abundance and species richness along the gradient change over time?
3. Which environmental factors, such as vegetation structure and microrelief, explain variation in Orthopteran abundance and species richness?

Methods

Study site

The research area was situated in the vicinity of Preda, located in eastern Central Alps, municipality of Bergün Filisur, within the canton of Grisons, Switzerland. Preda serves as an entrance to the “Parc Ela” which is, with its area covering 658 km^2, the biggest natural reserve of Switzerland (Verein Parc Ela 2025). Its lowest point is located in the Schinschlucht at 745 ma.s.l. and the highest on Piz Kesch reaching 3,418 m a.s.l. According to the Köppen-Geiger climate classification, the region is influenced by a continental subarctic climate that shapes its prevailing abiotic conditions (Beck et al. 2023). Bergün experiences a mean annual precipitation of approximately 1,336 mm, with an average yearly temperature of 1.3 °C and an average thickness of snow cover around 10 cm (Danko et al. 2023). With about 2,000 hours of sunshine per year, Parc Ela is one of the sunniest areas in Switzerland.

In recent decades, many alpine grasslands have been gradually abandoned and are now increasingly influenced by tourism (Bonzanigo et al. 2016). Today, vegetation forms a diverse mosaic of habitats, including subalpine forests, subalpine and alpine grasslands, spring communities, and dwarf-shrub heaths

and is strongly influenced by different ways of land use (Sergio and Pedrini 2007). This diversity of vegetation types and site characteristics offers valuable opportunities for detailed study and analysis.

The research covers several sub areas. The trail along Val Mulix, which the study site is parallel to, leads through distinct altitudinal zones. It featured altitudes ranging from 1,710 to 2,592 meters above sea level (m a.s.l.). This valley is underlain by silicate bedrock and includes habitats such as subalpine forests, alpine dwarf shrublands, and alpine grasslands. South-east to Preda train station, near the Naz village, lies the second site consisting mostly of subalpine meadows and pastures.

A total of 23 square plots were set up for sampling in Val Mulix as shown in Figure 1. The plots have been chosen in past summer schools for plant survey. Therefore, the options were limited by the relatively small number of plots that had also been surveyed for Orthopteran abundance. The plots were systematically positioned along an elevation gradient. The remaining plots were specifically selected to cover the altitudinal gradient in 100-m intervals and to represent the diversity of open ecosystems, particularly grassland habitats. To still gather a broad set of data from different locations, we plotted both sides of the Albula valley. We also examined plots that were established solely for additional orthoptera data in the past years (“ADD” plots) (Figure. 1).

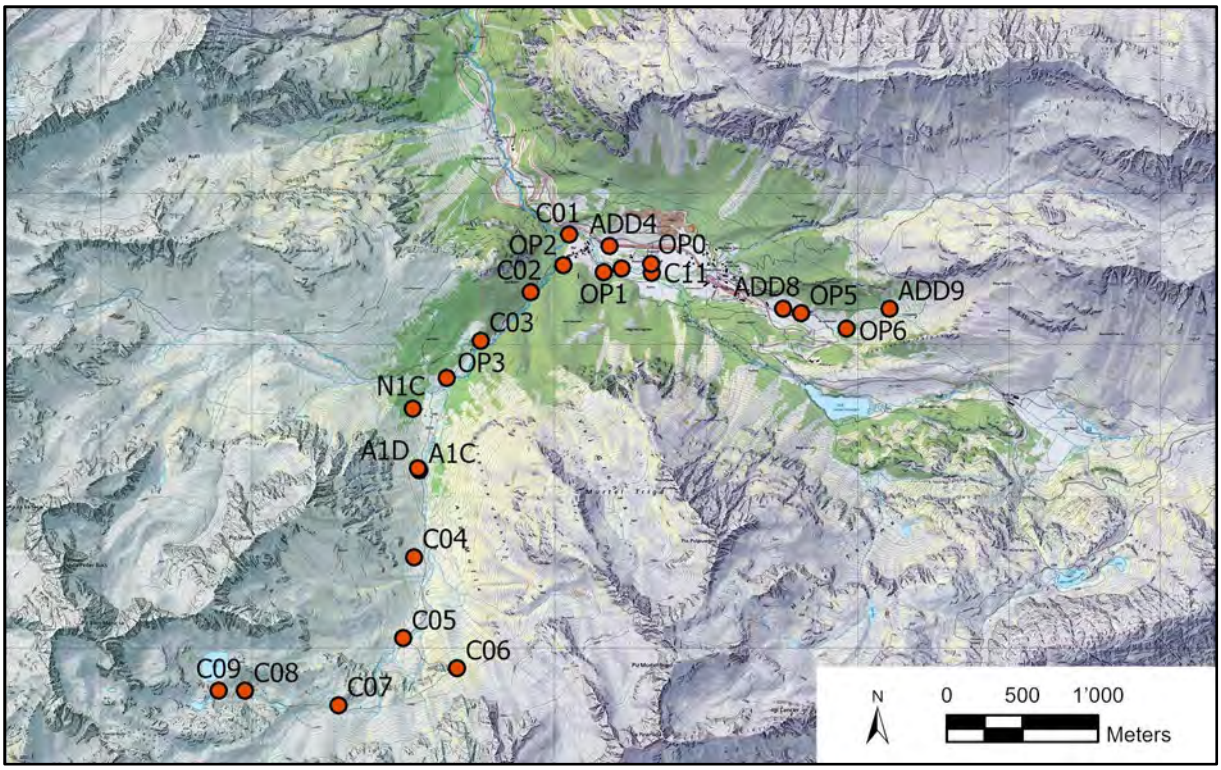

Figure. 1. Map of the research area with all plots sampled in 2025, Basemap: (Swisstopo 2022).

Field sampling

Sampling took place from August 19 to August 26, 2025. A research team of 2 to 4 members examined each plot. Orthoptera sampling adhered to the standardized EDGG (European Dry Grassland Group) survey methodology for orthopteroid insects, as detailed by Hilpold et al. (2020). One person positioned themselves with a sweep net at the SE corner of the plot to begin sampling, followed by others who could

collect Orthoptera missed by the person sweep netting, using small containers. This method was favored due to the type of vegetation in most plots. The search and trapping process lasted approximately 15 minutes in most cases. However, in plots with a particularly high abundance of individuals, we extended sampling time up to 30 minutes. Collected orthoptera specimens we categorized by gender and life stage. Identification was performed in the field, using English, German, and Polish reference books (Bellmann 2018; Baur 2010; Sardet et al. 2021). Alongside orthoptera data, we also compiled plant information for each plot.

Most of the 100 m² plots were surveyed for individual Orthopteran specimens under dry weather conditions. However, a few plots (C01, C02, C03, C10, C11) had to be surveyed during rainfall. The Summer School takes place over twelve fixed days each year, and this year the scheduled period coincided with unfavourable rainy weather conditions. To mitigate the effects of rain on our study, we primarily surveyed forest plots during rainy periods; these plots were excluded from further analyses due to the nature of our research questions.

Statistical Analysis

To examine patterns of abundance and species richness along the elevational gradient, we used data collected by our team in 2025, as well as data from previous years (2019, 2021, and 2023). We excluded forest plots from the analysis due to insufficient data. Because the research questions required different datasets, we applied different statistical approaches accordingly. We set the level of significance for all statistical models at $\alpha = 0.05$.

Abundance and species richness along the altitude gradient

To assess how abundance and species richness varied along the altitudinal gradient, we fitted simple regression models using base R functions. Abundance was analysed with a linear model (LM) including elevation as a predictor. Species richness was analysed using a **ge**neralized linear model (GLM) with a Poisson distribution, suitable for count data. All analyses were conducted in R (version 4.5.0; R Core Team, 2025).

Temporal variation of abundance and species richness patterns along the altitudinal gradient

To test whether elevational relationships remained consistent across years (2019–2025), we fitted generalized linear mixed-effects models (GLMMs) using the *glmmTMB* package (Brooks et al. 2017). We included elevation, year, and their interaction as fixed effects, and plot identity as a random factor to account for repeated counts within the same plots. We z-standardized elevation prior to analysis. We compared different error distributions (Poisson, NB1, NB2, Gaussian) using the *performance* package (Lüdecke et al. 2021) and inspected residual diagnostics with *DHARMa (Hartig 2016)*.

Influence of environmental factors on orthopteran abundance and species richness along the altitudinal gradient

To identify environmental factors explaining variation in Orthopteran species richness and abundance, we used only the 2025 dataset because environmental predictor data (Table 1) were incomplete for previous years. We transformed aspect into southness and eastness and excluded variables with high pairwise correlations ($|r| > 0.7$) to avoid multicollinearity. We z-standardized all continuous predictors prior to model fitting.

Table 1. Variables derived from sub-plot measurements. All percentage values are visual estimates.

Variable	Description	Unit
Elevation	Average plot altitude	m a.s.l.
Year	Year of collection	-
Inclination	Average inclination	–1 to +1
Max. microrelief	Maximum microrelief of subplot	cm
Vegetation total	Average vegetation coverage based on sub plots	%
Mean Ground Layer Height	Mean vegetation height (trees excluded)	cm
Max. Ground Layer height	Maximum vegetation height (trees excluded)	cm
Stone	Coverage by minerals > 63 mm	%
Gravel	Coverage by minerals 2 - 63 mm	%
Fine soil	Coverage by minerals < 2 mm	%
Southness	Southern orientation: −cos(Aspect·π/180)	-1 (north) to +1 (south)
Eastness	Eastern orientation: sin(Aspect·π/180)	-1 (west) to +1 (east)
Landuse	Land use through grazing, mowing or burning	-

We conducted model selection in two steps: (1) we compared candidate error distributions using the *performance* package and information criteria (AIC, BIC) as well as RMSE to assess overall model fit, and (2) we performed stepwise model reduction based on AIC using the *MASS* package (Ripley et al. 2013). We assessed multicollinearity among predictors using Variance Inflation Factors (VIF) calculated with the *performance* package and found no indication of multicollinearity (all VIF < 5).

We carried out all data preparation and statistical analyses in R (version 4.5.0; R Core Team 2025). For data manipulation and visualization, we used *dplyr* and *ggplot2* (Wickham 2016). We used AI tools (OpenAI 2025; Perplexity AI 2025; OpenAI 2025) to support model diagnostics, code validation, and text phrasing, and we critically verified all analyses for scientific accuracy.

Results

Abundance and species richness along the altitude gradient

Abundance

The linear model revealed a significant negative relationship between elevation and the number of individuals (log-transformed, p = 0.002). Elevation explained approximately 46 % of the variation in abundance (R^2 = 0.46) which is roughly 94 % decrease across 1'000 m of elevation. This R^2 suggests that there are other factors affecting the abundance (Figure 1). Residuals were symmetrically distributed, and model assumptions were met.

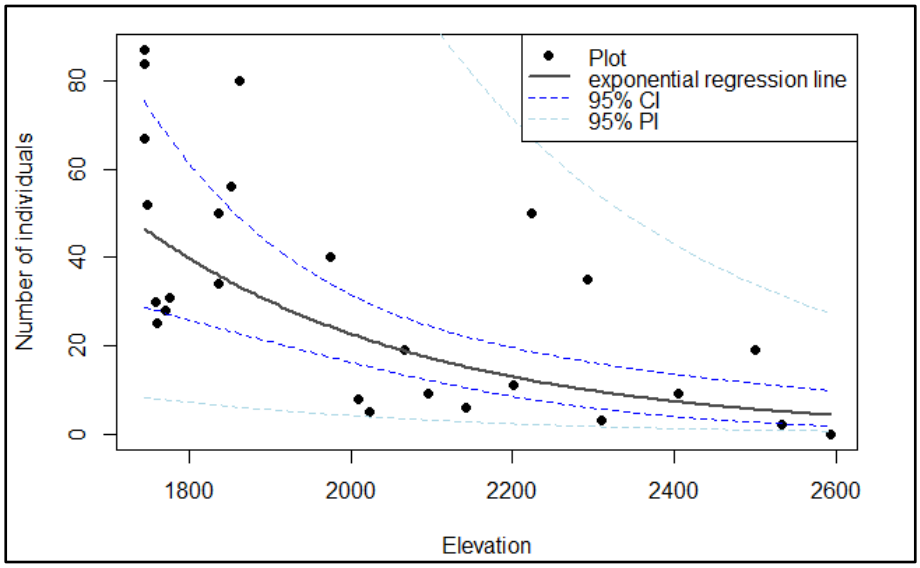

Figure 1: Abundance of species along the elevational gradient (m a.s.l.) across study years (2019–2025) based on a LM. CI = confidence interval. PI= prediction interval.

Species richness

GLM with Poisson regression indicated a statistically significant but weak decrease in species number with elevation (p = 0.0009). However the effect size was distinctly small (= 0.15 % decrease in expected species count per meter of elevation).

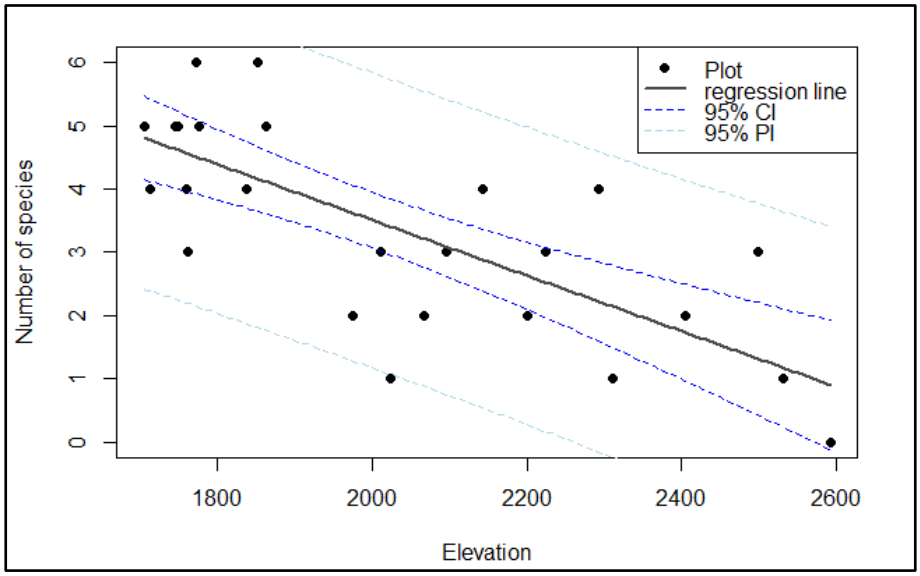

Figure 2. Number of species along the elevational gradient (m a.s.l.) across study years (2019–2025) based on a GLM. CI = confidence interval. PI= prediction interval.

Temporal variation of abundance and species richness patterns along the altitudinal gradient

Abundance

Generalized linear mixed-effects models (GLMMs) confirmed the elevational statistical patterns described above. We tested the interaction between elevation and year, but it was non-significant. Consequently, the negative effect of elevation on abundance can be seen as consistent across years (Figure 3). Thus we excluded the interaction term from the final model (Appendix table 4). Model comparison indicated that the negative binomial (NB1) distribution provided the best fit among all tested error structures (Poisson, Gaussian, NB1, NB2), as reflected by lower AIC, BIC and RMSE values and improved residual diagnostics (Appendix figure 5). The final model for abundance therefore included elevation and year as additive fixed effects, with plot identity as a random factor to account for repeated sampling.

The additive model without the interaction revealed a strong negative effect of elevation on abundance ($p = 0.001$). The factor Year was significant only for 2025 ($p = 3.46 \times 10^{-7}$), indicating a markedly lower abundance compared to the reference year 2019, while 2021 and 2023 did not differ significantly.

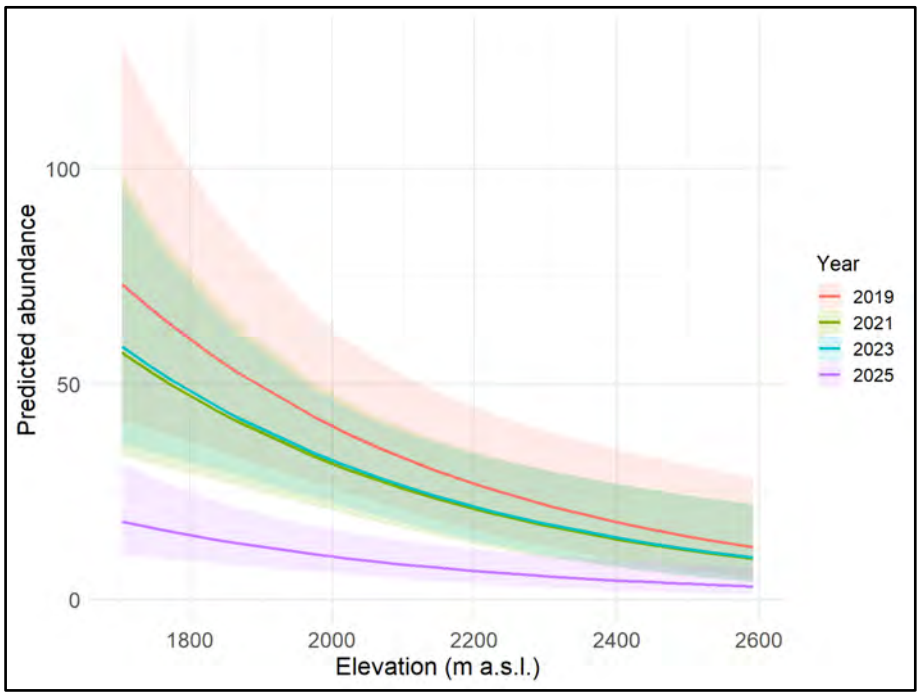

Figure 3. Predicted abundance of species along the elevational gradient (m a.s.l.) across study years (2019–2025) based on a generalized linear mixed-effects model (GLMM, negative binomial type 1 distribution, log link). The model included elevation (standardized) and year as fixed effects and plot identity as a random factor. Shaded areas indicate 95% confidence intervals. Predictions were bias-corrected to obtain unbiased estimates on the response scale.

Species richness

For species richness, the variance of the random intercept was very small ($\sigma^2 = 0.032$, SD ≈ 0.18), indicating minimal among-plot variation. Consequently, we tested generalized linear models (GLMs) without random effects in parallel. Among these, the most parsimonious model was a Poisson GLM including elevation as the single predictor, which showed the best overall performance.

Although the model including only elevation had the lowest AIC, BIC and RMSE, residual diagnostics indicated dispersion issues. Adding Year improved the diagnostics considerably (Appendix figure 5) while

increasing AIC only marginally (ΔAIC < 2). We therefore present the results of the additive model (Appendix table 5) with Elevation and Year. Elevation showed a strong negative effect on species richness ($p = 1.66 \times 10^{-6}$), whereas year had no significant effect (Figure 4).

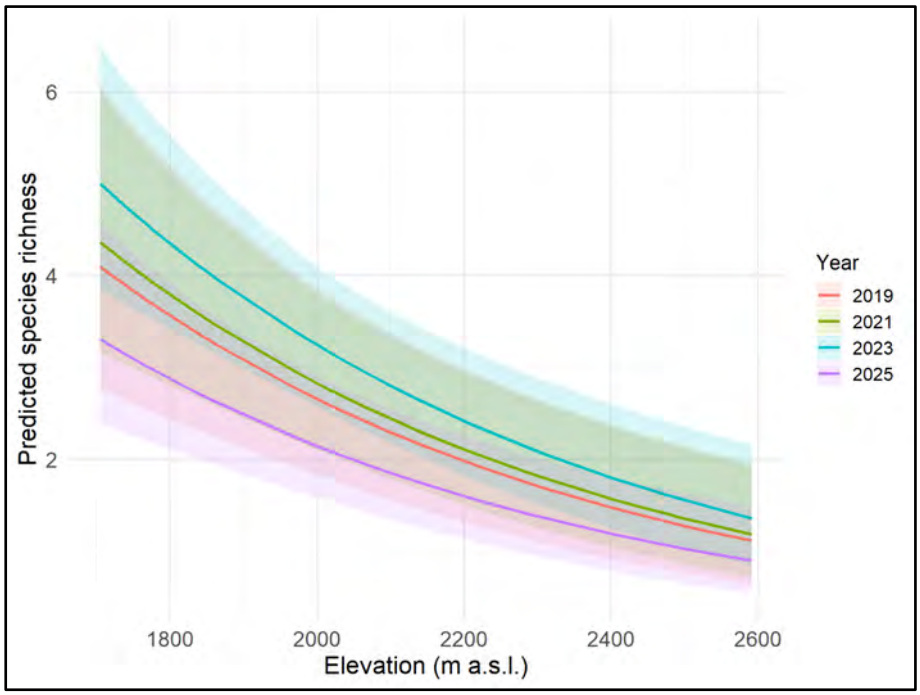

Figure 4. Predicted species richness along the elevational gradient (m a.s.l.) across study years (2019–2025) based on the best-fitting Poisson generalized linear model (GLM) including elevation (standardized) and year as fixed effects. Shaded areas indicate 95% confidence intervals. Predictions were bias-corrected to provide unbiased estimates on the response scale.

Influence of environmental factors on orthopteran abundance and species richness along the altitudinal gradient

In the 2025 dataset, Fine soil was highly correlated with vegetation cover, stone cover, and gravel cover (|r| > 0.7). We therefore excluded Fine soil and retained gravel, stone, and vegetation cover, as these variables are easier to estimate in the field and are considered more relevant for Orthopteran presence. The remaining predictors were included in the global model. Model comparison identified the negative binomial (NB1) distribution as the most appropriate for abundance. Stepwise AIC-based model selection yielded a final model comprising elevation (linear and quadratic terms), inclination, microrelief, mean and maximum vegetation height, stone and gravel cover, eastness, and land use as predictors.

Abundance

Model comparison indicated that adding a quadratic term for elevation improved the abundance model performance (ΔAIC > 2, lower RMSE etc.), supporting a unimodal relationship between abundance and elevation. Residual diagnostics confirmed an adequate model fit (Appendix figure 6) without signs of overdispersion. The final NB1 model therefore included both linear and quadratic elevation terms. Abundance peaked at intermediate elevations (linear term: p = 0.0011; quadratic term: p = 0.044). Steeper slopes (p = 0.0045) and higher maximum vegetation height (p = 0.037) were positively associated with abundance, whereas pronounced microrelief ($p = 8.74 \times 10^{-7}$) and coarse substrates such as stones (p = 0.061) and gravel ($p = 4.0 \times 10^{-4}$ ***) had negative effects. Land use also explained variation in abundance,

with mown plots supporting significantly higher abundances than grazed plots ($p = 3.77 \times 10^{-5}$ ***) (Table 2).

Table 2. Estimated coefficients (β), standard errors (SE), z-values and p-values from the best-fitting GLMM (negative binomial type 1, log link) for species abundance, including elevation (linear and quadratic terms).

Predictor	**Estimate (β)**	**SE**	**z**	**p-value**
Intercept	1.503	0.324	4.641	3.46×10^{-6} ***
Elevation (scaled)	1.184	0.362	3.268	0.001 **
Inclination (scaled)	0.534	0.188	2.841	0.005 **
Max. microrelief (scaled)	-1.007	0.205	-4.918	8.74×10^{-7} ***
Mean vegetation height (scaled)	0.309	0.208	1.485	0.138
Max. vegetation height (scaled)	0.425	0.204	2.082	0.037 *
Stone (scaled)	-0.572	0.306	-1.871	0.061 .
Gravel (scaled)	-1.079	0.305	-3.540	4.0×10^{-4} ***
Eastness (scaled)	-0.019	0.275	-0.070	0.944
Land use: Mowing	2.064	0.501	4.121	3.77×10^{-5} ***
Land use: None	0.733	0.442	1.658	0.097 .
Elevation² (scaled)	-0.471	0.234	-2.016	0.044 *

*Dispersion parameter = 0.78; AIC = 120.0; BIC = 132.2. Significance codes: ***p < 0.001, **p < 0.01, *p < 0.05, . p < 0.1*

Species richness

We modelled species richness using a Poisson generalized linear model (GLM). Model comparison across alternative error distributions (Gaussian, Poisson, NB1, NB2, Quasi-Poisson) indicated that the Poisson model provided the best overall fit, with the lowest AIC and highest performance score. Residual diagnostics (DHARMa) confirmed an adequate fit (Appendix figure 7), with slight underdispersion (dispersion = 0.56), indicating conservative significance testing but no violation of model assumptions. No evidence for zero inflation or non-uniformity was detected.

Stepwise AIC-based model selection yielded a final model (Table 3) including elevation, inclination, vegetation cover, southness, and eastness as predictors. Species richness decreased significantly with elevation (p = 0.0035), while steeper slopes (p = 0.013) and higher vegetation cover (p = 0.015) were positively associated with richness. Southness showed a marginally positive effect (p = 0.067), and eastness was not significant (p = 0.114). Variance Inflation Factors (VIF < 5) indicated no problematic multicollinearity among predictors.

Table 3. Estimated coefficients (β), standard errors (SE), z-values and p-values from the best-fitting Poisson GLM for species richness after stepwise variable selection (stepAIC).

Predictor	Estimate (β)	SE	z	p-value
Intercept	0.449	0.224	2.007	0.045 *
Elevation (scaled)	-0.635	0.218	-2.917	0.004 **
Inclination (scaled)	0.511	0.207	2.471	0.013 *
Vegetation total (scaled)	0.712	0.293	2.426	0.015 *
Southness (scaled)	0.339	0.185	1.829	0.067 .
Eastness (scaled)	0.323	0.204	1.578	0.114

*Residual deviance = 6.60 on 13 df; AIC = 62.3. Significance codes: ***p < 0.001, **p < 0.01, *p < 0.05, . p < 0.1*

Discussion

Abundance and species richness along the altitude gradient

Both orthopteran abundance and species richness decreased with increasing elevation. The effect on abundance was statistically significant and likely ecologically meaningful; however, for species richness the pattern is less clear. Although the model indicated a weak statistical relationship, visual inspection of the data made it clear that there was no real trend, and the apparent effect is unlikely to be ecologically meaningful. This discrepancy may result from the characteristics of the study area and the field sampling: species richness often declines already at relatively low elevations in many European grasslands, where most species are concentrated at lower altitudes. It is common at lower altitudes (0 - 1300 m.a.s.l.) to find more than ten species (Geppert et al. 2021).

Negative elevational trends are consistent with general biogeographic patterns observed for many insect groups in temperate mountains, where decreasing temperature, shorter growing seasons, and reduced vegetation productivity limit population density and species diversity. Reduced thermal energy and primary productivity at higher elevations likely constrain Orthopteran development, reproduction, and food availability. In case of abundance the results consolidate with that trend. Similar monotonic declines have been reported for grasshoppers and crickets in other alpine and subalpine systems (Hodkinson 2005).

In addition, vegetation structure changes along the gradient, with sparser and shorter vegetation at higher sites which may reduce habitat complexity and microclimatic buffering, both of which are known to promote Orthopteran diversity in lower elevations. The parallel decline in abundance and richness suggests that fewer individuals are able to persist under harsher high-elevation conditions, leading to species adapted to cooler environments, such as the Green Mountain grasshopper (*Miramella alpina*) and the Siberian grasshopper (*Gomphocerus sibiricus*), becoming more prevalent.

Temporal variation of abundance and species richness patterns along the altitudinal gradient

The consistent negative effect of elevation across years indicates that the elevational gradient exerts a stable, overriding control on Orthopteran assemblages. The absence of a significant elevation × year

interaction suggests that interannual variation in weather conditions or population dynamics does not substantially alter the underlying spatial pattern. However, abundance in 2025 was markedly lower than in previous years, which may reflect unfavourable weather conditions during the survey period or carry-over effects from preceding years, such as extreme weather events, drought, or phenological mismatches between Orthopterans and their vegetation resources.

The temporal stability of the elevational gradient suggests that Orthopteran communities are primarily structured by long-term abiotic constraints rather than by short-term fluctuations. The observation period (2019–2025) is clearly too short to assess potential effects of climate warming that could drive upward shifts in Orthopteran distributions and alter species diversity or dominance patterns. However, mechanisms determining altitudinal variation in species richness are yet poorly understood Continued long-term monitoring is therefore essential, as projected warming is expected to shift elevational limits and modify these relationships over time (Hodkinson, 2005).

Influence of environmental factors on orthopteran abundance and species richness along the altitudinal gradient

Our analyses of the 2025 dataset revealed that both topographic and vegetation-related factors shaped Orthopteran abundance and species richness along the elevational gradient. For abundance, the inclusion of a quadratic elevation term indicated a unimodal response, with highest densities at intermediate elevations. Such mid-elevation peaks are often interpreted as a trade-off between favourable thermal conditions and sufficient vegetation structure providing shelter and food. However, in our case this pattern is likely an artefact of limited data availability at certain elevations, caused by adverse weather conditions during field sampling. We therefore interpret this mid-elevation effect with caution, as a unimodal relationship would be expected primarily across a broader elevational range extending from lowlands to high mountains.

Microrelief, stone, and gravel cover negatively affected abundance. This might appear surprising, as heterogeneous microrelief often promotes Orthopteran diversity by increasing structural complexity. However, in our study, maximum microrelief likely reflected vegetation scarcity rather than fine-scale surface heterogeneity. Plots at higher elevations often contained more rocks and bare ground, resulting in higher microrelief values but reduced vegetation density. Consequently, maximum microrelief tended to be greater where vegetation was sparse. In addition, coarse and uneven substrates may hinder oviposition, further reducing Orthopteran abundance. In contrast, higher maximum vegetation height and steeper slopes were associated with greater abundance, possibly reflecting the availability of warmer microhabitats and dense, structurally complex vegetation that provides ample food biomass as well as refuges for thermoregulation and predator avoidance (Gardiner and Dover 2008).

Surprisingly, southness was not retained in the final model after stepwise variable selection, even though sunlight exposure is a key factor influencing thermal microhabitats and activity patterns of Orthopterans. A more suitable predictor might be potential solar radiation, which also accounts for slope inclination and aspect together, thereby providing a more realistic measure of surface warming.

In contrast to negative mowing effects reported from submontane grasslands (e.g. Rada et al., 2014), our data showed a positive effect of mown plots in comparison to grazed ones. This likely reflects differences in site productivity and vegetation structure rather than direct management effects. Mown plots were mostly located at lower elevations with denser vegetation, which may explain the higher Orthopteran abundance compared to grazed plots at higher, less productive sites.

Species richness clearly decreased with elevation, confirming the importance of temperature and resource availability as primary limiting factors for species occurrence. At higher elevations, fewer species can persist under the harsh climatic and structural conditions. Similar to abundance, richness increased in plots with greater vegetation structure and steeper slopes, emphasizing the role of structural heterogeneity in maintaining diverse Orthopteran assemblages. However, while abundance responded mainly to maximum vegetation height, richness was more strongly associated with vegetation cover South-facing slopes tended to support more species, consistent with the preference of Orthopterans for warm and dry microclimates, whereas eastness had no significant effect, likely reflecting the generally low thermal contrast between east- and west-facing slopes in this alpine region.

To assess whether the suborder *Ensifera* or *Caelifera* influenced the results, we also tested models including this categorical variable. However, adding suborder led to numerical instability and strong overdispersion. Although some interaction terms suggested biologically plausible differences between *Ensifera* and *Caelifera* (e.g. contrasting responses to land use, vegetation structure, and elevation), these effects should be interpreted with great caution. The model performed worse and was less stable than the simpler versions without suborder, indicating overparameterization and limited information to estimate all interaction effects reliably. We therefore regard these results as exploratory patterns rather than robust evidence for suborder-specific environmental responses.

From a functional perspective, a more informative predictor for habitat selection along the elevational gradient could be egg-laying strategy (ground vs. vegetation oviposition), as these reproductive types may respond differently to elevation and the associated environmental changes. For instance, species depositing their eggs in the soil are more dependent on suitable microclimatic and substrate conditions than species that lay eggs in vegetation (König et al. 2024). Thus, incorporating reproductive or life-history traits in future analyses might provide deeper insight into the mechanisms underlying elevational and land-use patterns in Orthopteran communities.

Conclusion

Overall, our findings highlight that both large-scale climatic gradients and fine-scale habitat characteristics jointly determine Orthopteran diversity in alpine grasslands. The models show that abundance and species diversity of grasshoppers in Preda along the elevation gradient are mainly influenced by altitude. Statistical analyses (GLMM/GLM) confirm a strong negative relationship between altitude and abundance as well as species diversity which was consistent over the past six years. However, while elevation captures the broad energy and productivity gradient, largely local vegetation structure mediates how these constraints are expressed at the community level. Maintaining habitat heterogeneity, especially through low-intensity mowing regimes and conservation of structurally diverse vegetation, appears crucial for sustaining Orthopteran populations under ongoing climate and land-use change.

References

Baur, B., Baur, H., Roesti, C., & Roesti, D. (2006). Die Heuschrecken der Schweiz. Haupt Verlag.

Beck, Hylke E., Tim R. McVicar, Noemi Vergopolan, et al. 2023. 'High-Resolution (1 Km) Köppen-Geiger Maps for 1901–2099 Based on Constrained CMIP6 Projections'. Scientific Data 10 (1): 724. https://doi.org/10.1038/s41597-023-02549-6.

Bellmann, Dr Heiko. 2018. Der KOSMOS Insektenführer. Franckh-Kosmos Verlags-GmbH & Co. KG.

Bonzanigo, Laura, Carlo Giupponi, and Stefano Balbi. 2016. 'Sustainable Tourism Planning and Climate Change Adaptation in the Alps: A Case Study of Winter Tourism in Mountain Communities in the Dolomites'. Journal of Sustainable Tourism 24 (4): 637–52. https://doi.org/10.1080/09669582.2015.1122013.

Brooks, Mollie, Kasper Kristensen, Koen van Benthem, et al. 2017. 'glmmTMB Balances Speed and Flexibility Among Packages for Zero-Inflated Generalized Linear Mixed Modeling'. The R Journal, December 1. https://digitalcommons.unl.edu/r-journal/675.

Danko, Hanna, Gabriela Filipowicz, and Karolina Gwardiak. 2023. Vascular Plant Communities in the Alluvial Plains around Preda: Diversity Patterns and Classification. Summer School Biodiversity Monitoring.

Fartmann, Thomas, Dominik Poniatowski, and Lisa Holtmann. 2022. 'Effects of Land-Use and Climate Change on Grasshopper Assemblages Differ between Protected and Unprotected Grasslands'. Basic and Applied Ecology 63 (September): 83–92. https://doi.org/10.1016/j.baae.2022.06.005.

Fumy, Florian, Steffen Kämpfer, and Thomas Fartmann. 2021. 'Land-Use Intensity Determines Grassland Orthoptera Assemblage Composition across a Moisture Gradient'. Agriculture, Ecosystems & Environment 315 (August): 107424. https://doi.org/10.1016/j.agee.2021.107424.

Gardiner, Tim, and John Dover. 2008. 'Is Microclimate Important for Orthoptera in Open Landscapes?' Journal of Insect Conservation 12 (6): 705–9. https://doi.org/10.1007/s10841-007-9104-7.

Geppert, Costanza, Greta La Bella, Francesco Boscutti, Francesco Sanna, Federico Marangoni, and Lorenzo Marini. 2021. 'Effects of Temperature and Plant Diversity on Orthopterans and Leafhoppers in Calcareous Dry Grasslands'. Journal of Insect Conservation 25 (2): 287–96. https://doi.org/10.1007/s10841-021-00300-3.

Hartig, Florian. 2016. 'DHARMa: Residual Diagnostics for Hierarchical (Multi-Level / Mixed) Regression Models'. August 26. https://doi.org/10.32614/CRAN.package.DHARMa.

Hilpold, Andreas, Philipp Kirschner, and Jürgen Dengler. 2020. 'Scientific Report - Proposal of a Standardized EDGG Surveying Methodology for Orthopteroid Insects'. Palaearctic Grasslands - Journal of the Eurasian Dry Grassland Group, July, 52–57. https://doi.org/10.21570/EDGG.PG.46.52-57.

Hodkinson, Ian D. 2005. 'Terrestrial Insects along Elevation Gradients: Species and Community Responses to Altitude'. Biological Reviews 80 (3): 489–513. https://doi.org/10.1017/S1464793105006767.

König, Sebastian, Jochen Krauss, Alice Classen, et al. 2024. 'Micro- and Macroclimate Interactively Shape Diversity, Niches and Traits of Orthoptera Communities along Elevational Gradients'. Diversity and Distributions 30 (5): e13810. https://doi.org/10.1111/ddi.13810.

Lüdecke, Daniel, Mattan S. Ben-Shachar, Indrajeet Patil, Philip Waggoner, and Dominique Makowski. 2021. 'Performance: An R Package for Assessment, Comparison and Testing of Statistical Models'. Journal of Open Source Software 6 (60). https://pure.mpg.de/rest/items/item_3316363/component/file_3316364/content.

Marini, Lorenzo, Paolo Fontana, Michele Scotton, and Sebastian Klimek. 2008. 'Vascular Plant and Orthoptera Diversity in Relation to Grassland Management and Landscape Composition in the European Alps'. Journal of Applied Ecology 45 (1): 361–70. https://doi.org/10.1111/j.1365-2664.2007.01402.x.

OpenAI. 2025. ChatGPT (October 2025 Version). V. October 2025. OpenAI, released. https://chat.openai.com/.

Perplexity AI. 2025. Perplexity AI (October 2025 Version). V. October 2025. Perplexity AI, released. https://www.perplexity.ai/.

R Core Team. 2025. R: A Language and Environment for Statistical Computing. V. 4.5.0. R Foundation for Statistical Computing, released. https://www.R-project.org/.

Ripley, Brian, Bill Venables, Douglas M. Bates, et al. 2013. 'Package "Mass"'. Cran r 538 (113–120): 822.

Sardet, Éric, Christian Roesti, and Yoan Braud. 2021. Grasshoppers of Britain and Western Europe: A Photographic Guide. Bloomsbury Wildlife.

Sergio, Fabrizio, and Paolo Pedrini. 2007. 'Biodiversity Gradients in the Alps: The Overriding Importance of Elevation'. Biodiversity and Conservation 16 (12): 3243–54. https://doi.org/10.1007/s10531-006-9113-y.

Swisstopo. 2022. 'Karten Der Schweiz - Schweizerische Eidgenossenschaft - Map.Geo.Admin.Ch'. https://map.geo.admin.ch/#/map?lang=de&center=2660000,1190000&z=1&topic=ech&layers=ch.swisstopo.zeitreihen@year=1864,f;ch.bfs.gebaeude_wohnungs_register,f;ch.bav.haltestellen-oev,f;ch.swisstopo.swisstlm3d-wanderwege,f;ch.vbs.schiessanzeigen,f;ch.astra.wanderland-sperrungen_umleitungen,f&bgLayer=ch.swisstopo.pixelkarte-farbe.

Verein Parc Ela. 2025. Parc Ela, Entdecken & Erleben. Broschüre. Verein Parc Ela. https://www.parc-ela.ch/sites/parc_ela/files/2025-04/Parc_Ela_Entdecken%26Erleben_2025.pdf.

Wickham, Hadley. 2016. 'Data Analysis'. In Ggplot2: Elegant Graphics for Data Analysis, edited by Hadley Wickham. Springer International Publishing. https://doi.org/10.1007/978-3-319-24277-4_9.

Appendix

Table 4. Estimated coefficients (β), standard errors (SE), z-values and p-values from the best-fitting GLMM (negative binomial type 1, log link) for species abundance, including elevation and year as fixed effects and plot identity as a random factor.

Predictor	Estimate (β)	SE	z	p-value
Intercept	3.581	0.227	15.809	2.0×10^{-16} ***
Elevation (scaled)	-0.567	0.172	-3.289	0.001 **
Year 2021	-0.246	0.213	-1.153	0.249
Year 2023	-0.222	0.201	-1.102	0.270
Year 2025	-1.400	0.275	-5.097	3.46×10^{-7} ***

*Random effect (Plot intercept variance = 0.63, SD = 0.79). Dispersion parameter = 7.03; AIC = 554.6; BIC = 569.9.

Significance codes: ***p < 0.001, **p < 0.01, *p < 0.05, . p < 0.1*

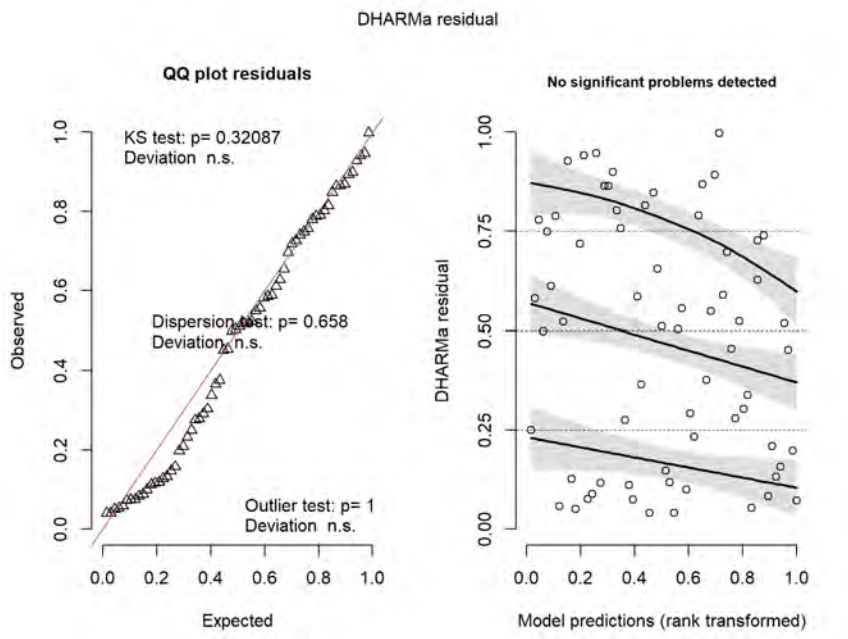

Figure 5. Residual diagnostics of the best-fitting GLMM (negative binomial type 1, log-link) based on DHARMa simulations. Left panel: quantile–quantile plot of scaled residuals with Kolmogorov–Smirnov (KS), dispersion and outlier tests (all n.s.). Right panel: residuals versus model predictions (rank transformed) with 95% confidence bands. No significant deviations from model assumptions were detected.

Table 5. Estimated coefficients (β), standard errors (SE), z-values and p-values from the best-fitting Poisson GLM for species richness, including elevation and year as fixed effects.

Predictor	Estimate (β)	SE	z	p-value
Intercept	0.951	0.192	4.964	6.90×10^{-7} ***
Elevation (scaled)	-0.41	0.086	-4.791	1.66×10^{-6} ***
Year 2021	0.063	0.241	0.260	0.795
Year 2023	0.199	0.222	0.898	0.369
Year 2025	-0.214	0.243	-0.880	0.379

*Residual deviance = 53.29 on 61 df; AIC = 239.6.Significance codes: ***p < 0.001, **p < 0.01, p < 0.05, . p < 0.1

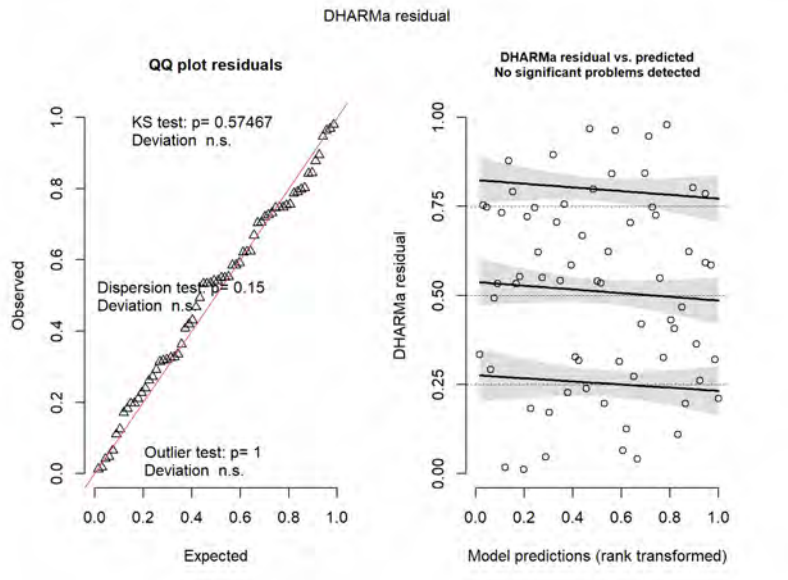

Figure 6. Residual diagnostics of the best-fitting GLM (Poisson, log-link) based on DHARMa simulations. Left: quantile–quantile plot of scaled residuals with Kolmogorov–Smirnov (KS), dispersion and outlier tests (all n.s.). Right: scaled residuals versus predicted values (rank transformed) with 95% confidence bands. No significant deviations from model assumptions were detected.

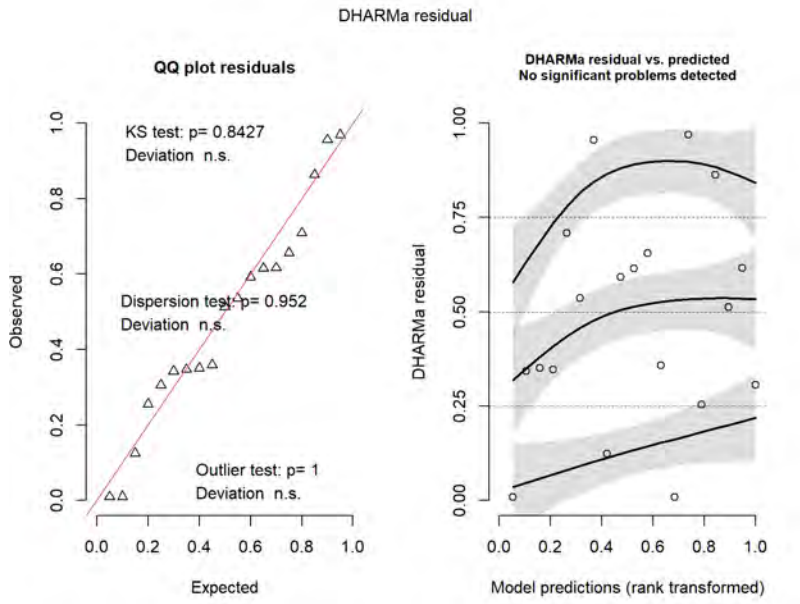

Figure 7. Residual diagnostics of the best-fitting GLMM (negative binomial type 1, log-link) based on DHARMa simulations. Left: quantile–quantile plot of scaled residuals with Kolmogorov–Smirnov (KS), dispersion and outlier tests (all n.s.). Right: scaled residuals versus predicted values (rank transformed) with 95% confidence bands. No significant deviations from model assumptions were detected.

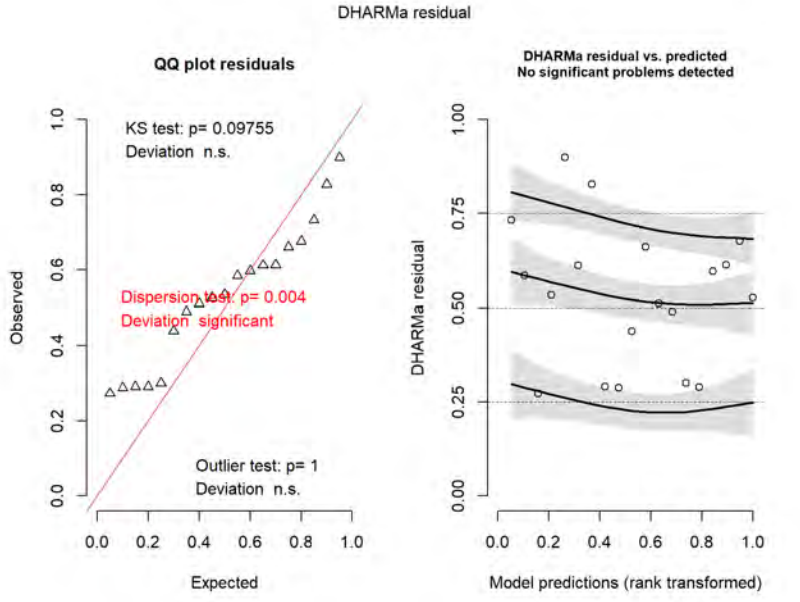

Figure 8. Residual diagnostics of the best-fitting Poisson GLM based on DHARMa simulations. Left: quantile–quantile plot of scaled residuals with Kolmogorov–Smirnov (KS), dispersion and outlier tests (dispersion significant at p = 0.002). Right: scaled residuals versus predicted values (rank transformed) with 95% confidence bands. No major deviations from model assumptions were detected.

Monitoring of small mammal diversity along an elevation gradient in Val Mulix and around Preda, Switzerland

Janick Ehrsam, Jonas Uhland & Joëlle Truniger

Abstract

Small mammals are key indicators of alpine biodiversity and ecosystem health. However, their elevational diversity patterns in the Swiss Alps have not been studied enough. This study aimed to quantify the diversity and activity of small mammals, as well as the environmental drivers, along an elevational gradient in Val Mulix near Preda in the Parc Ela nature reserve.

Between mid-June and late August 2025, 12 standardised camera traps were deployed at elevations ranging from 1735 m to 2635 m a.s.l. Species identification was conducted using DeepFaune and verified manually. Event-based datasets were used to calculate the probability of presence, species richness and Shannon diversity at each site, and linear models were applied to test the effects of elevation and climatic variables.

Both species richness and Shannon diversity declined with increasing elevation, showing near-significant negative relationships ($p \approx 0.06–0.07$). Lower elevations were dominated by generalist species such as *Clethrionomys glareolus* and *Apodemus sylvaticus* complex, while high-elevation sites were characterized by cold-adapted specialists including *Chionomys nivalis* and *Sorex alpinus*. Detection probabilities varied among species and elevations, with extended monitoring (three months) substantially increasing the likelihood of detecting rare taxa compared to previous one-week surveys. Exploratory analyses indicated that species activity responded to temperature but showed no clear relationship with precipitation.

These results demonstrate that small mammal diversity in alpine environments decreases with altitude and that longer monitoring durations are crucial for reliable detection and community assessment. The findings contribute to understanding how elevational and climatic factors shape small mammal assemblages in the Alps and provide methodological guidance for long-term biodiversity monitoring in mountain ecosystems.

Keywords

Alpine biodiversity, biodiversity monitoring, camera trapping, elevational gradient, Parc Ela, presence probability, small mammals, species richness, Val Mulix, weather-dependent activity

Introduction

Biodiversity patterns along elevational gradients provide key insights into the processes that shape species distributions in mountain ecosystems. These gradients are often characterized by sharp abiotic changes over relatively short spatial scales, which makes them particularly suitable for studying species richness, species turnover and ecological adaptations (Chen et al., 2020). Small mammals are important focal taxa in this context due to their ecological roles as prey, seed dispersers, and soil engineers, and their sensitivity to environmental variation (Chirichella et al., 2022; Ferrari et al., 2023; McCain, 2005).

This makes small mammals an important umbrella group for alpine biodiversity and valuable indicators of ecosystem health (Chirichella et al., 2022). However, monitoring efforts are distributed unevenly across mammal groups: large species such as ungulates and carnivores, which make up only a quarter of all mammals, are well studied, whereas small mammals like rodents and insectivores, which account for almost half, are underrepresented (Graf & Fischer, 2021; Kennerley et al., 2021).

Small mammals, particularly rodents and shrews, are key components of alpine and subalpine ecosystems. Voles (*Microtus* sp.) and field mice (*Apodemus sylvaticus* complex) are widespread in these habitats (Graf & Fischer, 2021). The snow vole (*Chionomys nivalis;* Martins, 1842) is typical of rocky screes and highly adapted to areas with many crevices (Müller & Wandeler, 2021). The alpine wood mouse (*Apodemus alpicola*; Heinrich, 1952) occupies various habitats from riparian zones to open pastures (Müller & Blant, 2021b). Among insectivores, the alpine shrew (*Sorex alpinus;* Schinz, 1837) prefers cool, moist alpine slopes, while the pygmy shrew (*Sorex minutus,* Linnaeus, 1766) and the common shrew (*Sorex araneus,* Linnaeus, 1758) occur in moist meadows and subalpine forests (Müller & Blant, 2021a, 2021c; Müller & Maddalena, 2021). In addition to their ecological importance and umbrella function, small mammals are widely distributed along mountain slopes and exhibit higher speciation rates and habitat-specific species turnover than larger mammals. These characteristics make them ideal model organisms for studying changes in species composition along elevational gradients (Sun et al., 2020).

The latest Swiss Red List for mammals reports that nearly a third of small mammal species (11 out of 37; excluding bats) and several small carnivores such as martens and weasels are threatened (infofauna, n.d.). Monitoring small mammals is therefore crucial to improving our understanding of this comparatively understudied species group and provides a scientific basis for future conservation measures. On a global scale, identifying regions that hold particularly high biodiversity or key ecological components is a fundamental step in conservation planning and spatial prioritization (Brum et al., 2017; Kennerley et al., 2021). Yet, for many small mammal species, especially rodents and eulipotyphlans, there remains a striking lack of ecological and distributional knowledge. In fact, around 17% of these species are currently listed as Data Deficient by the IUCN (2018), and many of them may indeed be at risk (Bland et al., 2015). In this context, the Swiss Alps, with their pronounced elevational gradients and high habitat heterogeneity, represent a key area for research. Studying small mammals in this region helps to assess their conservation status and population trends, thereby supporting evidence-based management and protection of alpine biodiversity (Granata et al., 2025).

Camera traps prove to be an efficient, non-invasive method for monitoring small mammal communities in alpine environments. They allow continuous recording of activity without the limitations and disturbance associated with live-trapping (Burton et al., 2015; Di Cerbo & Biancardi, 2013; Hofmeester et al., 2021). While previous studies (e.g. Hofmeester et al., 2021) have demonstrated the utility of camera traps for detecting small mammal diversity and behavior, long-term applications across full elevational gradients remain rare. Moreover, it is not yet well documented how monitoring duration and abiotic factors such as temperature and precipitation affect detection probability and species-specific activity patterns in alpine habitats.

Understanding species diversity of small mammals along elevational gradients is essential to reveal how environmental conditions shape ecological communities (Chirichella et al., 2022; Ferrari et al., 2023; McCain, 2005). Their distribution is influenced by multiple interacting factors, including temperature, precipitation, vegetation cover, plant species composition, and microrelief. These factors modify habitat structure and resource availability, such as foraging opportunities, nesting sites, and protective cover, which in turn affect where different species can thrive (Billman et al., 2021; McCain, 2005). Because these

conditions shift markedly with elevation, studying how species richness and community composition vary along elevational gradients provides valuable insight into ecological processes and adaptation. This is particularly important for small mammals, for which research remains limited. Additionally in the context of ongoing climate change that is expected to alter temperature and vegetation patterns, potentially reshaping their elevational ranges and community dynamics which could endanger small mammals further (Chen et al., 2020; Chirichella et al., 2022).

This study addresses these gaps by quantifying species richness, detection probability, and weather-dependent activity of small mammals along an alpine elevational gradient. Specifically, we ask: *How does small mammal biodiversity and activity vary along an elevational gradient in Val Mulix using camera traps, and to what extent are detection probability and weather conditions influencing the observed patterns?* This study aims to disentangle how both spatial (elevational) and temporal (climatic) drivers shape small mammal diversity in alpine environments. The results are expected to contribute to a better understanding of biodiversity dynamics in mountain ecosystems and to inform future monitoring designs. The ultimate aim of this study is to improve our understanding of small mammal diversity and inform evidence-based conservation strategies for endangered alpine species.

Methods

To assess small mammal biodiversity along an alpine elevational gradient, we combined automated camera trap monitoring, species identification using DeepFaune, and environmental data integration. The following subsections describe the study area, field sampling, data processing and statistical analysis.

Study site

The study was conducted in Val Mulix, situated near the village of Preda in the municipality of Bergün Filisur, within the canton of Grisons, eastern Central Alps, Switzerland (46.578° N, 9.750° E; Figure 1). The area lies within *Parc Ela*, Switzerland's largest regional nature park. Val Mulix extends south-east of Preda and represents a characteristic alpine valley system featuring diverse vegetation and habitat types.

The study transect followed the valley from approximately 1735 m to 2635 m a.s.l., covering a distinct elevational gradient. The underlying bedrock consists mainly of silicate substrates. Three major vegetation zones were represented along the gradient. Below 2000 m a.s.l., the landscape was dominated by subalpine coniferous forests, primarily composed of *Pinus mugo* subsp. *uncinata* in the lower valley and by *Pinus cembra* and *Larix decidua* at higher elevations. Between 2000 m and 2500 m a.s.l., the terrain opened into alpine meadows and dwarf shrub communities, whereas above 2500 m a.s.l., vegetation was increasingly restricted to sparse grasslands and scree slopes.

A total of 12 permanent square plots were included in the study. These plots were originally established by botanists in previous Summer Schools (see Dengler, 2020) for long-term vegetation monitoring. The plots were distributed systematically along the elevational gradient to represent major vegetation zones at approximately 100 m elevation intervals (Figure 2).

Because the locations of these plots were predefined, the small mammal group did not select new sites. Instead, photo boxes equipped with camera traps were installed within or in close proximity to the existing vegetation plots, ensuring spatial consistency across interdisciplinary research teams. This setup allowed small mammal monitoring to be directly related to vegetation structure and habitat characteristics already documented for each permanent plot.

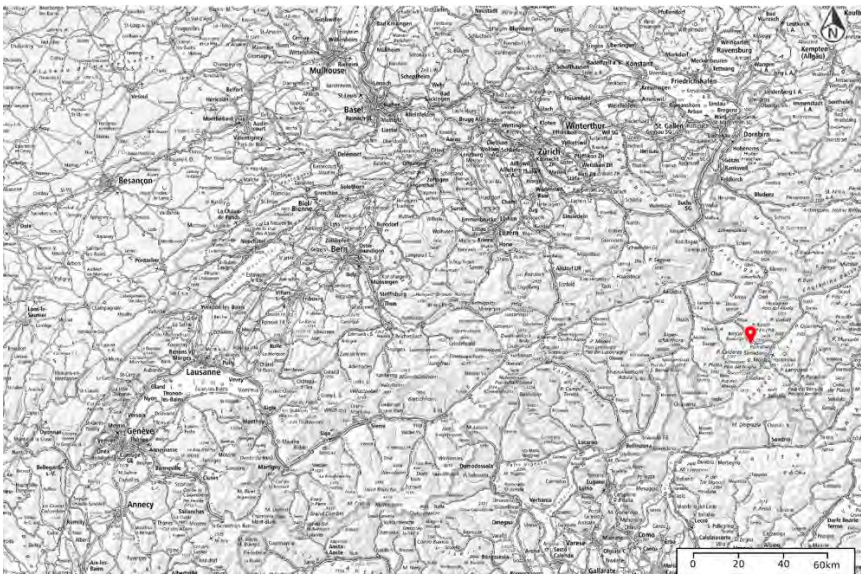

Figure 11. Location of the study area in Switzerland – Preda (Parc Ela, eastern Central Alps) (geo.admin, 2025).

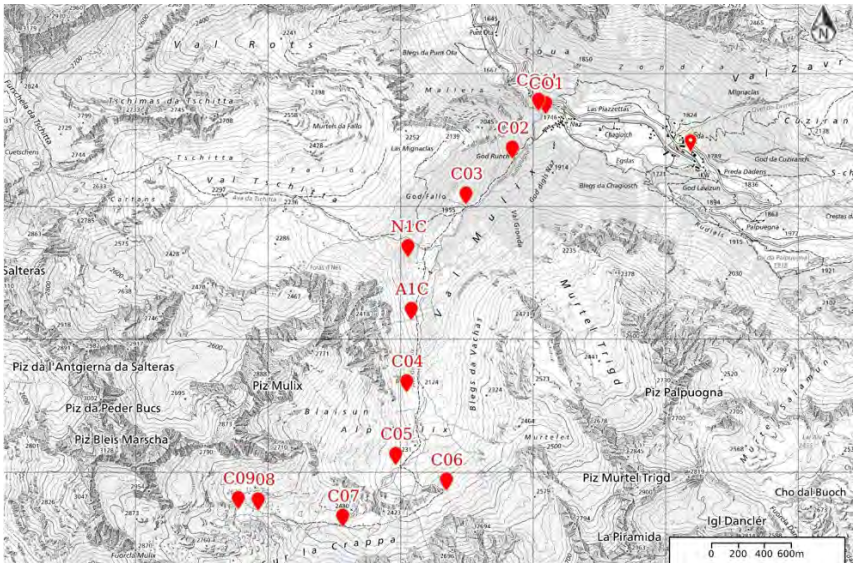

Figure 12. Study area with all plots sampled in 2025 in Val Mulix near Preda (geo.admin, 2025).

Field sampling

The wildlife research group deployed 12 white flash camera traps (Reconyx Hyperfire HC550; Reconyx, 2025) along the elevational gradient in Val Mulix. Ten cameras were placed at approximately 100 m elevational intervals, while two additional devices were installed at locations with potentially high small mammal activity (Table 1). All cameras were installed between 14 and 16 June 2025 and remained active until 18 to 24 August 2025, resulting in a continuous monitoring period of roughly three months.

Table 2. Overview of camera trap locations sampled in 2025

plot-ID	camera-ID	altitude [m a.s.l.]	x-coordinates – LV95 (CH1903+)	y-coordinates – LV95 (CH1903+)
C01	R20	1735	2'778'095	1'162'726
C01b	R21	1730	2'778'051	1'162'724
C02	R22	1840	2'777'838	1'162'351
C03	R23	1945	2'777'509	1'162'025
N1C	R24	2023	2'777'061	1'161'581
A1C	R25	2035	2'777'079	1'160'572
C04	R26	2194	2'777'079	1'160'572
C05	R27	2250	2'776'992	1'160'054
C06	R29	2355	2'777'353	1'159'864
C07	R58	2460	2'776'581	1'159'620
C08	R59	2565	2'775'946	1'159'718
C09	R60	2635	2'775'779	1'159'719

Each camera trap was installed in a standardized wooden photo box designed to attract small mammals and to minimize false triggers without baits (Figure 3). The cameras were positioned at similar heights above ground to ensure comparability across sites and optimal height to detect small mammals, with sensitivity adjusted to record both diurnal and nocturnal activity.

To account for differences in monitoring duration compared to previous years (which used shorter 7-day intervals), we later aggregated the three-month dataset into standardized time blocks. This enabled direct comparison of detection probabilities and the evaluation of optimal monitoring durations for reliable species detection.

Figure 13. Examples of standardized wooden photoboxes with wildlife cameras used along the elevational gradient in Val Mulix.

Species determination and event classification

All images were processed using the software DeepFaune (Rigoudy et al., 2023), which automatically generated an initial classification. These automated results were subsequently verified by manual inspection. Taxonomic identification was carried out conservatively (secure, higher-level taxonomy) to the lowest possible level (genus or species) using morphological criteria visible in the images (Figure 4). In cases of uncertainty, identifications were categorized as such and only identified by family e.g. *Neomys*

sp. (see identification key for all categories; Figure 4). Ambiguous images were shared among the research team for consensus classification.

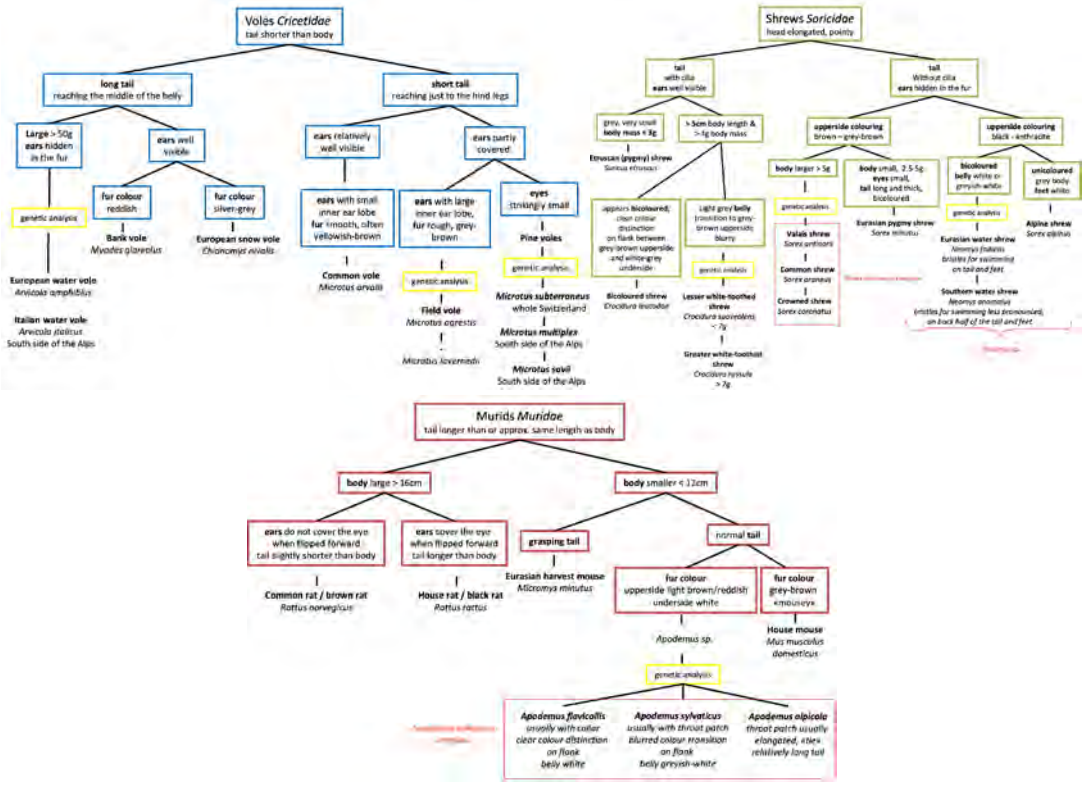

Figure 14. Adapted identification key (modifications shown in red) used for the classification and verification of small mammal detections (Reifler-Bächtiger & Stephani, 2019). For taxa where species-level identification required genetic analysis, individuals were assigned to species complexes. This applied to the *Apodemus sylvaticus* complex, comprising *Apodemus flavicollis*, *A. sylvaticus*, and *A. alpicola*, and to the *Sorex araneus* complex, comprising *Sorex antinorii*, *S. araneus*, and *S. coronatus*.

To quantify small mammal activity, we defined *events* as continuous sequences of the same individual in the frame. A new event was recorded when an individual was absent from the photo box for at least 40 seconds. This approach reduced the risk of pseudoreplication caused by repeated captures of the same individual within short intervals. We classified activity events based on the recorded images and compared species richness and diversity indices between elevations.

Two complementary species lists were derived from the camera trap data:

(i) a complete species list of all the events with small mammal individuals detected at camera trap sites R20, R21, R22, R23 and R27; and

(ii) an overall list of all the small mammal species recorded across the entire elevational gradient, based on combined data from all camera traps.

These data formed the basis for further statistical analyses of species composition, presence probability and diversity patterns. The corresponding visualisations are presented in the corresponding Results.

For subsequent analyses, we generated event-based datasets for each camera trap and elevation class to calculate diversity indices and presence probabilities for each species and site. Beyond biodiversity assessment, we also quantified the detection probability of small mammal species. In previous Summer

Schools in Preda, monitoring was limited to seven-day sampling periods (see Dengler, 2020). In this study, the monitoring duration was extended to three months, allowing us to track how detection probability accumulates over time. The longer observation period provided more robust and representative data on species presence and activity, thereby improving the reliability of biodiversity estimates and informing future survey designs.

Finally, we investigated the influence of weather conditions on small mammal activity. Due to the failure of the other loggers, temperature and precipitation data were only available from the lowest camera site. We tested whether activity patterns varied between wet and dry nights and between warm and cold conditions using these data. This exploratory analysis provides insights into potential short-term drivers of activity, particularly for alpine specialists such as *Sorex alpinus*, which may be more active under specific climatic conditions. The subsequent statistical analyses described below were based on the compiled event-based datasets.

Data preparation

Observation data on event level were imported from a CSV file using the readr package (Wickham et al., 2015). The dataset included camera ID, species identification event ID, timestamp, plot information, and geographic coordinates. Only relevant columns were retained for further analysis. Data were filtered to exclude entries with missing or unclear species identifications (e.g., empty values, "?") and non-target species and events that could only be detected on genus level. To ensure data consistency, a custom function was implemented to verify that each event contained observations of only a single species. Events with inconsistent species identifications were flagged and edited manually. The dplyr package (Wickham et al., 2014) was used to aggregate the data by event. For each event, the start and end timestamps were extracted, and the duration of the observation was calculated in seconds and formatted into a human-readable format (e.g., "1h 30m 15s") using a custom function. Additional metadata, such as geographic coordinates and altitude, were retained for the first observation in each event. The final dataset included aggregated event durations, the number of observations per event, and relevant spatial information. Data tables on species richness were manually prepared with a degree of structure which allowed for direct import and further processing.

Statistical analysis

All statistical analyses were performed in R version 4.5.1 (R Core Team, 2025). The interest of the performed analysis is to investigate, if the altitude of the plots is determining:

(a) The species richness per plot

(b) The Shannon index per plot, computed on an event-based list of observations

The analysis of species richness was be made on the data of each individual plot, while the analysis of Shannon diversity (Oksanen et al., 2001) was only done for five plots due to the labour-intensive process of making event-based data sets. Species lists were derived from event-based data when available and done manually by screening the preview of the footage on the data explorer for previously unreported species. Data entries which could not be identified at the species level were removed from the data set, as they do not hold information on the species richness or on the Shannon diversity. A linear model from “stats” (R Core Team, 2025) was deployed to assess the relation of diversity or species richness to the elevation of the observed plot.

Prior to statistical analysis, all numeric predictors were z-standardised to ensure the coefficients were comparable. Model diagnostics and residual checks were performed using the standard R Package “stats” (R Core Team, 2025) to assess fit and dispersion. Candidate models were compared based on the Akaike Information Criterion (AIC), and residual distributions were visually inspected to confirm the assumptions of the model (Table 2). Additional predictors for weather variables (temperature and precipitation) were included, using the on-site logger and Bergün station data described above. The significance level for all tests was set at $\alpha = 0.05$. To ensure reproducibility and transparency, data cleaning, event aggregation, and analytical scripts were independently reviewed by multiple team members, and data visualisations followed a standardised workflow using colour-blind-safe palettes (Okabe & Kei, 2002).

Table 3. Variables with corresponding units used in statistical analyses

Variable	Description	Unit
Elevation	Altitude of camera trap	m a.s.l.
Presence probability	Proportion of active weeks with detections	–
Shannon diversity	Diversity index based on species detections	–
Mean weekly temperature	Average local temperature per week	°C
Weekly precipitation	Total precipitation per week	mm

The presence probabilities of each species and camera site were compared between 2023 and 2025 in order to assess any temporal differences in detection patterns (Figure 7). Additionally, the relative species composition per 100-metre altitude band was visualised using stacked bar charts to illustrate elevational species turnover (Figure 8).

The methodological framework described above enabled us to quantify the diversity of small mammals, their species composition and their activity patterns along the elevational gradient. The following section presents the main results of these analyses.

Results

Species richness

Table 3 presents an excerpt of the event-based species list (i), comprising all small mammal detections recorded by camera traps R20, R21, R22, R23, and R27. This dataset served as the basis for calculating the Shannon diversity index across four elevational levels. Table 4 provides the overall species list (ii), which includes all species detected along the elevational gradient, regardless of detection frequency, and was used to determine species richness per elevation.

Table 4. Excerpt of the species list generated using DeepFaune and manually verified, showing all small mammal species detected by the camera traps during the 2025 monitoring period by camera id, event, date, plot id, altitude and x- & y-coordinates.

camera_ID	hyperlink sharepoint	Bestimmung	event	date	prediction	Plot	Bemerkungen	Mammal	Altitude	x_coordinates	y_coordinates	installation date
R20	IMG_0008.JPG	?	3	2025:06:16 21:18:13	Kleinsäuger	C01	nicht zu identifizieren	y	1735	778095	162726	45824
R20	IMG_0010.JPG	*Clethrionomys glareolus*	4	2025:06:16 22:13:55	Kleinsäuger	C01		y	1735	778095	162726	45824
R20	IMG_0011.JPG	*Clethrionomys glareolus*	4	2025:06:16 22:13:56	Kleinsäuger	C01		y	1735	778095	162726	45824
R20	IMG_0012.JPG	*Clethrionomys glareolus*	4	2025:06:16 22:13:56	Kleinsäuger	C01		y	1735	778095	162726	45824
R20	IMG_0013.JPG	*Clethrionomys glareolus*	4	2025:06:16 22:13:58	Kleinsäuger	C01		y	1735	778095	162726	45824
R20	IMG_0014.JPG	*Clethrionomys glareolus*	4	2025:06:16 22:13:59	Kleinsäuger	C01		y	1735	778095	162726	45824
R20	IMG_0015.JPG	*Clethrionomys glareolus*	4	2025:06:16 22:13:59	Kleinsäuger	C01		y	1735	778095	162726	45824
R20	IMG_0016.JPG	*Clethrionomys glareolus*	4	2025:06:16 22:14:00	Kleinsäuger	C01		y	1735	778095	162726	45824
R20	IMG_0017.JPG	*Clethrionomys glareolus*	4	2025:06:16 22:14:01	Kleinsäuger	C01		y	1735	778095	162726	45824
R20	IMG_0018.JPG	*Clethrionomys glareolus*	4	2025:06:16 22:14:02	Kleinsäuger	C01		y	1735	778095	162726	45824
R20	IMG_0019.JPG	*Clethrionomys glareolus*	5	2025:06:16 23:53:56	Kleinsäuger	C01		y	1735	778095	162726	45824
R20	IMG_0020.JPG	*Clethrionomys glareolus*	5	2025:06:16 23:53:57	Kleinsäuger	C01		y	1735	778095	162726	45824
R20	IMG_0021.JPG	*Clethrionomys glareolus*	5	2025:06:16 23:53:57	Kleinsäuger	C01		y	1735	778095	162726	45824
R20	IMG_0022.JPG	*Clethrionomys glareolus*	5	2025:06:16 23:53:58	Kleinsäuger	C01		y	1735	778095	162726	45824
R20	IMG_0023.JPG	*Clethrionomys glareolus*	5	2025:06:16 23:53:59	Kleinsäuger	C01		y	1735	778095	162726	45824
R20	IMG_0024.JPG	*Clethrionomys glareolus*	5	2025:06:16 23:54:00	Kleinsäuger	C01		y	1735	778095	162726	45824
R20	IMG_0034.JPG	*Apodemus sylvaticus complex*	9	2025:06:18 01:59:33	Kleinsäuger	C01		y	1735	778095	162726	45824
R20	IMG_0035.JPG	*Apodemus sylvaticus complex*	9	2025:06:18 01:59:34	Kleinsäuger	C01		y	1735	778095	162726	45824
R20	IMG_0036.JPG	*Apodemus sylvaticus complex*	9	2025:06:18 01:59:34	Kleinsäuger	C01		y	1735	778095	162726	45824

Table 5. Occurrence of small mammal species across all camera trap plots, indicating presence (✓) or absence (×) per site along the elevational gradient during the 2025 monitoring period as well as nocturnal (n), diurnal (d) or polyphasic (p) activity and whether they are habitat generalists (g) or specialists (s).

		Species													
		Apodemus sylvaticus complex	*Chionomys nivalis*	*Clethrionomys glareolus*	*Crocidura leucodon*	*Marmota marmota*	*Martes foina*	*Microtus arvalis*	*Mustela nivalis*	*Sciurus vulgaris*	*Sorex araneus complex*	*Sorex alpinus*	*Sorex minutus*	*Neomys* sp.	total
nocturnal / diurnal / polyphasic		n	d	n	n	d	n	p	p	d	p (n)	p	p	n	
habitat generalists / specialist		g	s	g	g	s	g	g	g	g	g	s	g	s	
Plot	C01	✓	×	✓	✓	×	✓	×	×	✓	✓	×	✓	×	7
	C01b	✓	×	✓	×	×	×	×	✓	×	✓	✓	✓	✓	7
	C02	✓	×	✓	×	×	×	×	✓	×	✓	✓	✓	×	6
	C03	✓	×	✓	×	×	×	×	×	×	✓	×	✓	×	4
	N1C	×	×	✓	×	×	×	×	×	×	✓	✓	×	×	3
	A1C	✓	✓	×	×	×	×	×	×	×	✓	×	✓	×	4
	C04	✓	✓	✓	×	×	×	×	✓	×	✓	×	×	✓	4
	C05	✓	✓	✓	×	×	×	×	✓	×	✓	×	×	✓	6
	C06	✓	✓	×	×	✓	×	✓	×	×	✓	×	×	×	5
	C07	✓	✓	×	×	✓	×	✓	×	×	×	×	×	×	4
	C08	✓	✓	✓	×	×	×	✓	×	×	✓	×	×	×	5
	C09	×	×	×	×	×	×	✓	×	×	✓	×	×	×	2

To assess the effect of elevation on small mammal diversity, the first dataset was employed to analyse species richness (Figure 5) and the second Shannon diversity (Figure 6). The corresponding model metrics are summarised in Table 5.

Table 6. Metrices of the linear models Species Count ~ Altitude and Shannon Index ~ Altitude.

Metric	Species Count ~ Altitude	Shannon Index ~ Altitude
Intercept	12.58 (±3.73)	3.86 (±0.97)
Slope (Altitude)	-0.0035 (±0.0017)	-0.0014 (±0.0005)
t-value (Altitude)	-2.03	-2.86
p-value (Altitude)	0.070	0.064
R^2	0.291	0.732
Adjusted R^2	0.220	0.643
F-statistic (DF)	4.11 (1, 10)	8.19 (1, 3)
p-value (Model)	0.070	0.064
Residual SE	1.78	0.22
Sample Size (n)	12	5

As illustrated in Figure 5, species richness (based on species list ii) showed a decreasing trend with increasing elevation. However, this relationship was not statistically significant ($p = 0.07$), and the explanatory power of the model was low ($R^2 = 0.29$).

When diversity was assessed using the Shannon index derived from event-based data (species list i; Figure 6), a similar decline with elevation was observed. Although this trend was also not statistically significant ($p = 0.065$), it approached the significance threshold ($\alpha = 0.05$) and exhibited a higher coefficient of determination ($R^2 = 0.73$), suggesting a stronger relationship between elevation and diversity in this model.

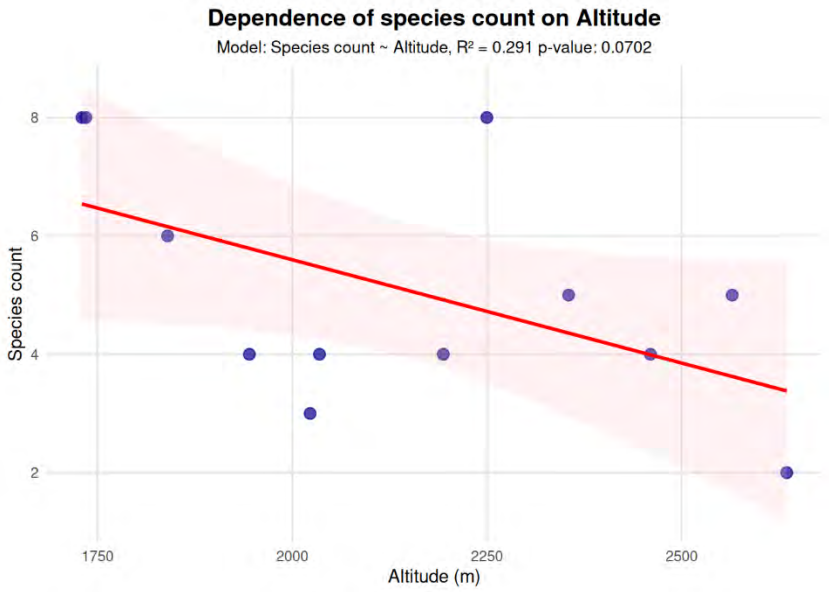

Figure 15**.** The linear regression plot illustrates the relationship between altitude [m] and species richness, showing a tendency for species richness to decrease (Species count = 12.68 – 0.0035 * altitude [m]) with increasing altitude ($R^2 = 0.92$, $p = 0.070$).

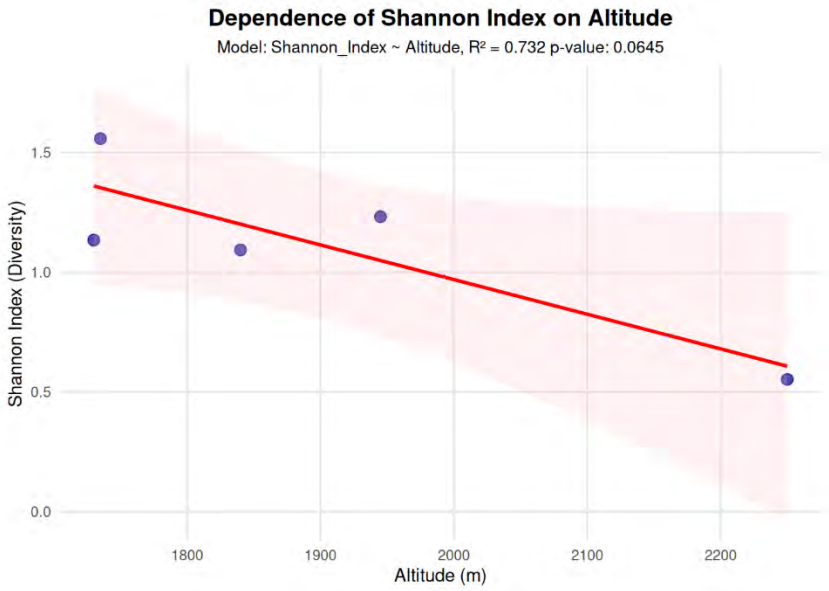

Figure 16**.** The linear regression plot depicts the relationship between altitude [m] and the Shannon Index, revealing a negative trend (Shannon index = 3.86 – 0.001447 * altitude [m]) in species diversity with increasing altitude ($R^2 = 0.73$, $p = 0.064$).

Species presence and detection probability

We detected small mammals across the elevational gradient using 12 camera traps deployed between 1735 and 2635 m a.s.l. The event-based dataset revealed clear differences in presence probability among sites. The five actively monitored plots (R20–R23, R27) yielded consistent detections across the three-month sampling period, whereas higher elevation sites showed fewer events overall.

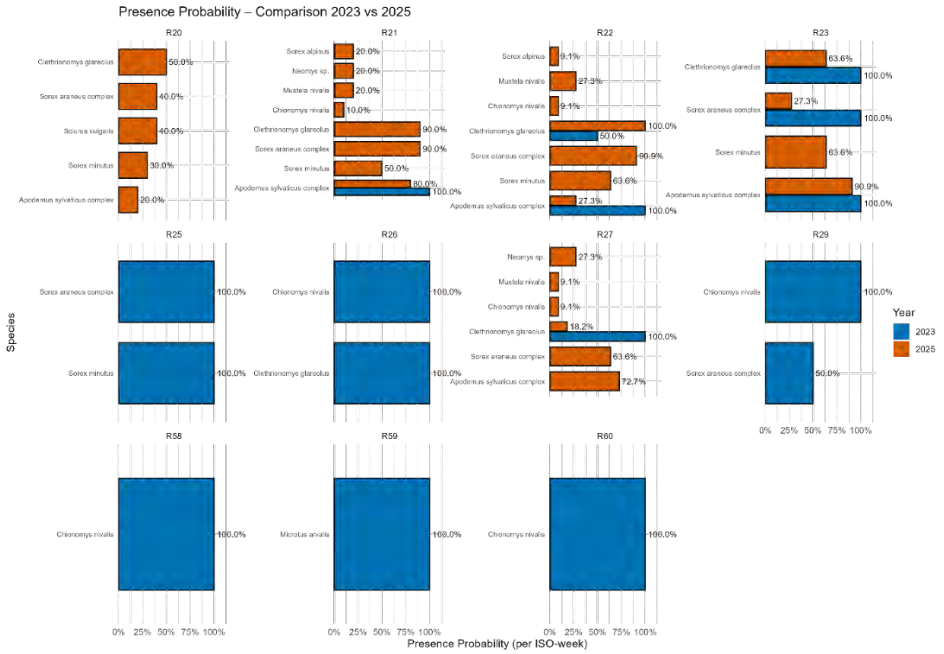

Figure 17. Relative presence probability in 7 days of small mammal species per camera trap location (R20-R23 & R27) in 2025 compared to 2023 (R21-R60). The bars show the average weekly probability of each species being present at the camera trap locations. Different colours are used to distinguish between the years 2023 and 2025, enabling a comparison of detection patterns over time along the elevation gradient.

The data show that species detection probability varied across both elevation and sampling years. The most frequently detected taxa were *Clethrionomys glareolus* (Schreber, 1780) and *Apodemus sylvaticus* complex, whereas *Sorex* species appeared less regularly. These differences indicate possible elevational and temporal effects on small mammal activity and detectability.

Species composition along the elevational gradient

Species composition (Figure 8) differed between low and high elevation sites. Lower plots were dominated by *Apodemus sylvaticus* complex and *Clethrionomys glareolus*, while higher plots contained a greater proportion of alpine specialists such as *Chionomys nivalis* and *Sorex alpinus*. Diversity appeared to decline with altitude, reflecting the harsher environmental conditions at higher elevations.

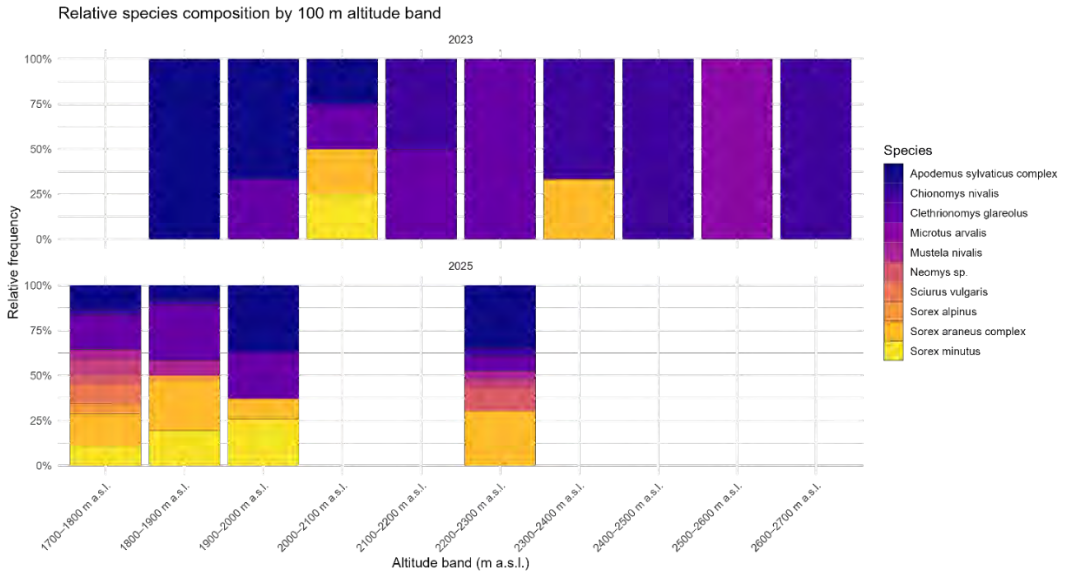

Figure 18. Relative species composition at 100-metre altitude intervals in 2023 and 2025. The stacked bars illustrate the proportionate contribution of each species of small mammal to the total number of sightings within 100-metre altitude bands. The colours illustrate changes in population composition with increasing altitude and over the years studied.

Mean presence probability along the gradient

When presence probabilities (Figure 9) were averaged across elevation bands, overall activity was higher at mid-elevations (≈ 1900–2300 m a.s.l.) compared to the uppermost plots (>2500 m a.s.l.). The results suggest that these intermediate zones provide optimal microhabitats, with greater vegetation cover and more stable microclimatic conditions.

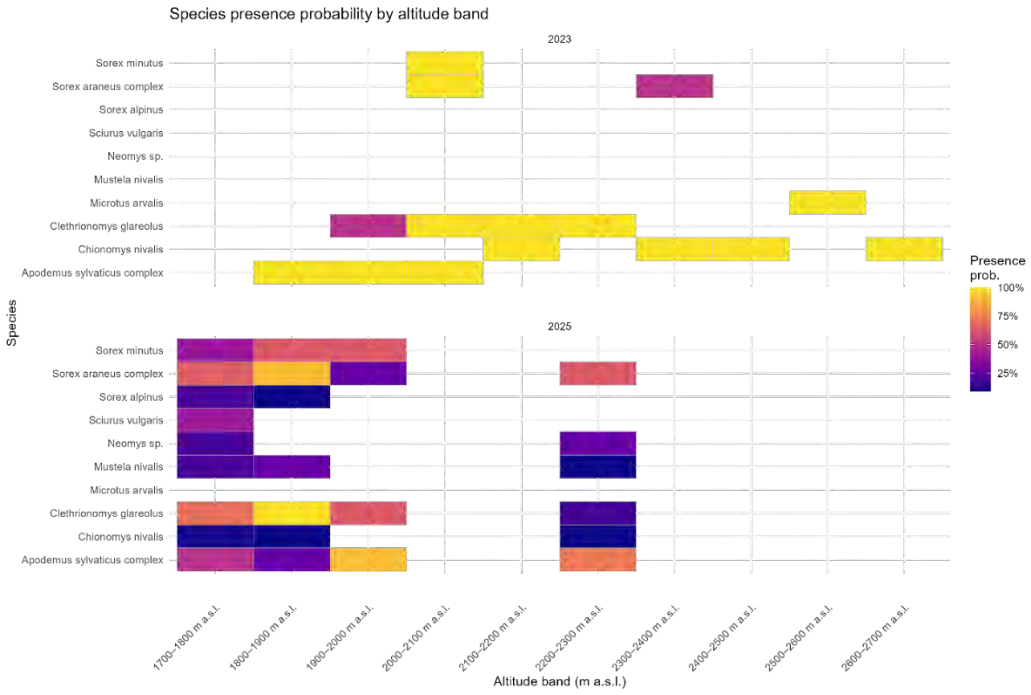

Figure 19. Mean presence probability of small mammal species along the elevational gradient in 2023 and 2025. The bars show the average occurrence probability of each species across all altitude bands, illustrating differences in activity along the gradient.

Temporal patterns of species observations regarding the weather

Air temperature (°C; measured approximately 10 cm above ground using a temperature logger) and precipitation (mm; data from weather station Bergün) were plotted against small mammal activity, represented by detection events from camera trap R20 at the lowest site (C01), to explore potential weather-dependent activity patterns (Figure 10). Since both local temperature records and event-based data (species list ii; Table 4) were available for this site, it provided an opportunity to examine temporal patterns of small mammal activity in relation to climatic variables. A total of five species were detected at C01 during the monitoring period. The visualization shows variation in detection frequency among species over time. *Sorex minutus* exhibited a clustered, high-intensity detection phase, whereas *C. glareolus* was recorded consistently throughout the observation period. No clear association between precipitation and detection events was apparent. The distribution of detections across temperature ranges further indicates the occurrence of both nocturnal and diurnal activity periods among the recorded species.

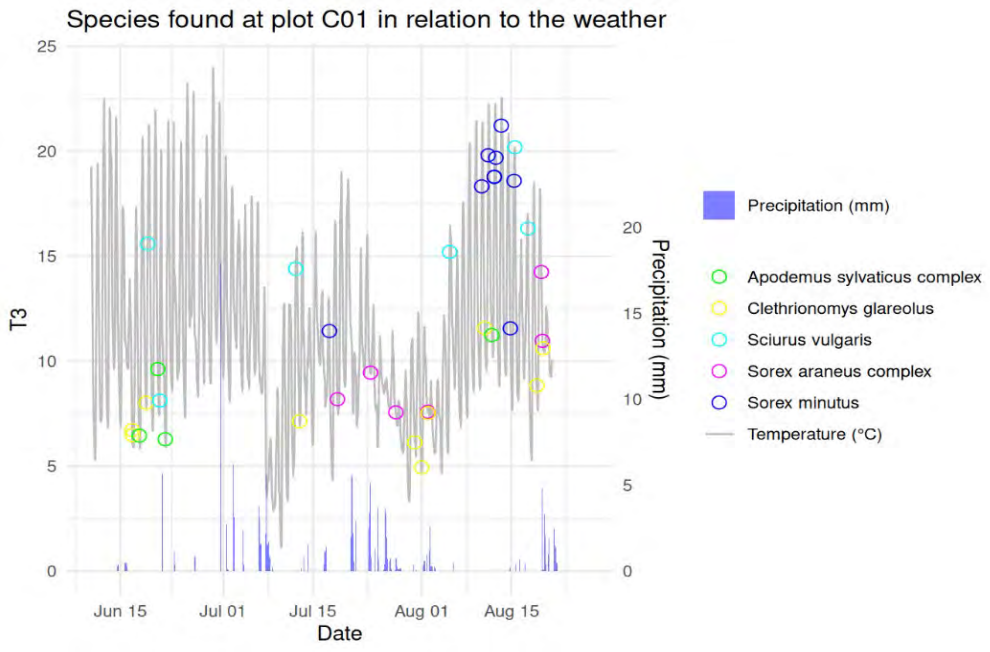

Figure 20. Species recorded in plot C01 (coloured circles) in relation to precipitation [mm] from the Bergün weather station.

Discussion

Species richness and diversity trends

Small mammal richness and diversity declined with increasing elevation in Val Mulix, as indicated by the negative relationship between Shannon index and altitude (Figure 6; $p = 0.0645$, $R^2 = 0.73$). Although not statistically significant, this trend likely reflects the limited number of sampled elevation levels. The pattern aligns with the globally observed decrease in biodiversity with elevation across taxa (Chen et al., 2020; McCain, 2005) and supports earlier findings from the study area (e.g. Dengler, 2020), confirming elevation as a major structuring factor in alpine small mammal communities.

This decrease in species diversity with elevation is typically linked to harsh weather conditions, shorter vegetation periods, and lower structural complexity at higher altitudes, all of which constrain resource availability and niche diversity (Chen et al., 2020; McCain, 2005). Furthermore, vegetation cover and soil productivity decrease with altitude, which likely limits foraging habitat and shelter, thereby reducing

species richness (Chen et al., 2020; McCain, 2005). In lower elevation zones, environmental and climatic conditions are more favorable and allow coexistence of multiple generalist species such as *Clethrionomys glareolus* and *Apodemus sylvaticus* complex. Their occurrence in these habitats may also reflect an anti-predatory strategy, as lower elevations provide more vegetation cover and complex microhabitats that facilitate concealment (Chirichella et al., 2022; Ferrari et al., 2023). In contrast, higher elevations are increasingly dominated by cold-adapted specialists such as *Chionomys nivalis*, which tolerate harsher abiotic conditions and reduced vegetation cover (Chirichella et al., 2022; Ferrari et al., 2023; Kamenišťák et al., 2020; Moritz et al., 2008).

Ecologically, these distributional shifts illustrate species-specific adaptations to temperature and vegetation (Chen et al., 2020). *C. glareolus* depends on dense understory vegetation for nesting and food, conditions typical of subalpine forests (Reifler-Bächtiger & Dietrich, 2021), while *C. nivalis* occupies rocky screes with abundant crevices, offering thermal buffering and protection from predators (Müller & Wandeler, 2021). The sharp decline in species richness at higher altitudes is consistent with the "climatic filtering" mechanism, where increasingly harsh temperatures restrict non-endemic and generalist species, leading to a community dominated by few cold-adapted taxa (Chen et al., 2020). Similar relationships between vegetation heterogeneity and small mammal diversity were documented on Mount Kinabalu, Malaysia, where diversity peaked at the transition between lowland and montane vegetation (Nor, 2001).

The results further support the spatial hypothesis, which attributes higher lowland diversity to larger historical habitat areas, lower extinction rates, and greater habitat heterogeneity (Camacho-Sanchez et al., 2019). The higher proportion of endemic species at greater elevations suggests that these taxa drive the turnover component of beta diversity, highlighting the role of historical biogeographic processes in structuring alpine communities (Camacho-Sanchez et al., 2019; Chen et al., 2020).

Interestingly, many global elevational studies on small mammals show mid-elevation diversity peaks (Chen et al., 2020; McCain, 2005), whereas our results indicate a continuous decline. This likely reflects the narrow elevational range examined and the strong climatic gradient in the central Alps, where high-elevation habitats (>2400 m) are characterised by shallow soils and limited vegetation. Nevertheless, the pattern supports the conclusion that small mammal richness in alpine environments is primarily shaped by temperature and resource availability rather than geometric or purely spatial constraints.

Detection probability and monitoring duration

Detection probability (Figure 7) varied markedly among species and elevations. Because detectability is species-specific (MacNeil et al., 2008), it is not possible to define a single optimal observation duration applicable to all taxa. Species detectability naturally increases with abundance but is also influenced by behavioral traits such as boldness and activity patterns (Benoit et al., 2018). Differences in detectability along elevational gradients can largely be attributed to ecological specialization (Ferrari et al., 2023). Common generalist rodents such as *A. sylvaticus* or *C. glareolus* complex are typically more active and adaptable to diverse habitats, which increases their likelihood of detection across elevations. In contrast, rare cold-adapted specialists such as *S. alpinus* or *C. nivalis* show more restricted activity windows and lower overall encounter rates, leading to reduced detectability in short-term surveys (Chirichella et al., 2022; Ferrari et al., 2023).

The higher species richness detected in 2025 compared to 2023 (Figure 8) is best explained by the longer monitoring duration. Extended sampling periods allow the accumulation of detections across fluctuating weather and activity cycles, which increases the chance of recording rare or less active species

(Hofmeester et al., 2021; Yang et al., 2025). This is particularly important in alpine and temperate ecosystems where species activity is temporally variable. Longer observation therefore enhances both detection probability and species presence estimates by reducing the likelihood of false absences (Yang et al., 2025). Therefore, the time required to reach reliable detection thresholds can be substantial. Our estimates suggest that 95 % detection probability (Appendix, Figure 11) may require 2 to 32 weeks depending on the elevation and species, underlining that one-week observations (such as in 2023) are insufficient to capture true community composition. Multi-week monitoring improves representation of rare taxa and provides more stable estimates for presence and abundance models (Li et al., 2021; Yang et al., 2025). Reliable detection and presence estimates thus require extended monitoring durations, ideally four to six weeks per site, to achieve representative coverage across elevational gradients.

Apparent higher detection probabilities in short-term datasets, such as in 2023, likely reflect a bias caused by low species numbers rather than genuine detectability. When only few dominant species are present, detection probabilities appear artificially elevated, masking the underrepresentation of rare or less active taxa (Skelton et al., 2023). Whereas in 2025, the larger number of species and longer observation time revealed more balanced community compositions. Weather differences and stochastic variation may have further influenced detectability (Chirichella et al., 2022; Li et al., 2021).

Weather dependency of species activity

Although only exploratory, our temperature analysis (Figure 10) from the lowest site (R20) indicated species-specific activity patterns related to temperature. *Sorex minutus* and *Sciurus vulgaris* (Linnaeus, 1758) were observed more frequently at higher temperatures throughout the monitoring, whereas *Sorex araneus* complex, *C. glareolus*, and *A. sylvaticus* complex were more active under cooler conditions. This aligns with general patterns of diurnal versus nocturnal activity, where the latter group is more active during the cooler night hours (Table 4). Chirichella et al. (2022) similarly found higher small mammal detections during night-time, when temperatures were lower, and reported that high daytime temperatures reduced detection rates. These trends are consistent with small mammal activity often correlating with microclimatic variables such as soil moisture and ambient temperature (Billman et al., 2021). However, our observations must be interpreted cautiously, given that they stem from a temperature logger in a single observed plot (C01). We also analysed mammal activity in relation to precipitation, but the results were inconclusive due to the low amount of sporadic rainfall. Future studies should deploy multiple loggers across the full gradient to disentangle local microclimatic effects and temporal variation.

In the context of climate change, these patterns are particularly relevant. Warming trends are expected to shift suitable habitats upward, potentially forcing cold-adapted species such as *C. nivalis* into increasingly restricted alpine refugia. These range shifts could impose additional stress on endemic specialists and potentially result in local extinctions if habitat availability decreases more rapidly than species can adapt or disperse (Ferrari et al., 2023; Moritz et al., 2008).

Methodological considerations and limitations

While the study provides valuable insights, several methodological limitations must be acknowledged. First, the unequal sampling effort among elevations and the limited subset of cameras analysed (due to over 60,000 images) reduce the representativeness of upper elevation zones. Consequently, statistical results should be interpreted with caution. Second, only one temperature logger was available, restricting the analysis of weather effects to a single site. Third, species identification from camera images can be

challenging, especially for morphologically similar taxa (e.g., *Sore*x *araneus* complex and *Sorex minutus*), and manual validation remains time-consuming.

Nonetheless, the study also has clear strengths. The use of non-invasive camera traps enabled continuous, disturbance-free monitoring over two months, far longer than in previous years, allowing for robust detection probability estimates. Integration with permanent vegetation plots further enhances the potential for cross-taxon analyses. Automated identification tools like DeepFaune considerably improved workflow efficiency and reproducibility, although human oversight remains essential for quality control. These methodological lessons contribute to refining protocols for alpine biodiversity monitoring, where harsh conditions and logistical constraints often limit sampling intensity.

Conservation and broader implications

The decline in species richness with elevation observed here echoes the general vulnerability of alpine small mammals to climate change and habitat loss. As highlighted in the Swiss Red List (infofauna, n.d.), nearly one-third of small mammal species are threatened, yet they remain underrepresented in monitoring programs. By providing quantitative evidence of how small mammal diversity and detectability vary along an alpine gradient, this study helps close critical knowledge gaps for conservation planning.

Our findings support the notion that lower and mid-elevation zones harbour the highest species richness, including many generalists that may serve as ecological indicators of community change. Conversely, cold-adapted specialists confined to higher elevations are likely most at risk under continued warming (Chirichella et al., 2022; Ferrari et al., 2023). Long-term monitoring in the Swiss Alps is therefore essential to detect population trends, anticipate range shifts, and inform evidence-based management.

Camera trapping proves to be a promising, low-disturbance tool for such monitoring efforts (Burton et al., 2015; Di Cerbo & Biancardi, 2013; Hofmeester et al., 2021). Its scalability and non-invasive nature make it ideal for integration into broader alpine biodiversity networks, such as Parc Ela or national initiatives like the Swiss Mammal Monitoring program. Coordinated long-term datasets will be crucial to detect changes in community composition and to guide conservation action for threatened small mammal species.

Conclusions and outlook

This study demonstrates that elevation strongly shapes small mammal diversity and activity in alpine ecosystems. The pronounced decline in species richness with altitude underscores the importance of temperature and habitat structure as key ecological drivers. Extended, continuous camera-trap monitoring over multiple weeks significantly enhances detection reliability and provides valuable insights into species' responses to environmental variation.

Future research should expand both the spatial (across valleys and mountain ranges) and temporal (year-round) coverage of monitoring. Integrating climatic data from multiple sensors and combining camera trapping with acoustic or genetic methods would allow a more comprehensive understanding of small mammal community dynamics.

Ultimately, long-term, standardized monitoring across the Swiss Alps will be fundamental to track biodiversity responses to ongoing climate change and to inform effective conservation of this ecologically important yet often overlooked mammal group.

References

Benoit, D., Jackson, D. A., & Ridgway, M. S. (2018). Assessing the impacts of imperfect detection on estimates of diversity and community structure through multispecies occupancy modeling. Ecology and Evolution, 8(9), 4676–4684. https://doi.org/10.1002/ece3.4023

Billman, P. D., Beever, E. A., McWethy, D. B., Thurman, L. L., & Wilson, K. C. (2021). Factors influencing distributional shifts and abundance at the range core of a climate-sensitive mammal. Global Change Biology, 27(19), 4498–4515. https://doi.org/10.1111/gcb.15793

Bland, L. M., Collen, B., Orme, C. D. L., & Bielby, J. (2015). Predicting the conservation status of data-deficient species. Conservation Biology, 29(1), 250–259.

Brum, F. T., Graham, C. H., Costa, G. C., Hedges, S. B., Penone, C., Radeloff, V. C., Rondinini, C., Loyola, R., & Davidson, A. D. (2017). Global priorities for conservation across multiple dimensions of mammalian diversity. Proceedings of the National Academy of Sciences, 114(29), 7641–7646. https://doi.org/10.1073/pnas.1706461114

Burton, A. C., Neilson, E., Moreira, D., Ladle, A., Steenweg, R., Fisher, J. T., Bayne, E., & Boutin, S. (2015). REVIEW: Wildlife camera trapping: a review and recommendations for linking surveys to ecological processes. Journal of Applied Ecology, 52(3), 675–685. https://doi.org/10.1111/1365-2664.12432

Camacho-Sanchez, M., Hawkins, M. T. R., Tuh Yit Yu, F., Maldonado, J. E., & Leonard, J. A. (2019). Endemism and diversity of small mammals along two neighboring Bornean mountains. PeerJ, 7, e7858. https://doi.org/10.7717/peerj.7858

Chen, Z., Li, X., Song, W., Li, Q., Onditi, K., Khanal, L., & Jiang, X. (2020). Small mammal species richness and turnover along elevational gradient in Yulong Mountain, Yunnan, Southwest China. Ecology and Evolution, 10(5), 2545–2558. https://doi.org/10.1002/ece3.6083

Chirichella, R., Ricci, E., Armanini, M., Gobbi, M., Mustoni, A., & Apollonio, M. (2022). Small mammals in a mountain ecosystem: The effect of topographic, micrometeorological, and biological correlates on their community structure. Community Ecology, 23(3), 289–299. https://doi.org/10.1007/s42974-022-00104-8

Dengler, J. (Ed.). (2020). International Master Summer School “Biodiversity Monitoring”, Preda, Parc Ela, Switzerland, 14–25 August 2019.

Di Cerbo, A. R., & Biancardi, C. M. (2013). Monitoring small and arboreal mammals by camera traps: Effectiveness and applications. Acta Theriologica, 58(3), 279–283. https://doi.org/10.1007/s13364-012-0122-9

Ferrari, G., Scaravelli, D., Mustoni, A., Armanini, M., Zibordi, F., Devineau, O., Cagnacci, F., Grasso, D. A., & Ossi, F. (2023). A Comparison of Small Rodent Assemblages after a 20 Year Interval in the Alps. Animals, 13(8), 1407. https://doi.org/10.3390/ani13081407

geo.admin. (2025). Basemap [Map]. Swisstopo.

Graf, R. F., & Fischer, C. (Eds.). (2021). Atlas der Säugetiere: Schweiz und Liechtenstein. Haupt Verlag, Bern.

Granata, M., Di Paolo, F., Luciano, L., Hofmeester, T. R., & Bertolino, S. (2025). How to catch a ghost? Comparing two camera trap-based monitoring methods for elusive small mustelids in the Italian Alps. Mammalian Biology, 13. https://doi.org/10.1007/s42991-025-00526-7

Hofmeester, T. R., Thorsen, N. H., Cromsigt, J. P. G. M., Kindberg, J., Andrén, H., Linnell, J. D. C., & Odden, J. (2021). Effects of camera-trap placement and number on detection of members of a mammalian assemblage. Ecosphere, 12(7). https://doi.org/10.1002/ecs2.3662

infofauna. (n.d.). Gefährdung und Schutz der Kleinen Säugetiere der Schweiz | info fauna. infofauna. https://www.infofauna.ch/de/beratungsstellen/kleine-saeugetiere/schutz/gefaehrdung-und-schutz#gsc.tab=0

Kamenišťák, J., Baláž, I., Tulis, F., Jakab, I., Ševčík, M., Poláčiková, Z., Klimant, P., Ambros, M., & Rychlik, L. (2020). Changes of small mammal communities with the altitude gradient. Biologia, 75(5), 713–722. https://doi.org/10.2478/s11756-019-00339-3

Kennerley, R. J., Lacher Jr., T. E., Hudson, M. A., Long, B., McCay, S. D., Roach, N. S., Turvey, S. T., & Young, R. P. (2021). Global patterns of extinction risk and conservation needs for Rodentia and Eulipotyphla. Diversity and Distributions, 27(9), 1792–1806. https://doi.org/10.1111/ddi.13368

Li, Z., Tang, Z., Xu, Y., Wang, Y., Duan, Z., Liu, X., Wang, P., Yang, J., Chen, W., & Prins, H. H. T. (2021). Habitat Use and Activity Patterns of Mammals and Birds in Relation to Temperature and Vegetation Cover in the Alpine Ecosystem of Southwestern China with Camera-Trapping Monitoring. Animals, 11(12), 3377. https://doi.org/10.3390/ani11123377

MacNeil, M. A., Tyler, E. H. M., Fonnesbeck, C. J., Rushton, S. P., Polunin, N. V. C., & Conroy, M. J. (2008). Accounting for detectability in reef-fish biodiversity estimates. Marine Ecology Progress Series, 367, 249–260. https://doi.org/10.3354/meps07580

McCain, C. M. (2005). Elevational Gradients in Diversity of Small Mammals. Ecology, 86(2), 366–372. https://doi.org/10.1890/03-3147

Moritz, C., Patton, J. L., Conroy, C. J., Parra, J. L., White, G. C., & Beissinger, S. R. (2008). Impact of a Century of Climate Change on Small-Mammal Communities in Yosemite National Park, USA. Science, 322(5899), 261–264. https://doi.org/10.1126/science.1163428

Müller, J. P., & Blant, M. (2021a). Alpenspitzmaus. In R. F. Graf & C. Fischer (Eds.), Atlas der Säugetiere: Schweiz und Liechtenstein (pp. 210–213). Haupt Verlag, Bern.

Müller, J. P., & Blant, M. (2021b). Alpenwaldmaus. In R. F. Graf & C. Fischer (Eds.), Atlas der Säugetiere: Schweiz und Liechtenstein (pp. 406–407). Haupt Verlag, Bern.

Müller, J. P., & Blant, M. (2021c). Zwergspitzmaus. In R. F. Graf & C. Fischer (Eds.), Atlas der Säugetiere: Schweiz und Liechtenstein (1. Auflage, pp. 208–209). Haupt Verlag, Bern.

Müller, J. P., & Maddalena, T. (2021). Waldspitzmaus. In R. F. Graf & C. Fischer (Eds.), Atlas der Säugetiere: Schweiz und Liechtenstein (1. Auflage, pp. 198–201). Haupt Verlag, Bern.

Müller, J. P., & Wandeler, P. (2021). Schneemaus. In R. F. Graf & C. Fischer (Eds.), Atlas der Säugetiere: Schweiz und Liechtenstein (1. Auflage, pp. 358–361). Haupt Verlag, Bern.

Nor, S. Md. (2001). Elevational diversity patterns of small mammals on Mount Kinabalu, Sabah, Malaysia. Global Ecology and Biogeography, 10(1), 41–62. https://doi.org/10.1046/j.1466-822x.2001.00231.x

Okabe, M., & Kei, I. (2002, November 20). Color Universal Design (CUD)—How to make figures and presentations that are friendly to Colorblind people. https://jfly.uni-koeln.de/color/

Oksanen, J., Simpson, G. L., Blanchet, F. G., Kindt, R., Legendre, P., Minchin, P. R., O'Hara, R. B., Solymos, P., Stevens, M. H. H., Szoecs, E., Wagner, H., Barbour, M., Bedward, M., Bolker, B., Borcard, D., Borman, T., Carvalho, G., Chirico, M., De Caceres, M., … Weedon, J. (2001). vegan: Community Ecology Package (p. 2.7-1) [Dataset]. https://doi.org/10.32614/CRAN.package.vegan

R Core Team. (2025). R: The R Project for Statistical Computing (Version 4.5.1) [Computer software]. https://www.r-project.org/

Reconyx. (2025). Professional Research Cameras. Reconyx. https://www.reconyx.com/market/professional?gad_source=1&gad_campaignid=130595127&gbraid=0AAAADshg2nbJxbuf5yLz6Fk4ejTqf95O&gclid=Cj0KCQjw_L_FBhDmARIsAItqgt56s8AqI4J8kjuIofeuNSd44N7KdhB_ZZ5o5EP0auxwbpn6JdOF9Q0aAueOEALw_wcB

Reifler-Bächtiger, M., & Dietrich, A. (2021). Rötelmaus. In R. F. Graf & C. Fischer (Eds.), Atlas der Säugetiere: Schweiz und Liechtenstein (1. Auflage). Haupt Verlag, Bern.

Reifler-Bächtiger, M., & Stephani, A. (2019). Small mammal Identification key [unpublished] [Chart]. Zhaw.

Rigoudy, N., Dussert, G., Benyoub, A., Besnard, A., Birck, C., Boyer, J., Bollet, Y., Bunz, Y., Caussimont, G., (…) Chamaillé-Jammes, S. (2023). The DeepFaune initiative: A collaborative effort towards the automatic identification of European fauna in camera trap images. European Journal of Wildlife Research, 69(6), 113. https://doi.org/10.1007/s10344-023-01742-7

Skelton, J., Cauvin, A., & Hunter, M. E. (2023). Environmental DNA metabarcoding read numbers and their variability predict species abundance, but weakly in non-dominant species. Environmental DNA, 5(5), 1092–1104. https://doi.org/10.1002/edn3.355

Sun, J., Wen, Z., Feijó, A., Cheng, J., Wang, Y., Li, S., Ge, D., Xia, L., & Yang, Q. (2020). Elevation patterns and critical environmental drivers of the taxonomic, functional, and phylogenetic diversity of small mammals in a karst mountain area. Ecology and Evolution, 10(19), 10899–10911. https://doi.org/10.1002/ece3.6750

Wickham, H., François, R., Henry, L., Müller, K., & Vaughan, D. (2014). dplyr: A Grammar of Data Manipulation (p. 1.1.4) [Dataset]. https://doi.org/10.32614/CRAN.package.dplyr

Wickham, H., Hester, J., & Bryan, J. (2015). readr: Read Rectangular Text Data (p. 2.1.5) [Dataset]. https://doi.org/10.32614/CRAN.package.readr

Yang, C., Mou, J., Qiao, J., Ruan, G., Jiang, Y., & Wang, J. (2025). Assessing the Impact of Elevation and Seasonality on the Detection of Medium- to Large-Sized Mammals by Camera Traps. Integrative Zoology, *20*(5), 1056–1060. https://doi.org/10.1111/1749-4877.12924

Appendices

Appendix A. Observed small mammal species

The following Table 6 lists all the small mammal species recorded by camera traps during the 2025 monitoring campaign along the altitude gradient in Val Mulix. It also shows all the species in the identification key that were not recorded (shown in red).

Table 7. observed small mammal species in camera traps

Species	Plot_C01	Plot_C01b	Plot_C02	Plot_C03	Plot_N1C	Plot_A1C	Plot_C04	Plot_C05	Plot_C06	Plot_C07	Plot_C08	Plot_C09
Apodemus sylvaticus complex												
Chionomys nivalis												
Clethrionomys glareolus												
Crocidura leucodon												
Marmota marmota												
Martes foina												
Microtus arvalis												
Mustela nivalis												
Sciurus vulgaris												
Sorex araneus complex												
Sorex alpinus												
Sorex minutus												
Neomys sp.												

Microtus agrestis complex
Microtus subterraneus complex
Arvicola amphibius complex
Rattus rattus
Rattus norvegicus
Micromys minutus
Mus domesticus
Crocidura sp.
Suncus etruscus
Martes martes
Eliomys quercinus
Dryomys nitedula
Glis glis
Muscardinus avellanarius

Appendix B. Additional taxa occasionally recorded

In addition to the focal small mammal taxa, the cameras occasionally recorded other vertebrates which were not included in the quantitative analyses. These observations are summarised below for the sake of completeness.

Table 8. Complete list of non-small-mammal species observed in Val Mulix during the Summer School 2025. Observations were made visually or with binoculars and are sorted by date. *N* indicates the number of individuals recorded, and the corresponding observation site is provided.

Datum	N	Species	Art	english	location
19.08.2025	3	*Rupicapra rupicapra*	Gämse	chamois	Val Mulix
19.08.2025	1	*Gypaetus barbatus*	Bartgeier	bearded vulture	Val Mulix
19.08.2025	2	*Marmota marmota*	Murmeltier	marmot	Val Mulix
20.08.2025	2	*Cervus elaphus*	Hirschkühe	red deer	Preda
20.08.2025	1	*Cervus elaphus*	Rothirsch	red deer	Preda
20.08.2025	1	*Vulpes vulpes*	Rotfuchs	red fox	Preda
21.08.2025	1	*Sciurus vulgaris*	Eurasisches Eichhörnchen	eurasian red squirrel	Preda
21.08.2025	2	*Capreolus capreolus*	Rehe	roe deer	Preda
21.08.2025	1	*Cervus elaphus*	Rothirsch	red deer	Preda
21.08.2025	5	*Cervus elaphus*	Rothirsch	red deer	Preda
21.08.2025	6	*Rupicapra rupicapra*	Gämse	chamois	Preda
22.08.2025	4	*Cervus elaphus*	Rothirsch	red deer	Preda
22.08.2025	1	*Cervus elaphus*	Rothirsch	red deer	Preda
22.08.2025	2	*Rupicapra rupicapra*	Gämse	chamois	Preda
23.08.2025	2	*Gypaetus barbatus*	Bartgeier	bearded vulture	Val Mulix
23.08.2025	2	*Rupicapra rupicapra*	Gämse	chamois	Preda
23.08.2025	5	*Capra ibex*	Alpensteinbock	alpine ibex	Fuorcla Crap Alv
24.08.2025	2	*Cervus elaphus*	Hirschkuh & -kalb	red deer	Val Mulix
24.08.2025	18	*Rupicapra rupicapra*	Gämse	chamois	Lai Negr
24.08.2025	1	*Gypaetus barbatus*	Bartgeier	bearded vulture	Val Mulix
24.08.2025	1	*Marmota marmota*	Murmeltier	marmot	Val Mulix

Appendix C. Weeks requested for a 95% detection probability

The following chart (Figure 11) shows the estimated quantity of weeks required for a 95% detection probability of every small mammal and elevational level.

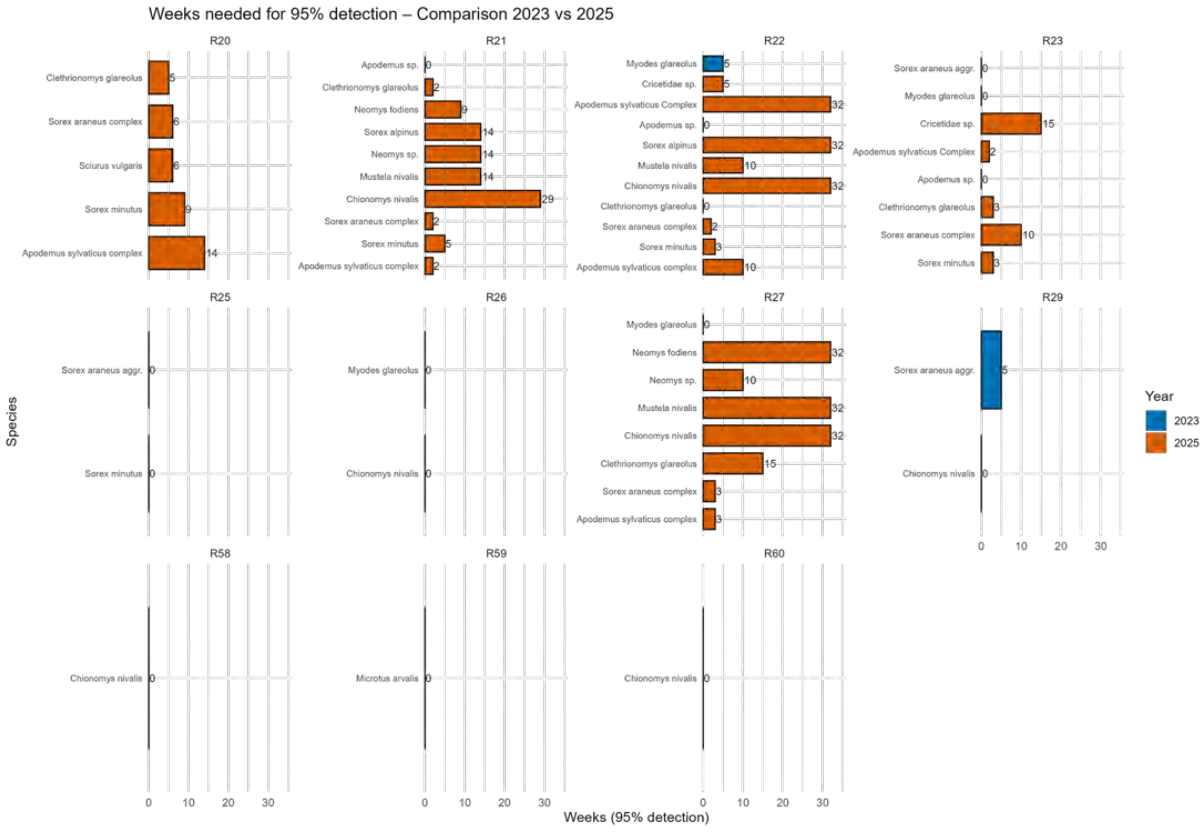

Figure 21. Weeks requested for a 95% detection probability

Appendix: Photo plates

Photographed by Anders Raagaard unless otherwise stated and compiled by Anders Raagaard

The Sonnenhof headquarters in Preda and the view down the Val Mulix.

Images from the field and from The 'lab' in Sonnenhof, where critical species were determined (top two images by Sophie Bürgi, middle right and bottom left images by Oksana Tyshchenko).

Botanical teams working on vegetation relevés (by Jürgen Dengler).

Animal life around Preda. From upper left to lower right: Caterpillar of Papilio machaon on *Laserpitum* siler (by Jürgen Dengler), *Nucifraga caryocatactes macrorhynchus* with a *Pinus cembra* cone, *Agrius convolvuli* (by Olha Chusova), alpine salamander (Salamandra atra), *Capra ibex, Marmota marmota, Ichthyosaura alpestris, Miramella alpina.*

Even though the field course was intense, there was time to enjoy the sights, swim in a lake, start a bonfire and even, for some this year, join a local mini festival (from top left to bottom right, images by Olha Chusova, Bartosz Norek, Fabian Rätz, Oksana Tyshchenko and Dunin Karwicki).

Alpine plants around Preda. From upper left to lower right: *Campanula cenisia*, *Saxifraga caesia*, *Leontopodium alpinum*, *Linaria alpina*, *Saxifraga aizoides* (middle photo by Jürgen Dengler).

Lab work and field work during the course, two top images show late night plant identification in Sonnenhof and a well-deserved snack in the field. Middle row shows plant plots in various habitats and aspects, including a wetland, a scree and the parking lot. Lower row: first image is a plot that is now covered by a recent rockslide, second is a lichen rich large rock habitat close to Preda. Image credits: top left, middle left and right and bottom right by Jürgen Dengler, middle center by Oksana Tyshchenko.

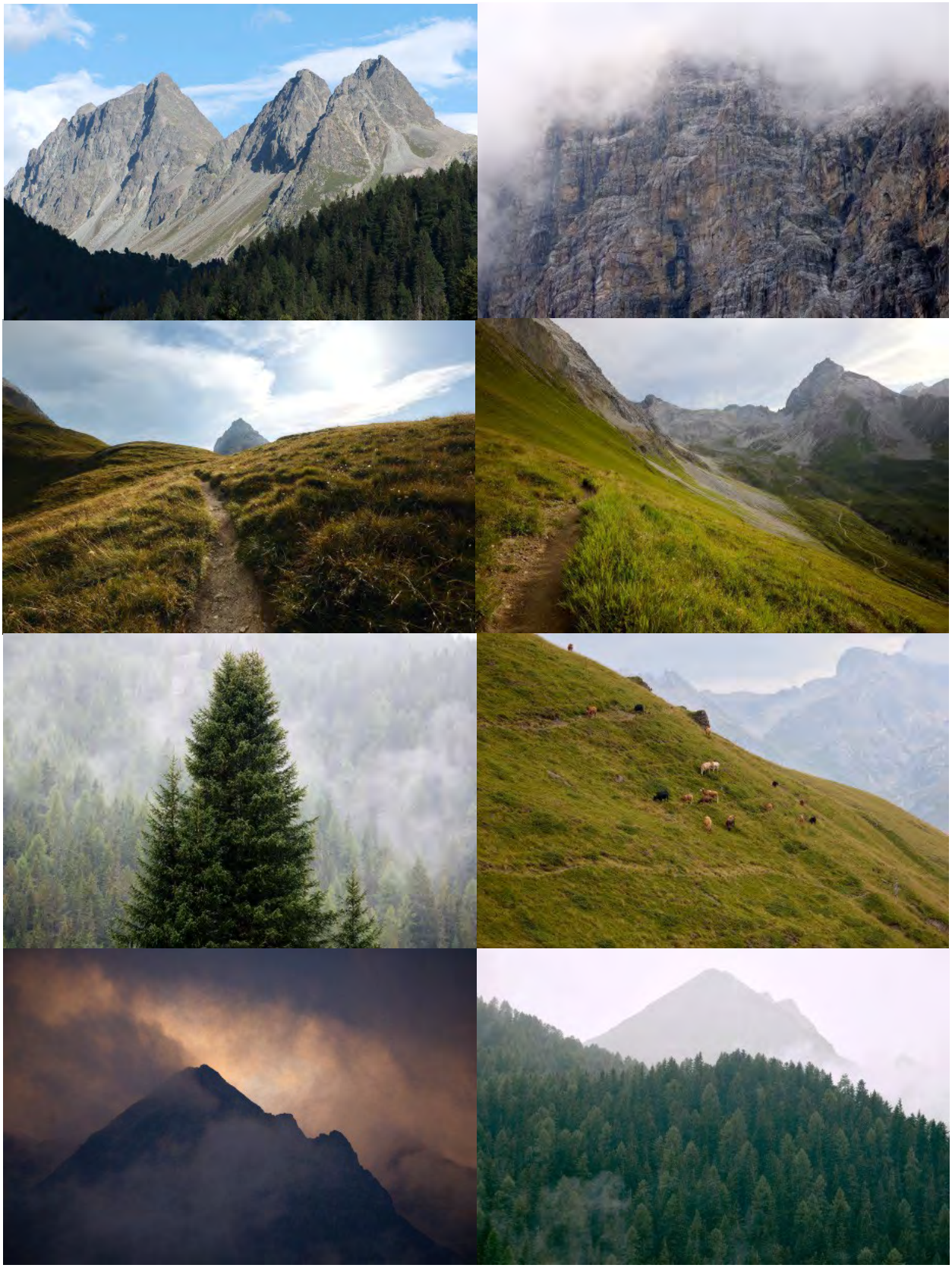

Some of the spectacular scenery around Preda. There was one free day on the course, where you can explore the vastness of the Swiss Alps (top left photo by Jürgen Dengler).

Subalpine plants around Preda. From upper left to lower right: *Gentiana asclepiadea*, *Scabiosa lucida*, *Huperzia selago*, *Centaurea rhaetica*, *Aconitum napellus*, *Aconitum variegatum*, *Dianthus superbus* (top left, center center and bottom right photos by Jürgen Dengler)